JPRS L/9264

21 August 1980

USSR Report

PHYSICS AND MATHEMATICS

(FOUO 7/80)

FBIS FOREIGN BROADCAST INFORMATION SERVICE

APPROVED FOR RELEASE: 2007/02/08: CIA-RDP82-00850R000300020036-7

NOTE

JPRS publications contain information primarily from foreign newspapers, periodicals and books, but also from news agency transmissions and broadcasts. Materials from foreign-language sources are translated; those from English-language sources are transcribed or reprinted, with the original phrasing and other characteristics retained.

Headlines, editorial reports, and material enclosed in brackets [] are supplied by JPRS. Processing indicators such as [Text] or [Excerpt] in the first line of each item, or following the last line of a brief, indicate how the original information was processed. Where no processing indicator is given, the information was summarized or extracted.

Unfamiliar names rendered phonetically or transliterated are enclosed in parentheses. Words or names preceded by a question mark and enclosed in parentheses were not clear in the original but have been supplied as appropriate in context. Other unattributed parenthetical notes within the body of an item originate with the source. Times within items are as given by source.

The contents of this publication in no way represent the policies, views or attitudes of the U.S. Government.

For further information on report content call (703) 351-2938 (economic); 3468 (political, sociological, military); 2726 (life sciences); 2725 (physical sciences).

APPROVED FOR RELEASE: 2007/02/08: CIA-RDP82-00850R000300020036-7

JPRS L/9264

21 August 1980

USSR REPORT

PHYSICS AND MATHEMATICS

(FOUO 7/80)

CONTENTS

ELECTRICITY AND MAGNETISM

UDC 533.09

A STUDY OF A LONG SLIDING SPARK

Novosibirsk ZHURNAL PRIKLADNOY MEKHANIKI I TEKHNICHESKOY FIZIKI in Russian
No 1, Jan-Feb 80 pp 111-115 manuscript received 14 Dec 78

[Paper by S.I. Andreyev, Ye.A. Zobov, A.N. Sidorov and V.D. Kostousov, Leningrad]

[Text] The flashover characteristics of sliding sparks up to 2.5 m long are studied for various gases at different pressures. Studies of sliding sparks in air at atmospheric pressure are described in the literature [1, 2]. The studies in this work were carried out in argon, neon, helium and air at pressures of from 10 to 1,600 mm Hg. The sliding discharge took place at the surface of a dielectric film which was enveloped by a metal tube connected to one of the electrodes (the so-called "initiator"). The diameter of the initiator was 40 mm. The film thickness was 0.4 to 4 mm. The length of the discharge gap varied from 0.25 to 2.5 m. The discharge was realized in a dielectric chamber 450 mm in diameter which was evacuated and then filled with various gases.

A cable transformer served as the voltage source [1, 2]. The voltage across the secondary winding had the form of a decaying cosinusoid at a frequency of from 30 to 120 KHz. The logarithmic decrement of the attenuation was 10^{-2}.

The experimental results. The breakdown voltage level, U_{pr}, was studied in all of the experiments. This quantity was defined as the lowest amplitude at which the sliding spark bridges the discharge gap.

The influence of the dielectric film thickness, Δ (in mm), can be expressed in terms of the specific film capacitance, $C_{ud} = 0.88\ \varepsilon/\Delta$, of which the breakdown voltage is a unique function.

The function U_{pr} (C_{ud}) is shown in Figure 1 for argon, neon, helium and air (curves 1 - 4 respectively), plotted for gap length of l = 1 m at

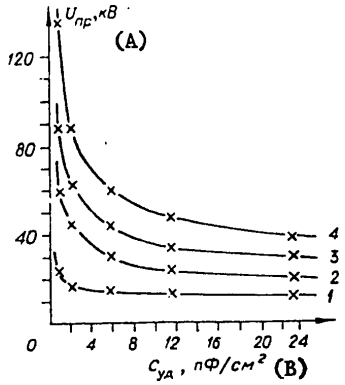

Figure 1.

Key: A. U_{pr} [breakdown voltage], KV;
B. C_{ud} [specific capacitance], picofarads/cm^2.

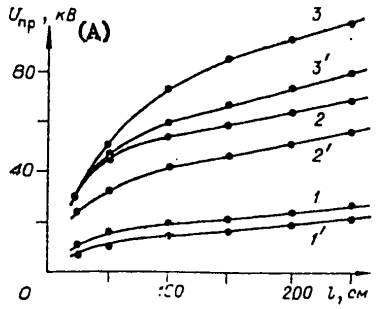

Figure 2.

Key: A. Breakdown voltage, KV.

atmospheric pressure. It can be seen that with an increase in C_{ud}, U_{pr} falls off rapidly at first. But starting at C_{ud} = 2 to 5 pFd/cm^2, the change in U_{pr} becomes minor. It is physically possible to explain this by the fact that the increase in C_{ud} initially leads to a rise in the capacitive current, and consequently, in the overall current through the uncompleted discharge channel. The rise in the current leads to a reduction in the channel resistance and the effective transfer of the high voltage electrode potential (from which the sliding discharge develops) to the head of the uncompleted leader channel. This potential provides for the occurrence of ionization processes at the head and the development of the leader. With a sufficiently high value of C_{ud}, the growth in the potential at the head experiences saturation.

It can also be seen from the data of Figure 1 that the ratio of the breakdown voltages for the various gases depends slightly on the quantity C_{ud} at rather high values of C_{ud}. This can likewise be explained by the decisive influence of ionization processes at the head of the uncompleted leader channel. The processes are basically determined by the area in front of the head, in which the multiplication of the electron avalanches and streamers takes place. U_{pr} is shown in Figure 2 as a function of the length of the discharge gap l for argon (1 and 1'), neon (2 and 2') and helium (3 and 3') for values of C_{ud} of 1.6 (curves 1 - 3) and 3.0 pFd/cm^2 (1' - 3').

As was noted earlier, an inflection point was observed in the curve for $U_{pr}(l)$ for the case of air [2]. For values of $l \geq l_{cr}$, the voltage increases practically linearly as a function of l (the field intensity in the section of the channel from l_{cr} to l remains constant). It turned out that the point of inflection (l_{cr},U_{cr}) is determined (at least in the range studied here) only by the quantity C_{ud} and the kind of gas (at an initial pressure

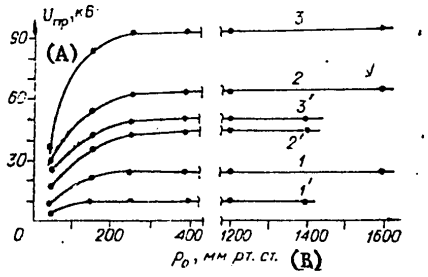

Figure 3.

Key. A. Breakdown voltage, KV;
B. p_o, mm Hg.

of $p \geq 200$ mm Hg) and does not depend on p:

$$U_{cr} = AC_{ud}^{-0.5}, \text{ KV}; \quad l_{cr} = BC_{ud}^{-0.5}, \text{ m.}$$

The constants are A = 80 and B = 1.15 for helium; A = 54 and B = 0.75 for neon; A = 17.2, B = 0.75 for argon. The values of the constant field intensities in the region above l_{cr} are as follows: E_{pr} = 14.5 KV/m for helium 8.3 KV/m for neon and 4.5 KV/m for argon.

When $l \geq l_{cr}$, the breakdown voltage can be determined from the formula:

(1) $U_{pr} = 1.1[U_{cr} + E_{pr}(l - l_{cr})]$, KV.

The given values for U_{cr}, l_{cr} and E_{pr} make it possible to determine U_{pr} using (1) with an error of around 10%. U_{pr} is shown in Figure 3 as a function of the gas pressure. In contrast to the Paschen curves, the pressure does not influence U_{pr} in a wide range [of pressures]. Curves 1 and 1' were obtained for argon, 2 and 2' were obtained for neon, 3 and 3' for helium; curves 1 - 3 apply to the case of a film thickness of Δ = 2 mm (C_{ud} = = 1.6 pFd/cm^2) for a length of l = 2 m, while 1' - 3' are for Δ = 0.5 mm (C_{ud} = 3 pFd/cm^2) for a length of 0.5 m.

The fact that the gas pressure does not influence the development of a leader in a wide range of pressures is evidence that in the case considered here, the quantity E/p (E is the field intensity at the head), which determines the intensity of the ionization processes at a given point in the gas, does not exert any substantial influence on the development of a leader. At the same time, the influence of C_{ud} is manifest when the pressure p changes (see Figure 3). It can be concluded as a result that the development of a leader is primarily determined by the overall current which flows into its head, while this quantity is in turn determined by the area over which the ionization processes take place. The intensity of these processes practically remains constant, since in the electrical field region at the head, there exists a large overvoltage and a change in E/p with a change in p under the conditions considered here does not increase the current feeding the leader head, while the area with the effective ionization does not change in this case (it is determined by the geometry of the unique capacitor formed by the conducting rod lying above the conducting plane).

In the range of comparatively low pressures, a leader apparently develops without substantial overvoltages at the head. For this reason, a change in p leads to a change in the intensity of the ionization processes and to a change in the current collecting surface in front of the head.

It is interesting that in such an electronegative gas as air, in contrast to the inert gases, the influence of pressure is marked throughout the entire range investigated from 37 to 800 mm Hg (Figure 4), if $l > l_{cr}$ (curves 1 and 2 apply to a discharge gap length of $l = 1.9$ m where $l_{cr} = 1.08$ m and 0.79 m respectively). In the case of a short discharge gap, $l < l_{cr}$ (curves 3 and 4 were obtained where $l = 0.35$ m and with the same values of l_{cr}), the influence of pressure falls off.

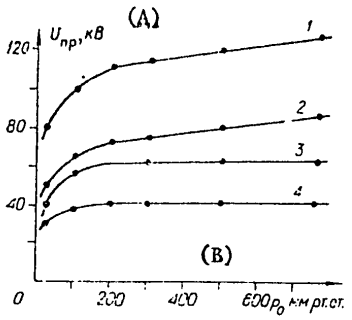

Figure 4.

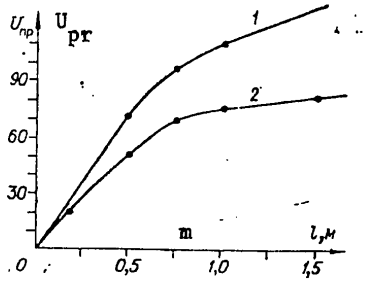

Figure 5.

Key: A. Breakdown voltage, KV;
B. p_o, mm Hg.

We will note that in the case of air where $l > l_{cr}$, the rise in the breakdown voltage with a rise in the pressure takes place linearly with a constant of 0.014 KV/mm Hg where $p \geq 200$ mm Hg. The dynamics of the process of slip discharge development [1] should also be brought into play to explain the data of Figure 4, which show the differing influence of p for short, $l < l_{cr}$, and long, $l \geq l_{cr}$, gaps.

Studies have shown that the breakdown in argon differs from the breakdown in other gases with a fast rate of leader channel development in the discharge gap; the breakdown in all of the cases studied here occurred over the time of the voltage rise.

In the case of helium, neon and air, the average rate of leader channel development is slower than in argon, and when $l \geq l_{cr}$, the development of the flahsover encompasses a region of voltage which changes sharply with time. In this case, the development takes place in a nonuniform fashion [1]. Characteristic stoppages and even "extinction" of the channel occur during the development, where these are determined both by the absolute level of the instantaneous voltage and its time derivative. This explains the multiplicity of flashover characteristics of a sliding spark which are found in the literature [3 - 8].

The conclusion can be drawn from an analysis of the timewise structure of the development of a sliding spark that the characteristic of the breakdown which depends on the gap length (on the breakdown time) is characterized by a range of flashover voltages falling between two maximum cases (Figure 5, air, 1 atm). Curve 1 applies to the case of breakdown with a single ("nonextinguishing") leader, which moves from one electrode to the other without stopping. Curve 2, which occurs with lower values of the breakdown voltages, corresponds to leader development with stoppages. The number of such stoppages exceeded under our conditions. In this case, the flashover occurs at a minimum value of the voltage.

In the first case, the average rate of leader travel is not too much different from the instantaneous value and amounts to $5 - 8 \cdot 10^8$ cm/sec, and in the second case, it is one to two orders of magnitude lower (from $5 \cdot 10^6$ to $7 \cdot 10^7$ cm/sec). Thus, formula (1) determines the lower flashover characteristic for the case of helium, neon and air, and the upper one in the case of argon.

We will note that to obtain a dense system of parallel discharges, the upper breakdown characteristic should be used.

The hypothesis can be put forward, in returning to the data of Figure 4, that a reduction in the influence of the pressure with a decrease in the length of the discharge gap is related to the transition from multistage breakdown to a single-pass flashover. In the case of a single-pass flashover in air, the excess voltage of the field at the head is rather high and the change in E/p with a change in p does not influence the flashover development process. In helium and neon, this influence is also not observed in the case of multipath breakdown.

The analysis of the set of data cited here from the point of view of the elementary processes makes it possible to explain the specific features of flashover in argon by the presence of more powerful ionizing radiation than in helium and neon. The specific features of breakdown in air are related to its electronegativity and large thermal capacity, which leads to a lower temperature and conductance (as compared to the inert gases).

The authors would like to express their gratitude to V.P. Sidorova for assisting in the work.

BBILIOGRAPHY

1. Andreyev, S.I., Zobov, Ye.A., Sidorov, A.N., "A Method of Controlling the Development and Generation of a System of Parallel Sliding Spark Channels in Air at Atmospheric Pressure", PMTF [JOURNAL OF APPLIED MECHANICS AND ENGINEERING PHYSICS], 1976, No 3.

2. Andreyev, S.I., Zobov, Ye.A., Sidorov, A.N., "A Study of a Sliding Spark in Air at Atmospheric Pressure", PMTF, 1978, No 3.

3. Toepler, E., "Stossspannung, Ueberschlag und Durchschlag bei Isolatoren" ["Shock Potential, Flashover and Breakdown in the Case of Insulators"], E.T.Z., 1924, Vol 45, p 1024.

4. Strigel, R., in "Electrische Stossfestigkeit" ["Electrical Breakdown Resistance"], Springer Verlag Publishers, 1955.

5. "Tekhnika bol'shikh impul'snykh tokov i magnitnykh poley" ["Large Pulse Current and Magnetic Field Engineering"], Collection edited by Komel'kov, V.S., Moscow, Atomizdat Publishers, 1970.

6. Roth, A., in "Hochspannungstechnik" ["High Voltage Engineering"], Springer Verlag Publishers, 1959.

7. Sirotinskiy, L.I., Lomonosov, V.I., Sergeyev, A.S., Panov, A.V., "Tekhnika vysokikh napryazheniy" ["High Voltage Engineering"], Vol 1, GEI Publishers, 1940.

8.. Skhanavi, G.I. "Fizika dielektrikov, Oblast' sil'nykh poley" ["The Physics of Dielectrics. The Region of Strong Fields"], Moscow, Fizmatgiz Publishers, 1958.

[8144/1380-8225]

8225
CSO: 8144/1380

UDC 537.523

HIGH-CURRENT COAXIAL DISCHARGE IN THE AIR STABILIZED BY A DIELECTRIC WALL

Moscow RADIOTEKHNIKA I ELEKTRONIKA in Russian Vol 25, No 6, 1980 pp 1218-1221

[Article by A. F. Aleksandrov, A. T. Savichev, O. I. Surov, I. B. Timofeyev, and A. R. Emil']

[Text] A continous emitting coaxial plasma sheath is produced by the electrical explosion of a vaporized metal coating deposited on a dielectric cylinder. Under certain experimental conditions the radiation of this discharge is close to equilibrium with the temperature of the emitting surface ~2 eV.

In recent years, high-current emitting discharges in atmospheric elements and in air produced by electrical explosions of thin metal wires have been investigated intensively [1] in regard to their use as high-intensity radiation sources in the visible and ultraviolet regions. At the present time, emitting discharges in the classical z pinch geometry [1] have been studied most thoroughly. However, linear discharges in spite of certain advantages, mostly in regard to the simple construction of such sources, have a small emitting surface and a relatively low resistance to the development of superheating (transparent discharges) and power (opaque discharges) instabilities.

Discharges with a return current [2] are more promising in this respect, especially since the emitting surface of such discharges can theoretically be as large as needed, and the duration of the steady state can be increased by a factor of R/r_p (R is the equilibrium radius of a discharge with a return current, and r_p is the radius of a linear z pinch). However, the generation of a dense emitting plasma with such a configuration presents some well-known difficulties. Thus, the formation of such discharges by a simultaneous explosion of many wires [2], in air for example, generally does not produce a single plasma sheath, but a discharge in the form of individual plasma channels.

A continuous emitting plasma sheath with a fairly large surface can prcbably be produced by an electrical explosion of thin metal foil or vaporized metal deposited on a dielectric of arbitrary shape (see [3] in this regard). Working with foil is difficult for purely technical reasons (it is difficult to construct a cylinder from thin foil with the correct shape). The use of a metal deposited on a dielectric cylinder to induce a reverse pinch is technologically advanced and presents certain advantages for a stationary inverse pinch, since the pressure of the inner plasma boundary is balanced by the dielectric wall. The so-called H-pinch discharge is formed, and the radius of the plasma sheath in it can be strictly controlled. In the present paper we investigate this type of discharge.

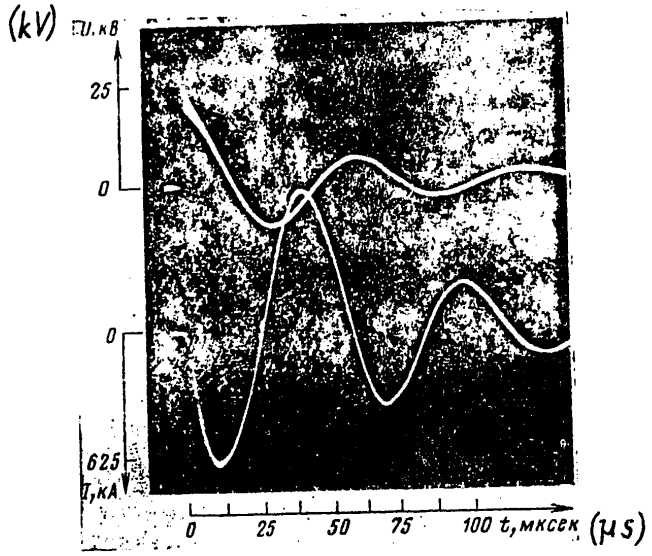

Fig. 1. Typical traces of the discharge current and voltage across the discharge gap (U_0=30 kV and $\underline{l}$=20 cm).

The experiments were performed on a Photon device with a capacitor bank of ≈500 μF and a voltage of 30 kV.

The discharge chamber was formed by two massive brass electrodes, with a dielectric cylinder 40 cm long pressed between them. A vaporized aluminum coating 300 - 500 Å thick was deposited on the cylinder surface. The cylinder diameters were

11 cm. To reduce the inductance of the discharge chamber, the upper electrode was connected to the "ground" of the device through eight brass rods placed uniformly about a circle with a diameter ≈50 cm.

In this paper, we used traditional methods of recording the basic discharge parameters - the shape and dimensions were obtained from end-on and side-on streak photographs, the current-voltage characteristics were recorded by Rogowski loops and ohmic voltage dividers, a time scan of the spectrum was provided by a rotating disk with slits (absolute calibration was by means of a Podmoshenskiy etalon), and the total radiation yield was obtained on an IKT-1M calorimeter [4]. The energy deposited in the discharge and the electrical conductivity of the plasma were determined from the current-voltage characteristics in the usual manner.

The experiments were performed for two values of the voltage across the capacitor bank: 25 and 30 kV. The stored energy amounted to ≈155 and 225 kJ in this case.

Figure 1 give typical traces of the discharge current and the voltage across the discharge gap. It is clear from these traces that the changes both in the discharge current and the voltage are close to periodic. The current period for the case U_0=30 kV and $\underline{l}$=20 cm (where U_0 is the initial voltage in the capacitor bank and $\underline{l}$ is the length of the discharge gap) equaled 70 μsec, and the amplitude at the first peak reached 625 kA. The maximum voltage drop across the electrode gap in this case was 25 kV. In the first half-period of the discharge current the energy deposited in the discharge equaled 46 kJ.

Figure 2 shows a typical side-on streak photograph of the development of the discharge. It is clear from the photograph that separate, brightly glowing and strongly branching channels (streamers) are observed in the initial stage of the discharge. As the discharge current increases, these channels expand and merge, and a single plasma layer with a fairly homogeneous

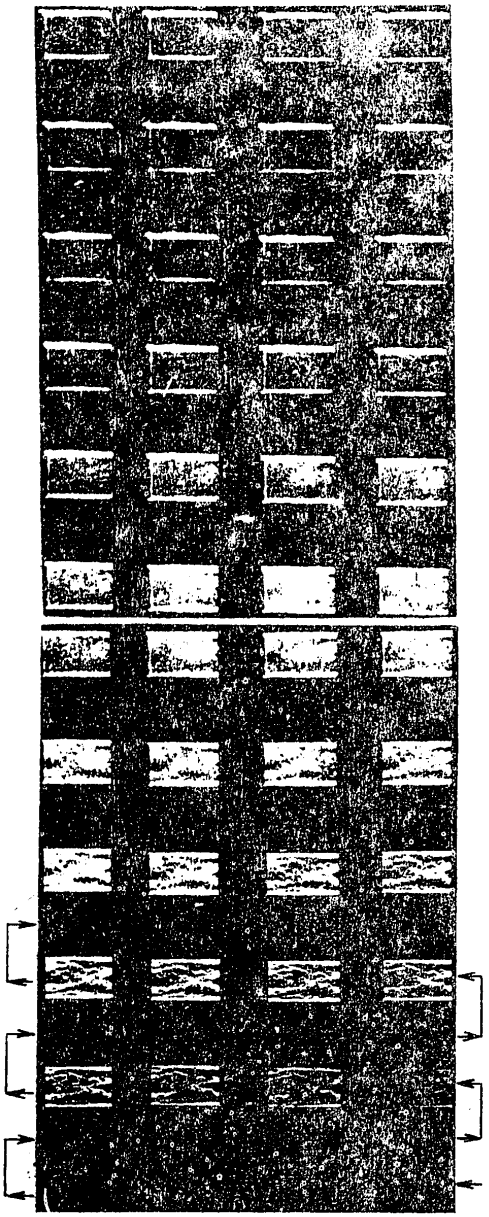

Fig. 2. Side-on streak photograph of the development of the discharge. The frames pass every 1 μsec.

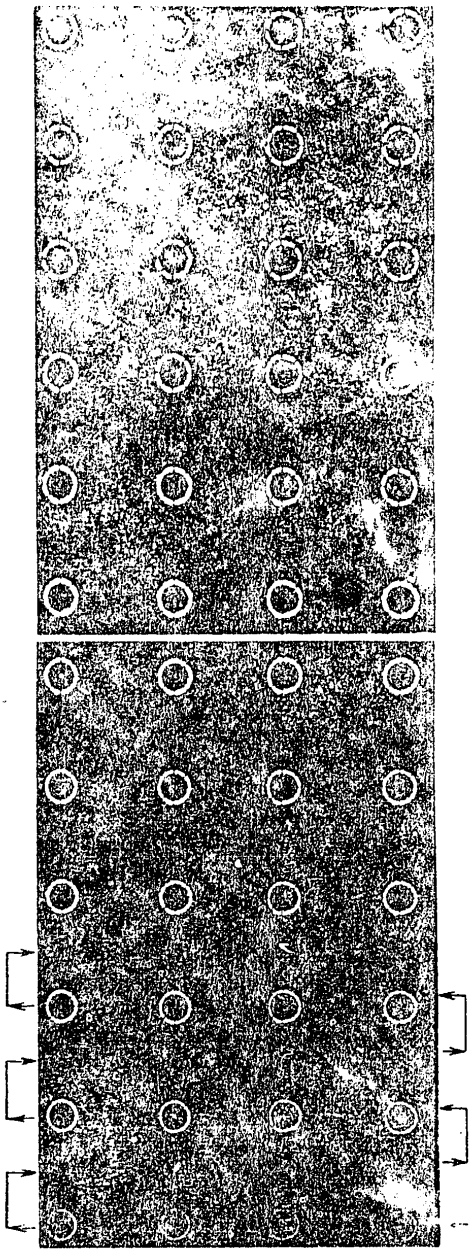

Fig. 3. End-on streak photograph of the development of the discharge.

glowing surface is formed approximately around 13 - 15 μsec. This feature is also confirmed by the end-on streak photograph of the discharge shown in Fig. 3. It is clear from the photographs that, as assumed, the inner dimension of the plasma sheath is strictly controlled by the position of the dielectric substrate to which the plasma is pressed by the magnetic pressure of the discharge current. Note that with small values of the initial voltage, the discharge channel during the entire lifetime of the discharge consists of separate glowing filaments ≈1 - 2 mm in diameter that undergo almost no expansion over time.

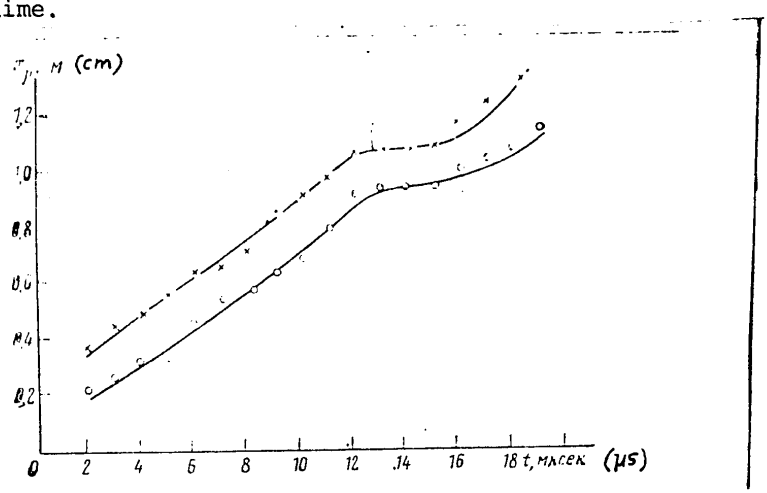

Fig. 4. Time dependence of the thickness of the plasma sheath x_p (1 - U_0=30 kV, $\underline{l}$=20 cm; 2 - U_0=25 kV, $\underline{l}$=20 cm).

Figure 4 gives the time dependence of the thickness of the plasma layer x_p for the first quarter of the discharge current period with two values of U_0 (25 and 30 kV), and the dependence was obtained by analyzing the end-on streak photographs. It is clear that in the first 12 μsec the discharge channel expands at a rate $\approx 10^5$ cm/sec, and a well-defined magnetic confinement stage is observed at times corresponding to ∿12 - 16 μsec (the maximum value of the power of the discharge current corresponds to ∿11 μsec). At subsequent times the expansion of the plasma continues due to a drop in the power of the discharge current.

Figure 5 shows a segment of the time scan of the radiation spectrum of the discharge. In the first half-period a continuous spectrum is observed, and its intensity increases with the increase in the power of the discharge current; the intensity maximum corresponds to the current maximum, and at later times

the discharge has a line spectrum.

The brightness temperature was determined over the continuous spectrum of the discharge. The radiation near the current maximum corresponds to absolute black-body radiation (the brightness temperatures for wavelengths λ_1=2800 A, λ_2=3000 Å, and λ_3=3600 Å coincided within the experimental error and equalled at the time of the current maximum T≈24,000 K and 19,000 K for an initial voltage of 30 and 25 kV, respectively). The change in T over time was similar in nature to the change in the power of the discharge current, as is evident from Fig. 6. The triangles in it represent the discharge temperature calculated from the conductivity in the usual manner with the use of the Spitzer equation. Clearly, it has a fairly good agreement with the brightness temperature of the discharge.

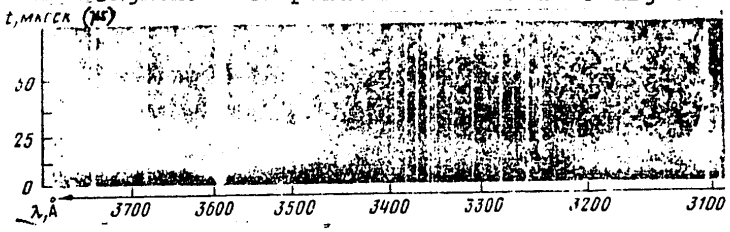

Fig. 5. A segment of a time scan of the spectrum.

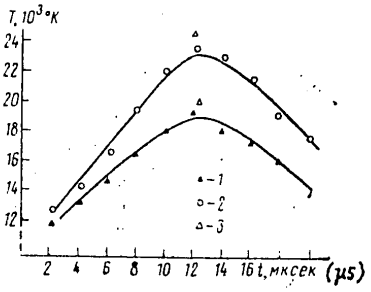

Fig. 6. Time dependence of the discharge current (1 - U_0=25 kV, $\underline{l}$=20 cm; 2 - U_0=30 kV, $\underline{l}$=20 cm; 3 - temperature calculated according to the conductivity).

If the time dependence of the discharge temperature is known, the balance equation $H^2/8\pi=(1+z)nkT$ can be used to estimate the charged particle density at the times corresponding to the magnetic confinement stage. For the time corresponding to the peak of the discharge current, such an estimate gives $n\approx 2\times 10^{18}$ cm^{-3}, but with a coating thickness of ≈500 Å the number of

particles is $n \approx 3 \times 10^{17}$ cm^{-3}. These results indicate that ambient air with a density of ≈ 0.1 is drawn from the atmosphere into the discharge channel.

An estimate of the energy balance in the discharge indicates that the main contribution to the balance is made by the radiation and the ionization energy. For a density of $n = 2 \times 10^{18}$ cm^{-3} the ionization energy is ~ 7 kJ and the escaping radiation is ~ 25 kJ.

Thus, the explosion of aluminum deposited on a dielectric cylinder has been used to produce a stationary inverse pinch (the H-pinch cylindrical discharge), whose characteristics are close to those of a discharge produced by the explosion of many wires but whose radiation is more uniform over the surface.

BIBLIOGRAPHY

1. A. F. Aleksandrov, V. V. Zosimov, A. A. Rukhadze, S. P. Kurdyumov, Yu. P. Popov, and I. B. Timofeyev, ZH. EKSP. TEOR. FIZ., 1971, 61, 1841; A. F. Aleksandrov and A. A. Rukhadze, Fizika sil'notochnykh elektrorazryadnykh istochnikov sveta [Physics of High-Current Electric-Discharge Sources of Light], Atomizdat, 1976.

2. A. F. Aleksandrov, V. V. Perebeynos, A. T. Savichev, and I. B. Timofeyev, ZH. EKSP. TEOR. FIZ., 1974, 44, 581; A. F. Aleksandrov and A. A. Rukhadze, USP. FIZ. NAUK, 1974, 112, No. 2, 193.

3. S. I. Andreyev, M. P. Vanyuk, and A. T. Starovoytov, ZH. EKSP. TEOR. FIZ., 1962, 43, 1616.

4. A. F. Aleksandrov, A. T. Savichev, O. I. Surov, and I. B. Timofeyev, FIZ. PLAZMY, 1978, 4, 1390.

[8144/1417-9370]

9370
CSO: 8144/1417

FLUID DYNAMICS

ABSTRACTS ON INHOMOGENEOUS FLUID DYNAMICS

Novosibirsk DINAMIKA NEODNORODNOY ZHIDKOSTI (Dinamika Sploshnoy Sredi 42) (Dynamics of Inhomogeneous Fluids (Continuum Dynamics 42) in Russian 1979 signed to press 18 Oct 79

[Abstracts from collection by Institute of Hydrodynamics, Siberian Affiliate of the USSR Academy of Sciences, 500 copies]

UDC 532.501.32

PERIODIC SOLUTIONS OF THE PROBLEM OF WAVES OVER A LEVEL BOTTOM

LOGINOV, B. V.

[Text] The problem of the potential fluid flow in a three-dimensional layer with a free upper boundary is considered with allowance for surface tension. Corresponding asymptotes of sets of periodic solutions in the neighborhoods of bifurcation points, representing fourfold eigenvalues of the linearized system are constructed. Methods of the theory of the branching of solutions of nonlinear equations under conditions of group invariance are used (Ref. Zh. Mat., 1971, 8B696, 10B698). The invariance of the problem with respect to a biparametric group of displacements serves to reduce the four-dimensional branching equation to its two-dimensional counterpart.

UDC 539.3

APPROXIMATE CALCULATION OF CAVERN DEPTH IN A SEMIINFINITE PARTITION

MERZHNEVSKIY, L. A. and RESNYANSKIY, A. D.

[Text] On the basis of a model of incompressible ideally plastic solids, the depth of the caverns forming upon the impact of spherical particles

against a semiinfinite obstacle are calculated. The findings are compared with experimental data. The range of applicability of the proposed approximation techniques is determined.

UDC 532.516

INTERACTION BETWEEN A LINEAR VORTEX AND A FREE SURFACE

NIKULIN, V. V.

[Text] An eddy filament in a viscous fluid is considered, with one end of the filament resting against the free surface of the fluid. It is assumed that the flow is symmetrical relative to the axis coinciding with the filament, and that the free surface is cone-shaped. The force of gravity is absent. The structure of solutions of Navier-Stokes equations is investigated. The existence theorem is demonstrated.

UDC 622.241.8

TEMPERATURE REGIME OF GAS WELLS

PAVLOV, N. N.

[Text] A simplified mathematical model of the motion of real gas in a well is examined as a function of the operating mode of the well. The unsteady-state heat transfer coefficient is derived to allow for unsteady-state heat exchange with ambient rocks. Sample calculations are presented.

UDC 517.946+551.51

EXISTENCE OF A GENERALIZED SOLUTION OF EQUATIONS OF ATMOSPHERIC DYNAMICS

SUKHONOSOV, V. I.

[Text] The existence and uniqueness theorem is demonstrated as a whole with respect to the time of the smooth solution of the initial boundary-value problem of the system of equations of atmospheric dynamics in case of plane-parallel motion.

UDC 539.374

VISCOSITY OF CYLINDRICAL SHELLS COMPRESSED BY PRODUCTS OF DETONATION

TRUNOV, V. L.

[Text] The effect of viscosity on the compression of cylindrical shells of revolution by the products of the detonation of an explosive is investigated. A numerical solution of the problem of the motion of a rotating ring of an imcompressible viscous fluid and the tagged-line method are used to measure the viscosity coefficients of copper, niobium, and aluminum. It is shown that viscosity affects markedly the motion of metal shells over a broad range of input data.

UDC 57.9+532.5

PERIODIC VISCOUS GAS FLOW

SHELUKHIN, V. V.

[Text] Two boundary-value problems with periodic data are considered. The first pertains to the barotropic viscous gas model and the second, to the heat-conducting viscous gas model. It is shown that only the first of these two problems displays periodic solutions. The class of periodic solutions applicable to the uniqueness theorem is isolated.

UDC 523.527+532.517

STABILITY OF THE FLOW OF IDEAL INCOMPRESSIBLE FLUIDS WITH CIRCULAR STREAM LINES

VLADIMIROV, V. A.

[Text] The behavior of pertubations with specified input data is considered. It is shown that flow of this type is always unstable with respect to perturbations belonging in a continuous spectrum. Solutins with singularities are investigated for perturbations having the form of normal waves. The form of the solution in the neighborhood of the critical point is derived. The rule for selecting the solution branch is formulated on the basis of the solution of the problem with specified input data. An analytic representation of the Reynolds stress distribution of the perturbation is obtained. Certain flow classes for which solutions with singularities do not exist are isolated. The applicability of the Rayleigh stability criterion is discussed.

UDC 517.53:517.947.42

SEQUENTIAL ROTATION OF QUASICONFORMAL PLANE MAPPINGS ONTO $\bar{R}^n$

KUD'YAVIN, V. S.

[Text] A method for finding linear coefficients of quasiconformality for pairs of regions in n-dimensional Moebius space $\bar{R}^n$, $n \geq 2$, based on the sequential rotation of plane quasiconformal mappings, is considered. The method is used to derive the linear coefficients of quasiconformality of certain pairs of n-dimensional, $n \geq 3$, annular regions, as well as to obtain n-dimensional analogues of the corresponding theorems of distortion in the presence of q-quasiconformal mappings of a 3-dimensional sphere onto itself.

UDC 517.946

THE DARBOUX PROBLEM AND A NONLINEAR HYPERBOLIC-PARABOLIC SYSTEM OF EQUATIONS IN A PLANE

ORAZOV, L.

[Text] The existence of a general solution of the Darboux problem for a system of nonlinear hyperbolic-parabolic equations is demonstrated.

UDC 532.031

A CASE OF CONVERGENCE OF THE ITERATIVE METHOD AND ITS APPLICATION TO THE THEORY OF JETS

PYKHTEYEV, G. N.

[Text] A case in which the nonlinear operator A(u) of the equation $u = \lambda A(u)$ (λ is a constant parameter), determined in Banach space, satisfies the Lipschitz condition in the sphere $0 \leq \|u\| \leq r$ is considered. Here the Lipschitz constant is a function of the radius of the sphere and tends toward infinity. Conditions for convergence of the iterative method in this case are established. The findings are used to determine two classes of streamline flow of incompressible fluids.

[157-1386]

1386
CSO: 1862

LASERS AND MASERS

UDC 621.373.826.038.823

ACTIVE MEDIA OF EXCIPLEX LASERS (SURVEY)

Moscow KVANTOVAYA ELEKTRONIKA in Russian Vol 7, No 4(94), Apr 80
pp 677-719

[Article by I. S. Lakoba and S. I. Yakovlenko]

[Text] In recent years, intense research in laser physics has centered around attainment of lasing on electronic transitions of diatomic molecules, which are called exciplexes in photochemistry [Ref. 1]. Exciplexes [from *excited complexes*] are chemical compounds (complexes) of a certain stoichiometric composition that are stable in electronically excited states and are easily dissociated in the ground state unless they are stabilized by external forces [Ref. 2]. An excimer is an exciplex that consists of identical atoms or atomic groups [Ref. 1, 2]. Following the suggestion of Ref. 3, it is natural to call lasers based on transitions of exciplexes and excimers "exciplex lasers."

The promising outlook of exciplex lasers, which is due primarily to their high specific energy characteristics, has led to a great deal of experimental research devoted to studying them. By now, effective amplification has been achieved on transitions of dimers R_2^* of heavy inert gases (R = Xe, Kr, Ar) and mercury Hg_2^* to the ground state, on transitions between electronically excited states of the helium dimer He_2 and monoxides of inert gases, and also on transitions to the ground state of the polyhalides of inert gases RX* (X = F, Cl, Br)[1] and mercury HgX* (X = Cl, Br, I)[2]. Preliminary systematization of rather disconnected information

[1]Except ArBr*. A report on lasing in XeI* [Ref. 4] is apparently due to a misunderstanding.

[2]The classification of HgX, XeF and possibly XeO as exciplexes requires an explanation. According to available data [Ref. 5-7], the energy of dissociation of the ground state of these compounds is much greater than the average energy of thermal motion under ordinary conditions. The instability of HgX and similar molecules is due to the fact that they are free radicals, and therefore quite reactive. However, with respect to structure and properties of excited states, they have much in common with the other exciplexes mentioned here.

relating to the properties of exciplex molecules and laser media based on them has been attempted in survey articles [Ref. 8-18] as experimental material has accumulated. At the present pace of development of new results in this field, the actual material presented in these surveys has become noticeably out of date within one or two years. Besides, most of these surveys deal with either specific exciplex systems or a limited number of general problems of amplification on exciplexes. At present the survey of Ref. 16 might be considered the most extensive in scope, but it contains considerable errors.

The main peculiarity of the active media of exciplex lasers is that a stage of chemical conversion with the participation of electronically excited particles and ions is necessarily a part of the process of molecule formation in the upper working state. In the general case, the relaxation kinetics of exciplex media (with consideration of plasma-chemical and radiation processes) is very complicated, which makes it difficult to analyze the problem of amplification on exciplexes. The solution of this problem requires construction of a sequential theory that gives joint consideration to the electronic state of exciplexes, the plasma chemistry of active media, and the behavior of the amplified emission. As the raw material for this theory we should take the most important experimental facts, which must be singled out, grouped, systematized and preanalyzed at least in general outline. This is the goal followed by our survey.

1. Molecular Terms. Optical Characteristics of Laser Transitions

Among the enumerated exciplexes, the helium dimer is the only one for which the structure of the terms has been established fairly completely with high experimental reliability [Ref. 19, p 198]. By now, quantum mechanical calculations of potential curves have been done for Xe_2 [Ref. 20], Ar_2 [Ref. 21], RO [Ref. 22], RF [Ref. 23], XeX [Ref. 24, 25], HgCl and HgBr [Ref. 26]. A qualitative form of the energy spectrum of mercury compounds is given for example in Ref. 27 (Hg_2) and Ref. 28 (HgX). The potential curves of some exciplexes are shown in Fig. 1. Here we note the low energy level of nucleonic terms for the halides RX* and HgX* due to the fact that the energy of electron affinity of the X atoms is considerable [Ref. 5], while atoms of R* and Hg* are close to the atoms of alkali metals in their capacity to donate electrons[1]. The localization of ionic states is unknown for monoxide molecules RO (according to Ref. 34, emission bands of 150 [ArO*], 180 [KrO*] and 237 nm [XeO] that have been observed correspond to radiative decay of these states). In contrast to the halides, between the ionic F and ground X states of RO there are terms that correlate with excited levels of the oxygen atom. All states are covalent for the dimers He_2^*, R_2^* and Hg_2^* (the electron affinity energy

[1]With this analogy, the authors of Ref. 33 were able to give a good estimate of the emission wavelength of RX* on transitions from the lower ionic state to the ground state, including for molecules with luminescence first observed in Ref. 33 and subsequently by other researchers.

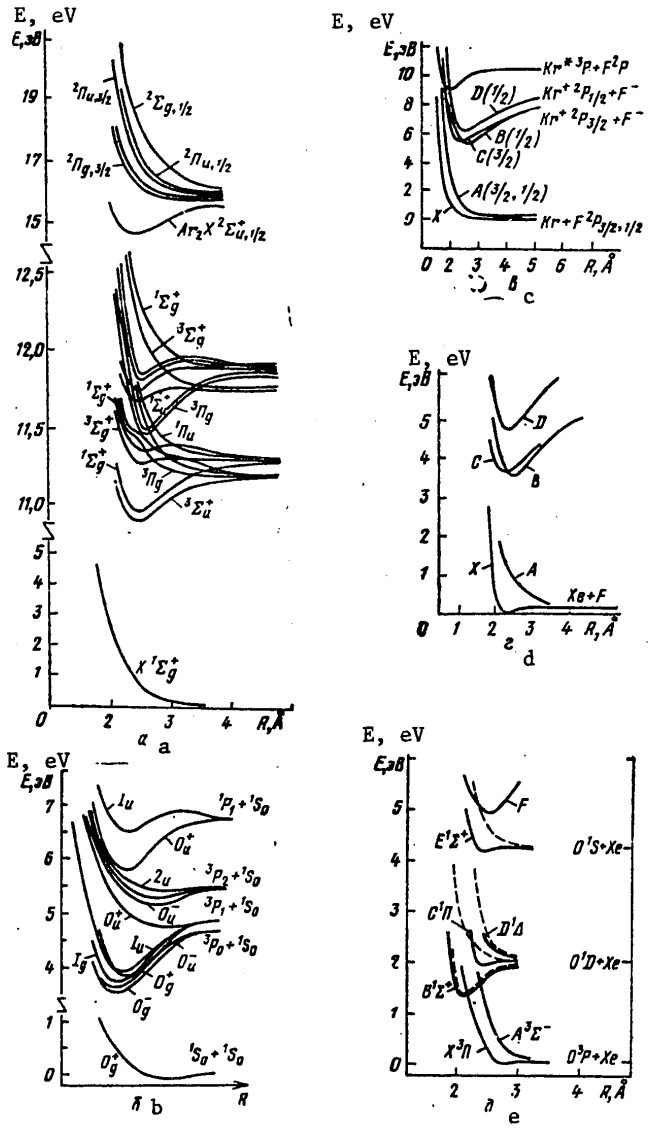

Fig. 1. Potential curves of some exciplexes: a--terms of argon dimer according to Ref. 21, 29, 30 (dimers of xenon, krypton and helium have analogous structure); b--states of mercury dimer according to Ref. 27; c--lower states of the molecule KrF according to calculations of Ref. 23, 24 (XeBr, KrCl, KrBr, ArF and ArCl belong to this type); d--terms of XeF according to Ref. 31 (analogs are XeCl and HgX); e--R-O system based on the example of XeO; solid curves from Ref. 32, broken curves -- Ref. 22

for atoms of R and Hg is close to zero, and possibly even negative [Ref. 5]). The structure of the potential energy curves of the exciplexes determines the characteristic values of possible laser transitions; if we know this structure, we can also get a better idea of the mechanisms and kinetics of relaxation of the corresponding active media.

The gain on molecular electronic transition $b \to a$ can be written as

$$\varkappa = \varkappa_+ - \varkappa_- - \varkappa_{cp}, \quad \varkappa_+ = [1 - (\bar{\sigma}^b_- / \bar{\sigma}_+)]\bar{\sigma}_+ M_b, \tag{1}$$

where $\bar{\sigma}_+$ is the cross section of the working phototransition; $\bar{\sigma}^b_-$ is the cross section of absorption of a light quantum on a transition from the upper working state to one lying above it (for example as a result of photoionization)[1]; M_b is the population of the upper working state; κ_- is the coefficient of absorption on the transition reverse to the working transition; κ_{cp} is the coefficient of absorption by impurities and other components of the active medium.

The expressions for $\bar{\sigma}_+$ and κ_- differ considerably in the case of bound-bound and bound-free transitions [Ref. 35, §§1, 22]. For photodissociative and the reverse (photoassociative) transitions, we have [Ref. 35, 36]

$$\bar{\sigma}_+ = (\lambda_0^2/4) A Q_\omega, \tag{2}$$

where λ_0 is the wavelength of the amplified emission; A is the probability of spontaneous transition; Q_ω is the Franck-Condon factor, i. e. the square of the integral of overlap of the nuclear wave functions (here the wave function of the continuous spectrum is normalized to the δ-function of frequency ω, so that Q_ω has dimensions of time);

$$\varkappa_- = \bar{\sigma}_+ N_A N_B (2\pi\hbar^2/\mu T)^{3/2} \Sigma (2l+1) \exp[-(E_{nl} - \hbar\omega_0)/T], \tag{3}$$

where N_A, N_B are the concentrations of atoms A and B that form exciplex AB; μ is the reduced mass of the molecule; T is gas temperature; n, l are the vibrational and rotational quantum numbers, E_{nl} is the energy of excitation of the exciplex to the vibrational-rotational state, reckoned from the electronic ground state of the atoms; $\hbar\omega_0$ is the energy of a quantum of the working radiation.

The Franck-Condon factor can usually be evaluated from the formula

$$Q_\omega \approx 1/\Delta\omega_{\text{разм}}, \tag{4}$$

---

[1]Just such a possibility of absorption of amplified emission by the upper working state is typical of electronic transitions of molecules, since they have broad absorption bands. As a rule, this effect does not inhere in atomic and vibrational-rotational transitions.

where the effective half-width of the line $\Delta\omega_{разл}$ is obtained by projecting the points of reversal of the vibrational level of the bound state onto the dispersion term, and from there onto the energy axis. Comparison with experimental data shows that Q_{ω}^{-1} and the observed half-width of the spontaneous emission band are close in order of magnitude.

For bound-bound transitions, only the superposed components of the vibrational-rotational structure are added:

$$\varkappa_+ = \sum_{n,\ l} \sigma_+^{nl}(\omega) M_{bnl} \approx \bar{\sigma}_+ M_b; \tag{5a}$$

$$\varkappa_- = \sum_{n,\ l} \sigma_-^{nl}(\omega) M_{anl} \approx \bar{\sigma}_- M_a; \tag{5b}$$

$$\bar{\sigma}_+ g_b = \bar{\sigma}_- g_a, \tag{5c}$$

where the subscripts b and a denote combining electron states; g_b and g_a are their statistical weights; $\bar{\sigma}_+$, $\bar{\sigma}_-$ are the effectively averaged cross sections. The cross section of the phototransition is written analogously to (2):

$$\bar{\sigma}_+ \approx \frac{\lambda_0^2}{4} A \frac{1}{\Delta\omega_{ab}}, \tag{2a}$$

but the effective half-width of the strongest line in band $\Delta\omega_{ba}$ is much less than $\Delta\omega_{разл}$.

The shape of the spontaneous emission spectra depends on the dipole moment of the transition and the relative location of the combining terms. If a photodissociative transition takes place to a steep section of the repulsion term and the energy of a vibrational quantum $\hbar\omega_{кол}^{b}$ of the upper working state is less than the dispersion energy for the atoms $E_p = E_{00} - \hbar\omega_0$, then the smooth curve for the distribution of spectral intensity is unimodal and asymmetric. This is typical for example of R_2^*. On the other hand if $\hbar\omega_{кол}^{b} \gtrsim E_p$, then, as shown in Ref. 37, oscillations of intensity may show up in the spectrum that are experimentally observed (in particular for KrF [Ref. 33] and ArCl [Ref. 34]). In either case, continuous tuning of the lasing wavelength is possible. The spectra of bound-bound transitions always have a more or less complicated structure, and amplification is frequently attained simultaneously in several vibronic bands.

While the absolute values of the cross sections of the induced radiation for bound-bound transitions as a rule are greater than on photodissociative transitions, amplification is not always attained more easily. Table 1 summarizes values of A and $\bar{\sigma}_+$ for exciplex transitions on which lasing is realized. It should be noted that these numerical characteristics are rough approximations.

TABLE 1

Characteristics of laser transitions of diatomic exciplexes

Molecule Молекула	Transition Переход	λ_0, nm, нм	A, c^{-1}	$\bar{\sigma}_{+}$, $см^2$
Xe_2	$(O_u^+, I_u) \to XO_g^+$	172	(2 [38] — 5 [39, 40])×$\times 10^{7}$ a)	(2 [41] — 7 [42])×$\times 10^{-18}$
Kr_2	»	146	$2{,}5 \cdot 10^8$ (O_u^+); $3 \cdot 10^6$ (I_u) [43, 44]*)	—
Ar_2	$(^1\Sigma_u^+, {}^3\Sigma_u^+) \to X^1\Sigma_g^+$	126	10^8 $(^1\sum_u^+)$; 10^7 $(^3\sum_u^+)$ [45]	$1{,}5 \cdot 10^{-18}$ a a)
$He_2^{***})$	$d^3\Sigma_u^+ \to b^3\Pi_g$	640	$\gtrsim 10^7$ [46]	—
Hg_2	$I_u \to XO_g^+$	335	$4{,}5 \cdot 10^6$ [47]	$0{,}97 \cdot 10^{-18}$ [47]
XeF	$B\,(1/2) \to X\,(1/2)$ $(B^2\Sigma_{1/2} \to X^2\Sigma_{1/2})$	353 351 349	(5,1 [48, 49] — —5,5 [50, 51]) $\cdot 10^7$; $8 \cdot 10^7$ [17, 25]	(2 [52] — 5 [53])×$\times 10^{-16}$
XeF	$C\,(3/2) \to A\,(3/2)$	470—480	$6 \cdot 10^6 - 10^7$ [25]	$5 \cdot 10^{-18}$ [132]
KrF	$B\,(1/2) \to X\,(1/2)$	249,5 248,5	$1{,}5 \cdot 10^8$ [23, 54]; $1 \cdot 10^8$ [55, 56]	$6 \cdot 10^{-17}$ [57]; $2{,}7 \cdot 10^{-16}$ [58]; $2{,}5 \cdot 10^{-16}$ [17]
ArF	» »	193	10^8 [59]; $2 \cdot 10^8$ [24]	$2{,}9 \cdot 10^{-16}$ [17]
XeCl	» »	307—308	$9 \cdot 10^7$ [25]	$4{,}5 \cdot 10^{-16}$ [17]
KrCl	» »	222	—	—
ArCl	» »	175	—	—
XeBr	» »	282	$5{,}7 \cdot 10^7$ [60]	$1{,}5 \cdot 10^{-16}$ [61]
KrBr	» »	206	—	—
XeO	$E^1\Sigma^+ \to B^1\Sigma^+$	538—544	10^{+6} [62]	10^{-17} [63]
KrO	» »	558	—	—
ArO	» »	558	$2{,}6 \cdot 10^5$ [62]	$2 \cdot 10^{-18}$ [64]
HgCl	$B^2\Sigma_{1/2} \to X^2\Sigma_{1/2}$	558	$4{,}5 \cdot 10^7$ [65]	$4{,}5 \cdot 10^{-16}$ [65]

Table 1 (continued)

Molecule Молекула	Transition Переход	nm λ_0, нм	A, c^{-1}	$\bar{\sigma}_+$, см²
HgBr	$B^2\Sigma_{1/2} \rightarrow X^2\Sigma_{1/2}$	502—504, 498	$4{,}3\cdot10^7$ [66]	$2{,}4\cdot10^{-15}$ [67]
HgJ	» »	443—445	$3{,}7\cdot10^7$ [66]	—

*) The effective values of A were found at rather high pressures. Typical times of radiative decay of the lower states of R_2^* show considerable dependence on the density of the gas (see for example Ref. 39, 68-70). This is due mainly to strong collisional mixing of populations of O_u^+ and I_u [Ref. 71]. Many researchers feel that the upper laser state of R_2^* is $O_u^*(^1\Sigma_u^+)$ alone.

**) The following values were used in the estimation: $A = 3\cdot10^7\ s^{-1}$, $\Delta\omega_{разл} = 0.5$ eV [Ref. 12].

***) Under the same conditions, less intense lasing has been achieved [Ref. 72] on other bound-bound transitions of He_2^*: $\lambda_0 = 400$, 403, 454 and 513 nm.

For excimers R_2^*, the corrections $\bar{\sigma}_-^b/\bar{\sigma}_+$ in (1) are due to photoionization. Usually photoionization can be disregarded as a consequence of the greater width of the photoionization band as compared with the photodissociation band. The problem of the ratio between the photoionization and photodissociation cross sections was qualitatively discussed in Ref. 73. According to calculations of Ref. 74, the cross section for photoionization of $Ar_2^*\Sigma_u^+$ at $\lambda = 126$ nm is about $4\cdot10^{-19}$ cm^2, i. e. it is considerably less than the estimated [Table 1] photoionization cross section. Transitions to repulsion or bound states lying above b are more likely than photoionization transitions. The effect that they have on the shape of the lasing spectra and gain is considerable for exciplexes that emit in the relatively long-wave region. In Ref. 58, 75, a continuous band was observed, and also a set of narrow absorption lines between the peaks (248.5 and 249.5 nm) of stimulated emission of KrF*, belonging to transitions from the working term to the covalent term, correlating with $Kr^*(^3P) + F$. In Ref. 28 the authors observed formation of highly excited atoms of $Hg(7^3S_1)$ accompanying laser photolysis of HgX_2 vapor. This was attributed to dissociative excitation of $HgX^*(B^2\Sigma_{1/2})$ due to absorption of self-radiation. The authors of Ref. 76 used a similar argument to explain failure to achieve lasing on the proposed transition $O_u^+ - XO_g^+$ of the mercury dimer ($\lambda = 485$ nm) [1].

[1]It can be concluded from Ref. 27 that there is no state O_u^+ in the group of lower states of Hg_2^*, and emission of the 485 nm band corresponds to photodissociative decay of trimers Hg_3^* rather than the dimers.

Losses of amplified radiation determined by κ_{cp} will be briefly discussed in Section 4.

2. Experimental Conditions for Achieving Lasing

Tables 2 and 3 give some data on experiments in which amplification has been achieved on diatomic excimers and exciplexes. Since problems of organizing optical feedback are nonspecific for exciplex lasers, we have given information mainly that determines the properties of the active media. Brief explanations are given below.

2.1. Pumping method. The use of high-current relativistic (subrelativistic) electron beams as the energy source is the most universal[1] and productive method of producing exciplex active media. Lasing (depending on the nature of the exciplex and a number of other factors) is realized with the following typical beam parameters: electron energy ~0.1-2 Mev, current density ~6-10^3 A/cm^2 (total current up to 150 kA), current pulse duration ~2-1400 ns. Let us note that the capabilities of present-day electron beams are not restricted to these limits (see for example Ref. 182).

Electric discharge methods are used to excite laser transitions corresponding to large values of $\tilde{\sigma}_+$ (RF*, HgX*): a self-maintained transverse discharge (TE-lasers) and its modifications utilizing preionization (electric, light beam, electron beam, x-rays [Ref. 151], radioisotope emission [Ref. 183]); a discharge in the traveling wave mode (this technique has been used to achieve amplification on ArCl* and KrBr* [Table 3] for which the $\tilde{\sigma}_+$ are relatively small); capacitive discharge [Ref. 126]. Series electric-discharge lasers have been developed [Ref. 184] that operate on XeF*, KrF* and ArF*. The characteristics of exciplex electric discharge lasers can be widely varied by modifying the design, but their capabilities are limited by the development of instabilities with breakdown of dense gases (discharge pinching, arc ignition and so on).

Arrangements for optical pumping of exciplexes [Ref. 185-189] were being discussed even before the development of the first exciplex lasers. For a long time, this method was used to achieve lasing only on bound-bound transitions of RO, XeF, HgBr and HgCl. Recently amplification has been realized on the photodissociative transition C(3/2) → A(3/2) of the molecule XeF [Ref. 133, 134].

The possibility in principle of nuclear pumping of excimers and exciplexes has been demonstrated in experiments [Ref. 85, 190]. When a nuclear charge is exploded, irtense superluminexcence of Xe_2^* is observed in nearby tubes containing dense xenon [Ref. 85]. Amplification in XeF*

[1]There is no basis for assuming that beam pumping is ineffective in the case of KrBr*, ArO* and HgI* since no serious attempts have been made to trigger lasers as yet by an electron beam in these exciplexes.

TABLE 2

Parameters of excimer lasers

Composition Состав среды	N, см$^{-3}$	τ_0, нс	Q, МВт/см^2	$\Delta\tau$, нс	τ, нс	$\frac{\Delta\lambda_{инд}}{\Delta\lambda_{сп}}$	$W_{пик}$, кВт	$\varepsilon_д$, Дж	L, см	$\varkappa$, см$^{-1}$	$\eta_{ср}$, %	Remarks Примечания	Ref. Литература
Molecule Молекула Xe_2													
Xe	$(3,8—8,5)\cdot10^{20}$	2,5	~100	2—12	3	0,12	—	—	2	—	—	—	[77]
Xe	$(4—6)\cdot10^{20}$	50	~30	20—40	30—60	~0,3	—	—	15	—	~1	—	[41, 78]
Xe	$(2—6)\cdot10^{20}$	40	≥100	10	~20	0,1	—	—	5	—	—	Угловая расходимость <5 мрад (1)	[79]
Ar:Xe≈0—9	$\leq1,7\cdot10^{21}$	—	—	—	—	—	—	—	—	—	—	С добавлением аргона повышается $\varepsilon_д$; максимум усиления достигается при более высоких давлениях (2)	[80]
Xe	$(2,5—6)\cdot10^{20}$	100	$2\cdot10^3$	>7	~10	0,23	$2\cdot10^4$	0,1	9	—	~1	—	[81]
Xe	$>3\cdot10^{20}$	20	—	—	—	0,07	—	0,1	9	—	—	Прогорели зеркала резонатора (3)	[82]
Xe	$4\cdot10^{20}$	20	~10	~5	~15	0,6	—	—	20	0,2	—	Ленточный пучок (4)	[83]
Xe Kr:Xe≈0—3	$\leq7,6\cdot10^{20}$	2,5	—	6—8 2	4—6 6—8	0,13 0,16	50	—	3	—	—	Для Xe оптимальное $N=4,7\cdot10^{20}$ см$^{-3}$; в смесях максимум $W_{пик}$ не достигнут (5)	[84]

For explanation of column headings and translation of the remarks see the page following the Table.

Table 2 (continued)

Composition Состав среды	N, $см^{-3}$	τ_0, нс	Q, МВт/$см^2$	$\Delta\tau$, нс	τ, нс	$\frac{\text{ширина}}{\Delta\nu}$	$W_{пик}$, кВт	$\varepsilon_д$, Дж	L, см	$\varkappa$, $см^{-1}$	$\eta_{др}$, %	Remarks Примечания	Ref. Литература
Xe	$(2,8—5,7)\cdot10^{20}$	—	—	—	—	—	—	10^{-7}	30	0,1—0,29	—	Источник накачки—γ-излучение ядерного взрыва; при $N<2,8\cdot10^{20}$ $см^{-3}$ усиления не наблюдалось (6)	[85]
Ar:Xe≳0—2 He:Xe≳0—2	$>4\cdot10^{20}$	50	~30	~40	~25	0,15	≳40	—	2,5	—	—	С повышением температуры газа интенсивность генерации падала; смеси эффективнее, чем чистый Xe (7)	[86]
Xe Xe + He	$3,5\cdot10^{20}$	2,5	10^3	—	3,5	0,09	10^3	—	~10	0,25	—	При $\tau_0=2,5$ нс интенсивность генерации у смесей меньше, а при $\tau_0=50$ нс больше, чем у Xe (8)	[87]
Xe; Ne:Xe≳2 Ar:Xe≳2	$\geqslant4\cdot10^{20}$	60	~100	≲5	10—90	—	$7,5\cdot10^4$	0,76	10	(0,2) (0,17) (0,2)	—	—	[88]
Xe	$(3,8—5,5)\cdot10^{20}$	3,0	—	8	4	—	10	—	2	—	—	Перестройка длины волны в пределах 169,5—174,5 нм (9)	[89]
Xe	$3,5\cdot10^{20}$	5	~10^3	—	3	0,09	$3\cdot10^3$	0,009	14	—	0,1	Перестройка длины волны в пределах 169—175 нм (10)	[90]
Ar—Xe	$(2—6)\cdot10^{20}$	10	70	—	—	0,06	—	0,2	4	—	—	— (11)	[91]
Xe	$3\cdot10^{20}$	25—30	100	—	8	—	$1,5\cdot10^4$	0,09	12	—	—	Чистота газа 99,99%	[92]
Xe	$4,2\cdot10^{19}$	1000	≳0,2	800	200	0,12	60	—	100	≳0,0005	—	—	[93]
Xe	$(1—2)\cdot10^{20}$	20	~10	5	10	0,25	~10^4	0,1	20	—	1,6	—	[94]

Table 2 (continued)

Composition Состав среды	N, $см^{-3}$	τ_0, нс	$\dot{Q}$, $МВт/см^3$	$\Delta\tau$, нс	τ, нс	$\frac{\Delta\lambda_{ген}}{\Delta\lambda}$	$W_{пик}$, кВт	$\varepsilon_д$, Дж	L, см	$\varkappa$, $см^{-1}$	$\eta_{ср}$, %	Remarks Примечания	Ref. Литература
Xe	$1,1 \cdot 10^{20}$	40	—	—	15	—	$6 \cdot 10^4$	—	50	0,05	2,5	(12) Очистка газа после каждого импульса повышает лазерный выход	[95]
Molecule Молекула Kr_2													
Kr	$(3,8—9,5) \cdot 10^{20}$	—	—	—	~10	0,06	—	—	—	—	—	(13) Линейный рост $W_{пик}$ с повышением N	[80]
Molecule Молекула Ar_2													
Ar	$5,7 \cdot 10^{20}—2 \cdot 10^{21}$	60	~100	15—27	4—15	0,18	$5 \cdot 10^4$	—	10	—	—	(14) Положение максимума в спектре зависит от давления	[96]
Molecule Молекула He_2													
He	$8 \cdot 10^{19}$	3	—	20	5	—	—	—	—	0,04	—	—	[46]
Molecule Молекула Hg_2													
Hg	$3,9 \cdot 10^{18}$	~20	~100	~200	~300	~1	—	—	24,5	0,0055	—	$400 < T \leqslant 520°C$	[47]

See next page for explanation of column headings and translation of the remarks.

Explanation of column headings for Table 2:

N--density of particles of the medium, cm^{-3}
τ_0, $\dot{Q}$--pumping duration and specific power, ns and MW/cm^3
$\Delta\tau$, τ--amplification delay and duration, ns
$\Delta\lambda_{СП}$, $\Delta\lambda_{ИНД}$--bandwidths of spontaneous and induced emission respectively
$W_{ПИК}$--peak power, kW
$\varepsilon_Л$--energy of laser radiation, J
L--length of the active region, cm
κ--gain, cm^{-1}
$\eta_{ср}$--efficiency of energy conversion in the medium, %
T--gas temperature
Numbers in parentheses show authors' estimates of κ. An electron beam was used as the pumping source everywhere except Ref. 85.

Key to translation of remarks in Table 2:

1--Angular divergence less than 5 mrad
2--Laser radiation energy is increased with the addition of argon; maximum gain is realized at higher pressures
3--The resonator mirror was burned through
4--Ribbon beam
5--Optimum particle density for Xe is $N = 4.7 \cdot 10^{20}$ cm^{-3}; maximum peak power is not attained in mixtures
6--The pumping source was gamma radiation of a nuclear explosion; amplification was not observed at $N < 2.8 \cdot 10^{20}$ cm^{-3}
7--Lasing intensity falls off with increasing gas temperature; mixtures are more efficient than pure Xe
8--At $\tau_0 = 2.5$ ns the lasing intensity is lower for mixtures, and at $\tau_0 = 50$ ns it is greater for the mixtures than for Xe
9--Tuning of wavelength over a range of 169.5-174.5 nm
10--Tuning of wavelength over a range of 169-175 nm
11--Gas purity 99.99%
12--Purification of gas after each pulse increases laser output
13--Linear increase in peak power with increasing particle density
14--The position of the maximum in the spectrum depends on pressure

---

was achieved in Ref. 190. A tube containing a mixture of NF_3-Xe-Ar covered inside with a thin layer of boron (isotope ^{10}B) was exposed to a neutron flux from a pulsed reactor. The direct source of pumping energy was the nuclear reaction $^{10}B(n,\alpha)^7Li$.

In Ref. 191 a proton beam was first used to stimulate an exciplex laser transition. Here are some of the characteristics of this laser: proton energy ~450 keV, current density ~10 A/cm^2, $\tau_0 \sim 50$ ns, mixture NF_3:Xe:Ar = 1:5:194, $p \sim 1$ atm, $\dot{Q} \gtrsim 1.5$ MW/cm^3, $\tau \sim 10$-20 ns, $\varepsilon_Л$ up to ~0.05 J, $L \sim 7.5$ cm, $\kappa \lesssim 0.052$ cm^{-1}, $\eta_{ср}$ up to 2.7%.

TABLE 3

Parameters of exciplex lasers

Pumping method / Способ накачки	Composition / Состав среды	p, атм	τ_0, нс	Q, МВт/см²	$\Delta\tau$, нс	τ, нс	$W_{имп}$, кВт	$\varepsilon_д$, Дж	L, см	$\varkappa$, см$^{-1}$	$\eta_{ор}$, %	Remarks / Примечания	Ref. / Литература
	XeF. Молекула XeF, переход $B \to X$ molecule, transition $B \to X$												
ЭП	NF_3:Xe:Ar=1:25:250	1,7	20	≲6	—	100	500	0,08	10	—	0,5	λ_0=351,1; 353,1 нм	[97]
ЭП	F_2:Xe:Ar=1:3:996	~4	100	~1	50	50	600	—	15	—	0,01	—	[52]
ТЕ	NF_3:Xe:He=1:3:196	0,4—1,3	20	—	30	20	—	≥0,007	100	—	—	λ_0=351,1; 353,1 нм	[96]
ТЕ	NF_3:Xe:He=1:3:100	0,26—0,53	10	~0,1	~40	~40	25	0,001	50	0,01	1,2	λ_0=353; 351 и 349 нм; частота повторения 20 Гц (1)	[99]
ТЕ	NF_3:Xe:He=1:4:100	0,1—1,5	—	~1	—	6	$2,8 \cdot 10^3$	0,017	30	—	~1	Частота повторения до 100 Гц (2)	[100]
Р-эл	SF_6:Xe:He=0,1:1:100	1—8	—	—	—	3—3,5	200	—	60	—	0,02	Оптимальное давление ~3 атм (3)	[101]
Р-эл	NF_3:Xe:He=1:1:81	~1	8	~1	—	4—20	$2,5 \cdot 10^4$	≤0,1	90	—	~1	Предионизация увеличивает выход лазерного излучения примерно на 30% (4)	[53]
ТЕ	NF_3:Xe:He=1:2:60	0,6	10	~10	—	6—40	10^4	0,006	50	—	0,5	—	[102]
ТЕ	NF_3:Xe:He=1:3:100	0,5	>2	—	—	≤2	—	~0,001	50	—	~0,1	Режим синхронизации мод (5)	[103]
Р-ЭП	NF_3:Xe:Ar=1:4:995	4	400	~1	~50	~50	—	0,01	20	—	0,3	(6) Лазерный импульс начинается до включения разряда; разряд становится неустойчивым через ~80 нс	[104]

For explanation of column headings and translation of the remarks see the page following the Table

Table 3 (continued)

Pumping method / Способ накачки	Composition / Состав среды	p, атм	τ_0, нс	$\dot{Q}$, МВт/см²	$\Delta\tau$, нс	τ, нс	$W_{имп}$, кВт	$e_д$, Дж	L, см	$\varkappa$, см$^{-1}$	$\eta_{ср}$, %	Remarks / Примечания	Ref. / Литература
ЭП	NF_3 (F_2):Xe:Ar=1:3:100	≤8	15	~10	25	15	—	$4\cdot10^{-5}$	3	—	—	—	[105]
Р-УФ	F_2(NF_3):Xe:He=3:10:987	≤2	—	≥1	—	—	—	0,065	60	—	≥1	—	[106]
ТЕ	NF_3:Xe:He=1:3,5:220	0,7	—	—	—	15	—	0,002	36	—	—	Генерация на шести электронно-колебательных переходах (7)	[107]
ТЕ	NF_3:Xe:He=2:5:500	~2	20	~0,3	—	~5; ≤0,2	50	—	68	0,128	—	Усиление сверхкороткого импульса третьей гармоники неодимового лазера (8)	[108]
ЭП	NF_3 (F_2):Xe:Ar=0,12:0,38:99,5	2,5	1400	~0,2	300	1000	10^4	0,3	100	0,02	0,5	—	[109]
ТЕ	F_2:Xe:He=4:3:193	0,6	10	~1	—	—	$5\cdot10^3$	0,05	87	—	~1	Достигнута расходимость ≤0,2 мрад (9)	[110]
ТЕ	NF_3:Xe:He=1:3:100	0,4—1	—	—	—	—	—	0,0064	50	—	—	Частота 200 Гц; средняя мощность 52 мВт (10)	[111]
Р-эл	NF_3:Xe:He=1:3:2700	≤10	<35	—	—	20—100	—	0,29	60	—	—	Перестраиваемый лазер: λ_0=353; 351; 348 нм; оптимальное давление ~5 атм (11)	[112]
Р-ЭП	NF_3—Xe—Ar	~1	1000	≤0,1	50—900	500	—	—	50	0,03	—	Порог генерации достигается при удельной мощности накачки $\dot{Q}\geq20$ кВт/см³ (12)	[113]

Table 3 (continued)

Pumping method / Способ накачки	Composition / Состав среды	p, атм	τ_0, нс	Q, МВт/см²	$\Delta\tau$, нс	τ, нс	$W_{имп}$, кВт	$\varepsilon_д$, Дж	L, см	$\varkappa$, $см^{-1}$	$\eta_{ср}$, %	Remarks / Примечания	Ref. / Литература
Р-Эл	F_2:Xe:He=1:24:3975	1,15	—	—	—	100	—	—	82	0,001	—	Усилитель (13)	[114]
Р-УФ	—	2	100	—	30	60	—	0,18	100	—	—	—	[115]
Р-УФ	NF_3:Xe:He=1:4:250 F_2:Xe:He=1:4:500	⩽2	20—25	⩽50	20	15	—	—	100	0,3 0,1	—	Составы смесей в варьировались в пределах 1:(2—15):(50—2000) (14)	[116]
ЭП	NF_3:Xe:He=1:3, 3:1660	⩽5	1000	0,5	—	—	—	~1	100	0,01	1,8	При замене Ar неоном $\varepsilon_д$ и $\eta_{ср}$ возросли более чем в 3 раза (15)	[117]
Р-ЭП	SF_6:Xe:Ar=0,6:1:150	2	5000	—	~100	~1000	—	0,18	100	—	1,44	—	[118]
ТЕ	NF_3:Xe:He=1:1:100	0,4—1	—	—	—	10—15	—	0,024	37	—	0,9	—	[119]
Р-УФ Р-ЭП	NF_3:Xe:He=4:14:982 NF_3:Xe:Ar=1:10:80	1	— 70	—	—	— 50	—	0,001 0,12	100 36	—	—	Расходимость ~1 мрад (16)	[120]
ОН	XeF_2:N_2:Ar=0,4:7:93	1	—	—	—	~2000	—	0,001	70	—	—	— (17)	[121]
ЭП	NF_3—Xe—Ar; NF_3:Xe:Ne=1:4:1000	⩽3	500—5000	~10	—	400	20	—	14	—	—	При замене аргона неоном выходная мощность возросла в 3 раза; снизился порог генерации	[122]
ТЕ	NF_3:Xe:He=1:3:500	1—7	20	⩾10	—	—	—	0,36	100	—	—	—	[123]
ТЕ	NF_3:Xe:He=1:3:200	0,9	60	3	—	20	30	0,006	30	—	0,25	Частота повторения до 500 Гц; средняя мощность до 3,3 Вт; прокачка рабочей смеси (18)	[124]
Р-ЭП	NF_3:Xe:Ne=1:3:1300	1—5	1000	0,2	—	1000	—	—	—	0,0185	1,75	Увеличение лазерного сигнала при наложении электрического поля (19)	[125]

Table 3 (continued)

Pumping method / Способ накачки	Composition / Состав среды	p, атм	$\tau_н$, нс	Q, МВт/см²	Δτ, нс	τ, нс	$W_{имп}$, кВт	$\varepsilon_д$, Дж	L, см	$\varkappa_{-1}$, см$^{-1}$	$\eta_{ср}$, %	Remarks / Примечания	Literature type / Литература Ref.
												рического поля осабсвует с ростом давления. p=3 атм. Сильная зависимость от концентрации NF_3 (20)	
ЕР	NF_3:Xe:Ne:He= 1:2:48,5:48,5	0,2—1	200	~10	—	10	—	$3,5\cdot10^{-6}$	10	—	1	При замене He или Ne аргоном генерации нет. Резонатор волноводного типа. Оптимум при p~100 мм рт. ст. (21)	[126]
Р-УФ	NF_3:Xe:He=1:3,5:100	1	—	—	—	— 2—	—	0,011	≤77	0,37	0,8	Генерация в режиме свеpхизлучения (22)	[127]
Р-УФ	NF_3:Xe:He=1:3:100	0,4—1,2	—	—	—	— 30	—	0,025	50	0,2	—	—	[128]
Р-ЭП	NF_3:Xe:Ar=1:10:2220	1	—	~0,1	—	1000	—	0,18	100	—	0,5	Прекращение действия пучка сопровождалось контрагированием разряда и срывом генерации (23)	[129]
ТЕ	NF_3:Xe:He=1:3:800	1—7	10—20	20	—	—	—	0,1	60	—	0,5	Частота повторения до 50 Гц (24)	[130]
ЭП	NF_3:Xe:Ne=1:8:994	2; 3	900	~0,1	—	750	—	≤25	100	—	до 5,4	$\eta_{ср}$ немонотонно зависит от исходной температуры смеси; максимум $\eta_{ср}$ для p=3 атм получен при T=150K (25)	[131]

Table 3 (continued)

Pumping method / Способ накачки	Composition / Состав среды	p, atm / p, атм	τ_0, ns / τ_0, нс	$\dot{Q}$, MW/cm² / $\dot{Q}$, МВт/см²	$\Delta\tau$, ns / $\Delta\tau$, нс	τ, ns / τ, нс	W_{max}, kW / $W_{макс}$, кВт	$\varepsilon_д$, J / $\varepsilon_д$, Дж	L, cm / L, см	$\varkappa_i$, cm^{-1} / $\varkappa_i$, см$^{-1}$	η_{op}, % / $\eta_{ор}$, %	Remarks / Примечания	Ref. type / Литера тура
					Молекула XeF, переход C→A XeF molecule, transition C→A								
EP / ЭП	NF_3:Xe:Ar; 10—25 мм рт. ст. NF_3+2—3 мм рт. ст. Xe mm Hg	16	2	—	~10	~10	—	—	—	—	—	При λ=488 и 476 нм зарегистрировано усиление до 8% за один проход резонатора, энергосъем 0,1 Дж (26)	[132]
OH	XeF_2:N_2:Ar=1:80:500 XeF_2:N_2=1:230	1,5 0,6	~10^4	⩾0,05	—	~1500	—	0,004	70	—	—	Накачка излучением открытого разряда; λ_0=470 нм; $\Delta\lambda_{изл}$=30 нм (27)	[133]
OH	XeF_2+Ar; 1—4 мм рт. ст. XeF_2 mm Hg	3	1000	—	400	500	—	~0,001	—	$4\cdot10^{-3}$	—	Источник накачки — сверхзвуковая струя Xe_2^*, λ_0=480 нм; $\Delta\lambda_{изл}$=12 нм. Добавление SF_6 увеличивает лазерный выход (28)	[134]
					Молекула KrF Molecule								
EP / ЭП	F_2:Kr:Ar=1:10:989	1,3—4,2	100	⩽1	20	100	—	0,008	15	—	0,4	—	[135]
EP / ЭП	F_2:Kr:Ar=1:25:500	4,2	50	⩽1	—	50	$1,15\cdot10^3$	5,6	40	—	~3	λ_0=248,4 и 249,1 нм (29)	[136]
P-EP / Р-ЭП	F_2:Kr:Ar=1:20:979	~1	100	1,6	100	⩽90	—	0,006	20	—	0,19	—	[137]
EP / ЭП	NF_3:Kr:Ar=1:130:1300	2,25	125	~1	—	10	—	0,1	—	—	1	—	[138]
TE	NF_3:Kr:He=1:50:500	0,5—0,9	10	15	—	25	32	0,008	50	—	0,05	λ_0=248,5 и 249,5 нм (30)	[139]
EP / ЭП	F_2:Kr:Ar=1:25:350	~2	55	3,5	~20	~50	$1,9\cdot10^3$	108	180	—	~3	—	[140]
TE	NF_3:Kr:He=1:50:500	1,1	—	~1	—	4	10^3	0,004	30	—	0,4	Частота повторения до 100 Гц (31)	[100]
P-EP / Р-ЭП	SF_6:Kr:He=0,1:1:100	1—8	—	—	—	1,5—2	$2\cdot10^3$	—	60	—	0,15	Выходная энергия растет с давлением (32)	[101]

Table 3 (continued)

Pumping method Способ накачки	Composition Состав среды	p, атм	$\Delta\tau$, нс	$\dot{Q}$, МВт/см²	τ, нс	τ, нс	$W_{имп}$, кВт	$\varepsilon_{д}$, Дж	L, см	$\varkappa$, $см^{-1}$	$\eta_{ср}$, %	Remarks Примечания	Literature type Литература	Ref.
Р-эл	NF_3:Kr:He = 0,1:(2—10)	0,6—1,1	—	~4	—	25	$1,5 \cdot 10^8$	0,03	90	—	0,3	Предыонизация увеличила лазерный выход на 50% (33)	[53]	
ТЕ	NF_3:Kr:Ar = 1:25:3500	0,9	—	~10	—	30	55	0,0016	~50	—	0,06	Два импульса генерации (34)	[102]	
Р-УФ	F_2:Kr:He = 3:150:847	≤2	400	≥1	—	—	—	0,13	60	—	1,3	—	[106]	
ТЕ	NF_3—Kr—He	1,2	—	—	—	17	—	0,0005	36	—	—	$\Delta\lambda_{осц}/\Delta\lambda_{инд} \sim 7$	[107]	
ТЕ	F_2:Kr:He = 1:6:93	0,8	10	~1	—	10	$5 \cdot 10^8$	0,05	87	—	~1	Расходимость ≤0,2 мрад (с нестабильным резонатором) (35)	[110]	
Р-ЭП	F_2—Kr—Ar	~1	1000	~0,1	~800	500	—	—	50	—	—	Порог генерации при $\dot{Q} \geq 20$ кВт/см² (36)	[113]	
ЭП	F_2:Kr:Ar = 1:20:300	~3	—	—	—	300	—	—	22	0,0044	—	—	[58]	
Р-эл	F_2:Kr:He = 1:30:370	1	—	—	—	110	—	—	82	0,002	—	Усилитель (37)	[114]	
Р-УФ	F_2—Kr—He	2	100	—	30	60	—	0,3	100	—	—	Состав менялся (38)	[115]	
Р-УФ	F_2:Kr:He = 4:100:900	1,3	—	—	—	20	—	0,1	100	—	—	Обнаружено поглощение излучения молекулой CF_4 в полосе генерации (39)	[141]	
ЭП	F_2:Kr:Ar = 1:15:550	35	70	~10	—	—	$1,5 \cdot 10^4$	1,2	20	—	3	— (40)	[142]	
ТЕ	SF_6: NF_3: N_2F_4:Kr:He = (0,4—0,7):16:2250	~3	—	~10		7—10	$2,5 \cdot 10^8$	0,02	80	—	0,2	Наиболее эффективным фторагентом является N_2F_4	[143]	

Table 3 (continued)

Pumping / Накачка	Composition / Состав среды	p, atm / p, атм	τ_0, ns / τ_0, нс	Q, MW/cm² / Q, МВт/см²	$\Delta\tau$, ns / $\Delta\tau$, нс	τ, ns / τ, нс	W_{max}, kW / $W_{макс}$, кВт	$\varepsilon_д$, J / $\varepsilon_д$, Дж	L, cm / L, см	$\varkappa$, cm^{-1} / $\varkappa$, см$^{-1}$	$\eta_{ср}$, %	Remarks / Примечания	Ref. Type / Литера Тип
ТЕ	$NF_3-Kr-He$	—	—	—	—	—	—	0,03—0,13	—	—	1,3	Частота до 400 Гц; средняя мощность до 3,3 Вт (41)	[15]
Р-УФ	F_2:Kr:He=1:18:1500	≤6	—	—	—	17—20	—	0,6	60	—	0,5	—	[144]
Р-УФ	$F_2-Kr-He$	1	70	—	—	25	—	0,1	60	—	—	Перестройка $\lambda_{ген}$ в пределах 2 нм(42)	[145]
Р-УФ	F_2:Kr:He=0,25:6:94	1, 5	—	—	—	40	—	0,75	80	0,0043	0,8	—	[146]
РБВ	F_2:Kr:He=1:10:90	0,5—1	—	—	~30	~20	90	0,0017	160	0,019	—	Длительность фронта импульса накачки ~2,5 нс (43)	[147]
ЭП	F_2:Kr:He=1:6:94	1	1200	0,6	—	—	—	0,35	100	—	—	Для накачки (44) использованы как прямой, так и обратный токи пучка	[148]
ЕР	F_2:Kr:He=1:10:89	0,3—0,9	200	~10	—	3	—	0,00005	10	—	1	При замене He аргоном $\varepsilon_д$ снизилась в 4 раза. Оптимум p~500 мм рт. ст. Резонатор волноводного типа (45)	[126]
Р-УФ	F_2:Kr:He=1:18:1800	1—6	200	—	25—35	25	—	0,88	60	—	—	—	[149]
Р-УФ	F_2:Kr:He=1:20:3600	2,8	10—500	—	—	20	$2\cdot10^4$	0,18	—	—	1,2	—	[150]
Р-Х	F_2:Kr:He=1:1,6:7500	1—5 1—8	10	—	—	30	—	0,02	35 15	—	0,5 ≲1	Оптимальное давление 2,5 атм без предионизации и 4 атм—с предионизацией (46)	[151]
ТЕ	F_2:Kr:He=1:6:136	~1	—	—	—	—	—	≤0,1	70	—	0,13—1,6	С быстрой прокачкой смеси удалось достичь частоты повторения $f_{пов}$ = 1 кГц в среднем (47)	[152]

Table 3 (continued)

Pumping method / Способ накачки	Composition / Состав среды	p, атм	τ_0, нс	Q, МВт/см³	$\Delta\tau$, нс	τ, нс	$W_{пик}$, кВт	$\varepsilon_д$, Дж	L, см	$\varkappa$, см$^{-1}$	$\eta_{ср}$, %	Remarks / Примечания	Ref. / Литература
ЭП	1 мм рт. ст. NF_3+ +75 мм рт. ст. Kr+ +1,5 атм Ar+ +5,5 атм Ne	⩽8	30	0,1	20	30	—	2,1	50	—	⩽7	Оптимальная смесь. Без Ar $\eta_{ср}$ была несколько ~4,5% (49)	[153]
						Molecule / Молекула Ar F							
Р-эл	SF_6:Ar:He=0,1:1:100	1—8	—	—	—	3	10	—	60	—	0,003	Оптимум по давлению не достигнут (50)	[101]
Р-УФ	$F_2(NF_3)$—Ar—He	⩽2	400	⩾1	—	—	—	0,06	60	—	0,6	Состав варьировали (51)	[102]
ЭП	F_2:Ar=1:350	⩽2	55	3,5	~12	~50	$1,6\cdot10^4$	92	180		1,6	—	[140]
РБВ	F_2:Ar:He=1:10:90	0,5—1	—	—	~20	~30	—	0,001	160	0,017	—	—	[147]
ТЕ	NF_3:Ar:He=1:55:630	2—3,5	—	—	—	15	50	$(2,5—8)\times$ $\times10^{-4}$	36	—	—	Перестраиваемый лазер. Интервал перестройки 0,9 нм, $\varepsilon_д$ расчет. (52)	[154]
Р-УФ	F_2:Ar:He=1:10:300	⩽6	—	—	—	17	—	0,3	60	—	0,25	—	[144]
Р-УФ	F_2—Ar—He	1	70	—	—	25	—	0,03	60	—	—	Перестройка λ_0 в пределах 2 нм (53)	[145]
						Molecule / Молекула XeCl							
ЭП	Cl_2:Xe:Ar=0,1:10:90	>2	100	⩽1	100	30	3	$\sim5\cdot10^{-5}$	15	—	—	—	[135]

Table 3 (continued)

Pumping method / Способ накачки	Composition / Состав среды	p, атм	τ_0, нс	$\dot{Q}$, МВт/см²	$\Delta\tau$, нс	τ, нс	$W_{имп}$, кВт	$\varepsilon_д$, Дж	L, см	$\varkappa$, см$^{-1}$	$\eta_{ср}$, %	Remarks / Примечания	Ref. / Литература
ЭП	Cl_2:Xe:Ar=1:50:800	3	50	~10	—	—	15	—	40	—	—	CCl_4 менее эффективен, чем Cl_2 (54)	[155]
Р-УФ	XZ—Xe—He	2	—	—	—	10	—	0,001	36	—	—	XZ=CCl_4, BCl_3, CF_2Cl_2, C_2F_5Cl	[107]
ТЕ	BCl_3:Xe:He=2:15:1000	4—7	5	≤10	10—12	5	—	0,0025	40	—	0,3	—	[156]
ЭП	CCl_4:Xe:Ar=1:75:2000	≤8	25	—	—	—	$5,2\cdot10^3$	0,13	20	—	14?	CH_3Cl, CH_2Cl_2, $C_2H_4Cl_2$ менее эффективны (55)	[157]
ТЕ	XZ:Xe:He=(0,05—0,5):(0,5—4):100	0,5—2,7	30	~1	—	30	—	0,11	60	—	0,8	XZ=HCl, Cl_2, CCl_4, BCl_3: наиболее эффективен HCl; генерация на шести электронно-колебательных переходах (56)	[158]
Р-ЭП	CCl_4:Xe:Ar	≤4	25	—	—	—	—	0,205	20	—	~2	—	[159]
ТЕ	BCl_3:Xe:He=3:20:2200	≤3	100	—	—	5—7	$1,7\cdot10^3$	0,012	—	—	—	—	[160]
Р-ЭП	HCl:Xe:Ar=1:20:480	~1	1000	$\sim3\cdot10^{-3}$	—	500	—	—	120	—	0,7	—	[161]
ТЕ	XZ:Xe:He=(0,4—1):20:310	1	—	—	—	—	—	≤0,025	—	—	≤0,9	XZ=CCl_4 (наиболее эффективен), CH_2Cl_2, $CHCl_3$, $C_2H_2Cl_2$, $C_2F_3Cl_3$, C_2HCl_3 (57)	[162]
ТЕ	—	—	—	—	—	—	—	0,009	—	—	—	Частота до 400 Гц; средняя мощность до 1,6 Вт (58)	[15]
Р-УФ	HCl:Xe:He=1:25:474	3,4	—	—	—	30	—	0,18	120	—	—	λ_g=308,43; (59) 308,17; 307,92 и 307,65 нм. Снижения лазерного выхода не наблюдалось даже после 10000 импульсов	[163]
ЭП	HCl:Xe:He=2:15:1500	1—5	1000	—	—	500	—	1,15	100	0,026	5	Оптимум при p=4 атм (60)	[164]

Table 3 (continued)

Pumping method Способ накачки	Composition Состав среды	p, атм	τ_0, нс	$\dot{Q}$, МВт/см³	$\Delta\tau$, нс	τ, нс	$W_{имп}$, кВт	$\varepsilon_д$, Дж	L, см	$\varkappa$, см⁻¹	$\eta_{ср}$ %	Remarks Примечания	Ref. Литература
ТЕ	CCl_4:Xe:He=1:40:719	1	—	—	—	—	—	0,007	—	—	0,5	f=10 Гц, прокачка смеси в замкнутом цикле через молекулярные сита. За $1,8 \cdot 10^6$ выстрелов энергия генерации уменьшилась лишь вдвое (61)	[165]
						Molecule							
						Молекула KrCl							
ЭП	Cl_2:Kr:Ar=1:20:670	4,4	50	~10	20	30	—	0,05	10	—	0,007	—	[166]
ЭП	Cl_2:Kr:Ar=1:40:600	4	50	~10	30	30	50	—	15	—	—	—	[167]
РБВ	Cl_2:Kr:He=1:10:90	0,5—1	—	—	~20	~20	~60	0,0013	160	0,018	—	— (62)	[113]
Р-УФ	HCl:Kr:He=3:200:1800	3,9	—	—	—	10	—	0,1	120	—	—	После 6000 имп. пульсов интенсивность генерации снизилась вдвое	[163]
						Molecule							
						Молекула ArCl							
РБВ	Cl_2:Ar:He=1:15:84	0,5—1	—	—	40	10	20	$2 \cdot 10^{-4}$	160	0,012	—	См. также [14] (63)	[147]
ЭП	Cl_2:Ar=5:995	2,7	3	—	—	—	—	—	—	—	—	—	[168]
						Molecule							
						Молекула XeBr							
ЭП	Br_2:Xe=(0,1—1):100	0,6—1,8	50	~10	~20	~15	0,2	—	15	0,003	—	—	[60]
ЭП	Br_2:Xe=9:991	~1,1	—	—	~20	—	—	—	—	—	—	—	[3]
ЭП	HBr:Xe=1:10	1—2	50	≥10	—	—	1	—	40	—	—	—	[61]

Table 3 (continued)

Тип лазера	Состав смеси	λ, мкм	τ_0, нс	Q, Мдж/см^3	$\Delta\tau$, нс	τ, нс	$W_{пик}$, квт	$\varepsilon_{пр}$, Дж	L, см	$\varkappa$, см$^{-1}$	$\eta_{ср}$, %	Литература Примечания
Р-УФ	HBr:Xe:He=1:50:949	⩽3,8	35	—	20	20	—	⩽0,06	120	—	—	[169] Оптимальное давление зависит от содержания HBr. Низкий ресурс работы (в отличие от смеси с HCl) (64)
ЭП	XZ—He—Ar	2—6	50	⩽7	3—25	15	$3\cdot10^3$	⩽0,05	20	—	0,4	[170] XZ=Br$_2$, $C_2F_4Br_2$, $CHBr_3$, $C_2H_4Br_2$. Лучшие результаты дает $C_2F_4Br_2$. $\Delta\tau$ падает с ростом давления (65)
РБВ	He—Kr—Br$_2$	~1	—	—	—	—	—	—	—	—	—	[14]
ЭП	10 мм рт. ст. O_3+Xe	12	70	⩾10	~100	~80	100	0,01	10	0,005	—	[171] λ_g=538 и 544 нм
ОН	N_2O:Xe=1:150	0,7	—	—	5000	$(4—5)\cdot10^3$	—	—	80	⩽0,002	—	[172] T=170K
ОН	N_2O:Xe:Ar=1:40:250	1,75	—	—	$(2,5—10)\cdot10^3$	$(3—8)\cdot10^3$	—	0,6	80	0,0015	—	[62] T=160K
ОН	N_2O—Xe—R', R'=Ar, He	⩽3	$\sim2\cdot10^4$	—	—	8000	—	⩽2,2	70	0,0035	—	[173] Состав варьировался. Оптимальное давление ~1,5 атм. Энергия генерации немонотонно зависит от содержания компонентов. При T>210 K генерация не была (66)
ЭП	5 мм рт. ст. O_3+Kr	15	70	⩾10	~100	~80	—	0,005—0,01	10	~0,005	—	[171]
ЭП	5 мм рт. ст. O_3+Kr	14	80	—	500	—	—	—	100	0,0015	—	[11]
ОН	2 мм рт. ст. N_2O+Ar	⩽40	—	—	250	10 000	—	—	50	~0,0002	—	[64]

Molecule
Молекула KrBr

Molecule
Молекула XeO

Molecule
Молекула KrO

Molecule
Молекула ArO

Table 3 (continued)

Способ накачки Pumping method	Composition Состав среды	p, atm	τ_0, ns	$\dot{Q}$, MW/cm³	$\Delta\tau$, ns	τ, ns	$W_{имп}$, kW	$\varepsilon_д$, J	L, cm	$\varkappa$, cm^{-1}	$\eta_{ср}$, %	Remarks Примечания	Ref. Литература
Молекула HgCl													
ЭП	CCl_4:Hg:Xe:Ar = 11:21:111:857	—	150	~0,5	30	40	140	—	15	—	0,5	$T = 260°C$	[174]
ЭП	CCl_4:Hg:Xe:Ar = 2:40:110:850	≤1,5	50	—	40	15	—	$5 \cdot 10^{-6}$	15	—	—	$T = 250°C$; λ_g = 557,6 и 558,4 нм	[175]
Р-ЭП	Cl_2:Hg:Ar = 8:10:1500	~2	400	—	400	100	—	—	46	—	0,01	$T = 200°C$	[176]
Р-ЭП	Cl_2:Hg:Ar = 2:5:993	~2	400	—	200	150	10	0,005	40	—	0,02	$T = 250°C$	[177]
Р-УФ	1—10 мм рт. ст. $HgCl_2$+He	0,5—1,2	50	2	—	—	—	0,003	50	—	0,3	$T > 225°C$. $\varepsilon_д$ и $\eta_{ср}$ увеличиваются при добавлении в смесь азота (67)	[178]
ОН	$HgCl_2$:He = 1:375	~0,3	—	—	—	50	—	10^{-6}	—	—	—	$T = 400$ K. Источник Xe_2-лазер (68)	[65]
Молекула HgBr													
ЭП	HBr:Hg:He:Ar = 8:2:6:108:864	—	150	~0,5	—	—	50	—	15	—	0,25	λ_g = 501,8 и 498,4 нм	[67]
ОН	0,45 мм рт. ст. $HgBr_2$+He	0,35	30	—	25	25	—	$2,5 \cdot 10^{-4}$	20	—	3,5	$T = 125°C$. Источник накачки — ArF-лазер (69)	[179]
Р-эл	$HgBr_2$ — He	1	70	—	—	50	—	10^{-4}	—	—	—	$T = 150°C$; λ_g = 502,0; 502,3; 503,6; 503,9; 504,2; 504,6 нм	[180]

Table 3 (continued)

Pumping Способ накачки method	Composition Состав среды	p, атм	τ_0, нс	Q, МВт/см²	$\Delta\tau$, нс	τ, мс	$W_{имп}$, кВт	$\varepsilon_д$, Дж	L, см	$\varkappa$, $см^{-1}$	$\eta_{ср}$, %	Remarks Примечания	Литература Ref.
ОН	$HgBr_2$—SF_6	1	30 000	—	—	2 000	—	—	50	—	—	T=246°C. Источник накачки — открытый сильноточный разряд (70)	[181]
Р-ЭП Р-УФ	$CBrCl_3$:Hg:Ar=2:5:993 1—10 мм рт. ст. $HgBr_2$+He mm Hg	≤2 0,5—1,2	400 50	— 2	200 —	— —	— —	0,001 0,0075	40 50	— —	— 0,5	T=250°C T=225°C	[177] [178]
Molecule Молекула HgJ													
Р-УФ	mm Hg 1—10мм рт. ст. HgI_2+He	0,5—1,2	50	2	—	—	—	$3\cdot10^{-4}$	50	—	0,3	T=225°C. Генерация на 6 линиях в полосе 443—445 нм (71)	[178]

Explanation of pumping methods:

ЭП--electron beam
TE--self-maintained transverse discharge
Р-эл--discharge with electric preionization
Р-УФ--discharge with UV preionization
Р-ЭП--discharge stabilized by an electron beam
Р-Х--discharge with x-ray preionization
РБВ--discharge in the traveling wave mode
ЕР--capacitive discharge
ОН--optical pumping

See next page for explanation of column headings and translation of the remarks.

FOR OFFICIAL USE ONLY

APPROVED FOR RELEASE: 2007/02/08: CIA-RDP82-00850R000300020036-7

Explanation of column headings for Table 3:

p--pressure, atmospheres
τ_0, $\dot{Q}$--pumping duration and specific power, ns and MW/cm^3
$\Delta\tau$, τ--amplification delay and duration, ns
$W_{пик}$--peak power, kW
$\varepsilon_л$--energy of laser radiation, J
L--length of the active region, cm
κ--gain, cm^{-1}
$\eta_{ср}$--efficiency of energy conversion in the medium, %
λ_0--lasing wavelength

Key to translation of remarks in Table 3

1--λ_0 = 353, 351 and 349 nm; repetition rate 20 Hz
2--Repetition rate up to 100 Hz
3--Optimum pressure about 3 atm
4--Preionization increases the output of laser emission by about 30%
5--Mode-locked operation
6--Laser pulse starts before activation of discharge; discharge becomes unstable within about 80 ns
7--Lasing on six vibronic transitions
8--Amplification of ultrashort pulse of the third harmonic of a neodymium laser
9--Divergence of about 0.2 mrad or less
10--Repetition rate 200 Hz; average power 52 mW
11--Tunable laser: λ_0 = 353, 351, 348 nm; optimum pressure about 5 atm
12--Lasing threshold reached at specific pumping power of 20 kW/cm^3 or more
13--Amplifier
14--Mixture compositions varied over a range of 1:(2-15):(50-2000)
15--When neon was substituted for argon, the $\varepsilon_л$ and $\eta_{ср}$ were more than tripled
16--Divergence about 1 mrad
17--When neon was substituted for argon, the output power was tripled; emission threshold was reduced
18--Repetition rate up to 500 Hz; average power up to 3.3 W; circulation of the working mixture
19-20--Intensification of laser signal with application of electric field falls off with increasing pressure. Optimum pressure p = 3 atm. Strong dependence on NF_3 concentration
21--Lasing does not occur when argon is substituted for He or Ne. Cavity of waveguide type. Optimum at pressure of about 100 mm Hg
22--Lasing in the superradiation mode
23--Beam interruption was accomapnied by pinching of the discharge and cutoff of lasing
24--Repetition rate up to 50 Hz
25--$\eta_{ср}$ depends nonmonotonically on the initial temperature of the mixture: the maximum $\eta_{ср}$ for p = 3 atm is reached at T = 450 K

Key to Table 3 (continued)

26--At $\lambda = 488$ and 476 nm, amplification of up to 8% per trip through the cavity is recorded; energy input about 0.1 J
27--Pumping by radiation of an open discharge; $\lambda_0 = 470$ nm, $\Delta\lambda_{инд} = 30$ nm
28--Pumping source was superluminescence of Xe_2^*. $\lambda_0 = 480$ nm; $\Delta\lambda_{инд} =$ 12 nm. Addition of SF_6 increases the laser output.
29--$\lambda_0 = 248.4$ and 249.1 nm
30--$\lambda_0 = 248.5$ and 249.5 nm
31--Repetition rate up to 100 Hz
32--Output energy increases with pressure
33--Preionization increased laser output by 50%
34--Two lasing pulses
35--Divergence of 0.2 mrad or less (with unstable cavity)
36--Lasing threshold at $\dot{Q} \geqslant 20$ kW/cm^3
37--Amplifier
38--Composition was varied
39--Absorption of radiation by the CF_2 molecule was observed in the lasing band
40--The most effective fluorine agent is N_2F_4
41--Repetition rate up to 400 Hz; average power up to 3.3 W
42--Tuning of λ_0 in a range of 2 nm
43--Rise time of pumping pulse about 2.5 ns
44--Both direct and reverse beam currents were used for pumping
45--When argon is substituted for He, the $\varepsilon_л$ fell to 1/4 the initial value. Optimum pressure about 500 mm Hg. Cavity of waveguide type
46--Optimum pressure about 2.5 atmospheres without preionization, and 4 atmospheres with preionization
47-48--With rapid circulation of the mixture, a repetition rate of f = 1 kHz was attained with average lasing power of 10 W
49--Optimum mixture. The $\eta_{ср}$ was somewhat lower (about 4.5%) without Ar
50--Pressure optimum not attained
51--The composition was varied
52--Tunable laser. Tuning range 0.9 nm, $\varepsilon_л$ increases with p
53--Tuning of λ_0 over a range of 2 nm
54--CCl_4 less effective than Cl_2
55--CH_3Cl, CH_2Cl_2, $C_2H_4Cl_2$ are less effective
56--XZ = HCl, Cl_2, CCl_4, BCl_3. HCl is most effective. Lasing on six vibronic transitions
57--XZ = CCl_4 (most effective), CH_2Cl_2, $CHCl_3$, $C_2H_4Cl_2$, $C_2F_3Cl_3$, C_2HCl_3
58--Repetition rate up to 400 Hz; average power up to 1.6 W
59--$\lambda_0 = 308.43$, 308.17, 307.92 and 307.65 nm. No reduction in laser output was observed even after 16,000 flashes
60--Optimum at p = 4 atm
61--f = 10 Hz, circulation of the mixture in a closed cycle through a molecular sieve. After $1.8 \cdot 10^5$ flashes, the lasing energy had only fallen off by a factor of 2.
62--After 6000 flashes lasing intensity fell to one-half

Key to Table 3 (continued)

63--See also Ref. 14
64--Optimum pressure depends on HBr content. Short work life (in contrast to HCl)
65--XZ = Br_2, $C_2F_4Br_2$, $C_2H_4Br_2$, $CHBr_3$. Best results obtained with $C_2F_4Br_2$. $\Delta\tau$ falls with increasing pressure
66--The composition was varied. Optimum pressure about 1.5 atm. Lasing energy depends nonmonotonically on the content of components. No lasing was observed at temperatures above 210 K.
67--T > 225°C, ε_{Π} and η_{cp} increase when nitrogen is added to the mixture
68--T = 400 K. Pumping source Xe_2 laser
69--T = 125°C. Pumping source ArF laser
70--T = 246°C. Pumping source was an open high-current discharge
71--T = 225°C. Lasing on six lines in the 443-445 nm band

2.2. Initial medium. The working mixtures listed in tables 2 and 3 are gas-phase[1]. The particle density N (pressure p of exciplex media) lies in a range of $5 \cdot 10^{18} \leqslant N \leqslant 2 \cdot 10^{21}$ cm^{-3} ($0.15 \leqslant p \leqslant 70$ atm). The necessary density is frequently attained by adding a buffer gas (Ar, Ne, He, N_2, SF_6) to the mixture, primarily to increase the specific absorbed energy and accelerate relaxation processes. The concentration of buffer gas may be of the order of 99% or more (for RX* and HgX*). Lasing is often unattainable without buffer gas additives. We note that changing from a heavy buffer gas to a lighter one as a rule is accompanied by a reduction of the lasing threshold and increased laser output [Ref. 86, 117, 122 and elsewhere]. Vice versa, when a heavy buffer gas is substituted for a lighter one, the lasing characteristics deteriorate to the point of disappearance of emission (especially in electric discharge lasers) [Ref. 115, 126]. Apparently the curve for emission intensity as a function of N passes through a maximum for all exciplexes.

In the case of lasing on heteronuclear exciplexes (RX*, RO*, HgX*), the initial medium usually contains from two to four components. In addition to the free halides and oxygen, the chemical compounds of these elemenets are frequently used as their donors. Sometimes different researchers diverge considerably in their quantitative "recipes" for the same compositions of active media. One may also encounter contradictory recommendations on the effectiveness of different halide donors. Here the problem of optimizing the medium with respect to composition and density is one of the most important jobs, and also one of the most complicated;

---

[1]Ref. 192, 193 report onset of a directional effect and narrowing of the spectral line of luminescence of liquid xenon when it is exposed to an electron beam. These reports stimulated the development of gas-phase excimer lasers. An attempt to stimulate a laser transition in solid xenon was unsuccessful [Ref. 194]. See Section 6 concerning amplification in solutions containing polyatomic organic exciplexes.

so far there has been no theoretical resolution of this question in any cases.

2.3. Energy characteristics. To achieve lasing, it is necessary to exceed the threshold values of the specific input power $\dot{Q}$ or energy Q (for pumping with a short pulse). No systematic studies have been done on the threshold characteristics of $\dot{Q}$ and Q as a function of the properties of the medium and pumping conditions. An experiment has been done [Ref. 113] in which the measured threshold value of specific power was about 20 kW/cm^3 for XeF* and KrF*. This value of $\dot{Q}$ is indicative for the specific media and pumping method. An estimate of this quantity for lasing on XeCl, according to data of Ref. 161, gives $\dot{Q} \approx 3$ kW/cm^3. In Ref. 190, noticeable amplification (after many passes through the cavity) on XeF* is achieved with specific power of nuclear pumping of only 40 W/cm^3.

Estimates of laser efficiency rely on the actual efficiency of the facility η, the efficiency of energy conversion in the medium $\eta_{ср}$ and the quantum efficiency η_q. In these estimates $\eta_{ср} = \varepsilon_л/\varepsilon_{нак}$, where $\varepsilon_л$ is the energy of the extracted laser emission, $\varepsilon_{нак}$ is the energy of the source, including the active volume, $\varepsilon_q = \hbar\omega_0/E_0$ (E_0 is the average energy expended in forming one exciplex molecule). The quantum efficiency is usually measured in tens of percent; however, $\eta_{ср}$ so far has not risen above 7% [Ref. 153][1]. It should be noted that estimates of $\eta_{нак}$ are not always reliable (e. g. in Ref. 157). It is natural to expect the maximum quantum yield in the case of selective arrangements for stimulating a laser transition (optical pumping). The theoretical value of η_q for a beam is somewhat lower than for a discharge, but as a rule the efficiency of conversion $\eta_{ср}$ is higher. Also higher are the power and energy characteristics of beam-controlled exciplex lasers: $\varepsilon_л \approx 108$ J, $W_{имп} \approx 2$ GW [Ref. 140]. Ref. 196 reports attainment of $\varepsilon_л \approx 350$ J (KrF*, electron beam); it can be anticipated that we will shortly achieve a laser emission energy $\varepsilon_л$ of the order of 1 kJ or more.

2.4. Time characteristics. A laser signal delay with respect to the pumping pulse is typical of exciplex lasers. The duration of the delay depends in a complicated way on the pumping parameters and the composition of the medium. The delay time usually decreases with increasing density of the medium and intensity of energy input. At high pumping powers, excimers R_2^* usually show early interruption of lasing due to destruction of the cavity mirrors and overheating of the gas (for more detail see Ref. 12, 35 and below). The longest amplification pulses on exciplexes have been attained with comparatively weak pumping. One of the principal tasks in looking for ways to increase the efficiency of exciplex lasers is to match the duration and specific power of pumping to each other and the parameters of the medium and to optimize composition.

[1]Recently by optimizing optical feedback conditions, $\eta_{ср}$ was brought up to 11.4% [Ref. 195] (KrF*, electron beam, $\varepsilon_л \approx 80$ J).

The possibility of achieving continuous lasing on exciplexes so far remains unclear. Lasing duration in experiments with electric discharges has been brought up to about 1 μs [Ref. 109, 125, 129], with optical pumping -- to about 10 μs [Ref. 62, 64], and with nuclear pumping [Ref. 190] amplification has been observed for about 30 ms. We note that there are electric discharge lasers that operate in the pulse-periodic mode. A pulse repetition rate of 1 kHz has already been achieved in the case of KrF* [Ref. 152]. Attempts to develop an excimer laser on Xe_2^* with a pulse repetition rate of 10 Hz were undertaken in Ref. 197, but apparently were unsuccesful.

2.5. Temperature dependence. Usually the initial temperature of the gas mixture is close to room temperature. Sometimes the necessary density of the vapor of the working materials is created by preheating (for example in experiments with mercury and its salts).

No detailed investigation has been made of the influence that temperature has on lasing; however, it is clear that there are critical temperatures T_{cr} above which amplification is interrupted. This effect may be due to an increase in the photoassociation coefficient (see Ref. 12, 35, and formula (3)), thermal dissociation of the upper working state, the destruction of this state by electron impacts with increasing concentration as the temperature rises (see for example the calculations of Ref. 73), or to other causes. In Ref. 86 an abrupt drop in laser emission of Xe_2^* was observed when the initial temperature of heavy particles was increased from 240 to 350 K. In pumping of xenon by a high-power beam [Ref. 81], not only was lasing interrputed, but the intensity of spontaneous emission dropped as well[1]. In experiments with XeO* [Ref. 62, 172] the duration and intensity of the laser signal increased with falling temperature to 160-170 K. In the case of stimulated emission of XeF* in a supersonic flow [Ref. 122] the gas temperature ranged from room temperature down to about 80 K. Some decrease of intensity was noted at temperatures below 120 K. In Ref. 199 when a working mixture of F_2-Kr-Ar pumped by an electron beam was heated from 150 to 400 K the intensity of spontaneous and induced emission of KrF* increased about ten-fold, and above 400 K the increase changed to an abrupt drop. In mixtures containing no argon this effect practically disappeared. No such analogous behavior was observed for mixtures of Ar-Xe-F_2. In Ref. 131 a mixture of Ne-Xe-NF_3 was heated to about 500 K from room temperature. It was found that beginning at approximately 350 K the laser output increases and reaches a maximum, after which it begins to fall once more. As the initial pressure of the mixture increases, the maximum η_{cp} is reached at a higher temperature. These facts show the complicated interdependence of the properties of the active medium and pumping conditions.

[1]Attenuation of the intensity of luminescence of Xe_2^* with increasing temperature has also been observed in Ref. 198.

3. Mechanisms of Formation of the Populations of Working Levels

3.1. Purification of the lower working state. In lasing on photodissociative transitions, the lower state is quite rapidly depopulated due to dispersion of atoms. The dispersion time [see Ref. 12] is determined by the slope of the ground term in the vicinity of internuclear distances of the transition. For molecules with a fairly steep repulsion term the condition of predominance of photodissociation over photoassociation boils down primarily to the requirement of a low gas temperature: $T < T_{cr} \approx 0.1$ eV (for more detail see Ref. 12, 35). For some polyhalides with a mildly sloping ground term (for example XeBr*, KrF*), electron sticking and other collisional processes may be additional channels of purification of the lower level.

In amplification on bound-bound transitions of exciplexes, collisional purification is predominant. In mercury polyhalides, apparently the major role is played by vibrational relaxation of high ($n \sim 20$) vibrational levels of the ground state: according to estimates [Ref. 180], at $p \sim 1$ atm the time of vibrational de-excitation is <10 ns. Besides, in the case of HgX, and to a greater degree for XeCl and XeF, it is possible that the molecule in a highly excited vibrational state may be dissociated by collisions with heavy particles. Calculated values and measurements of the rate constants of dissociation of XeF in helium and neon are given in Ref. 200, 201. The authors of Ref. 131 attribute an increase in η_{cp} when a mixture of Ne-Xe-NF_3 is heated chiefly to accelerated thermal dissociation of XeF X(1/2). Among the other mechanisms of purification we note de-excitation by electron impact (He_2^*) and predissociation (RO*). In contrast to photodissociative transitions, the problems of purification on bound-bound transitions of exciplexes are analogous to a great extent to those encountered in lasing on atoms (see Ref. 35, Chapter 5) and stable molecules.

3.2. Channels of population of the upper laser level. The simplest case of a single-component active medium in which excimers R_2^* are formed was discussed in some detail in Ref. 8-10, 12, 35, 73. The formation of populations of heteronuclear exciplexes is much more complicated. So far the available data can give us only a general idea of the pattern of relaxation of a complex composition.

Elementary acts of interaction of a source of energy with a medium as a rule do not lead to direct population of the upper working state of exciplexes[1]. Ionization of the medium and formation of excited atoms are the major processes on the pumping stage. Mixtures that contain stable compounds of xenon (XeF_2) and mercury (HgX_2) are an exception: exciplexes XeF* and HgX* are effectively formed by dissociative excitation of the molecules of these compounds [Ref. 65, 121, 178-181]. Let us note

[1]The formation of exciplexes by photoassociation or excitation by a fast electron in a ternary collision is unlikely.

that amplification arrangements based on chemical dissolution of stable substances may hold promise, in particular in the search for new lasing exciplex media (research of this kind should be done for instance with the higher fluorides, oxyfluorides and oxides of xenon, HgF_2, organo-mercury compounds and so on).

Recombination relaxation of a multicomponent plasma takes place through several atomic and molecular channels that are intensively mixed as a result of plasma-chemical reactions. Elastic and inelastic collisions determine the concentration and energy distribution of the electronic component of the plasma [Ref. 35, Chapter 4]. Channels of losses of electrons and positive ions include:

dissociative recombination, for example:

$$AB^+ + e \rightarrow A^* + B; \tag{6}$$

ternary recombination, for example:

$$A^+ + e + Y \rightarrow A^* + Y \tag{7a}$$

(Y = e, A; R' is an atom of inert buffer gas);

$$A_2^+ + e + Y \rightarrow A_2^* + Y; \tag{7b}$$

$$AB^+ + e + Y \rightarrow AB^* + Y \text{ (e. g. see Ref. 202);} \tag{7c}$$

sticking of an electron to neutral particles, for example:

$$AB + e \rightarrow A + B^-; \tag{8a}$$

$$B + e + Y \rightarrow B^- + Y \tag{8b}$$

(Y is an unexcited neutral particle).

For slow electrons the rates of processes (8) are quite considerable [Ref. 203-207]. It should be noted that in media with a high content of electronegative molecules (halides X, their compounds XZ, etc.) an ionic plasma may even be formed in which heavy particles carry the main negative charge. This may involve new effects (for more detail see Ref. 208).

A negative and a positive ion may recombine both in a binary process (charge exchange)

$$A^+ + B^- \rightarrow A^* + B, \tag{9}$$

and in ternary collisions

$$A^+ + B^- + Y \rightarrow AB^* + Y. \tag{10}$$

Processes (10) predominate in a dense medium ($N > 10^{18}$ cm^{-3}). The coefficients of reaction rates for these processes were recently calculated for A = Y = He, Ne, Ar, Kr, Xe and B = F [Ref. 209]; A = Hg, Y = Ar, B = F, Cl, Br, I [Ref. 210]; A = Kr, B = F, Y = He, Ne, R [Ref. 211]. It was shown in the latter research that the coefficient of the reaction rate of (10) depends on the type of Y, and reaches a maximum at different densities N for different buffer gases. Ion-ion recombination with the participation of molecular ions may take place in analogy with (10) or by dissociative mechanisms, in particular [Ref. 115]:

$$\begin{aligned} A_2^+ + B^- &\rightarrow AB^* + A, \\ A^+ + BZ^- &\rightarrow AB^* + Z. \end{aligned} \tag{11}$$

Let us now enumerate the most important reactions that intermix atomic and molecular states. In addition to (6), (7), (10) and (11) these include the conversion of atomic ions, for example:

$$A^+ + B + Y \rightarrow AB^+ + Y \tag{12}$$

(molecular ions may interact analogously); collisional association, for example:

$$A^* + B + Y \rightarrow AB^* + Y; \tag{13}$$

transfer of a molecule to a dispersion term by electron impact

$$AB^* + e \rightarrow A^* + B + e; \tag{14}$$

transfer of excitation and charge exchange with interaction of particles made up of dissimilar atoms (see 17, 199, 212); substitution reactions, for example:

$$A^* + BZ \rightarrow AB^* + Z. \tag{15}$$

Among the most important channels of formation of excited states of exciplexes are processes (10), (13) and (15). Dimers, including He_2^* and Hg_2^* are formed chiefly by association of an excited and an unexcited atom. It is conventionally assumed [Ref. 62, 171, 213] that a major role in populating RO* ($E^1\Sigma^+$) is played by the reaction $R + O^*(^1S) + R \rightarrow RO^* + R$.

Reactions of type (15) are especially effective when they take place by the harpoon mechanism (see Ref. 214, 215):

$$A^* + BZ \rightarrow [A^+B^-Z] \rightarrow AB^* + Z. \tag{15a}$$

In this case the exciplex AB* is formed in one of the ionic states. The rate constant of the harpoon reaction is determined by the relation

between the electron bonding energy in atom A*, the electron affinity energy for BZ and B, the depth of the ionic term AB* and energy of rupture of the bond B-Z in the negative ion BZ^-. This dependence shows up in the considerable scatter of values of this rate constant for different A* and BZ. When A = Xe, Kr and BZ = Cl_2, F_2, the cross section of the harpoon reaction may reach ~10^{-14} cm^2 [Ref. 216]. However, this does not imply that the main channel of formation of exciplexes RX* is associated with excitation of R and subsequent drift into the harpoon reaction. Actually, interaction of R* with other halide donors is sometimes considerably less effective, up to the point where RX* molecules as a result of reaction (15a) are practically unobserved. In particular, this is the situation in the case of XZ = SF_6 [Ref. 216]. Nevertheless, emission has been achieved on mixtures of R'-R-SF_6 [Ref. 101, 118, 129]. The experimentally established effectiveness of SF_6, HCl, HBr and other halide donors that are not active with respect to (15a) is apparently due to the fact that population of AX* (A = R, Hg) in a plasma of composition R'-A-XZ takes place chiefly due to ion-ion recombination (15). This is indicated by the high values (up to $3 \cdot 10^{-6}$ cm^3/s) of the rate constants of (10) as calculated in Ref. 209-211, and the results of numerical modeling of the kinetics of such media (see Ref. 217 for example), and also to some extent by the fact that it has not been possible to achieve lasing in such media so far by selective pumping.

3.3. Destruction of the upper laser level. Side reactions. For heteronuclear exciplexes, just as for excimers, destruction of the upper working state may take place due to the working radiative transition (it is desirable that it should predominate), collisions with electrons (of the first and second kind) and excited particles (see Ref. 12, 35). In contrast to excimers, reactions of quenching by unexcited particles of the working components of the medium may be important for many exciplexes. For example the effective rate constant of quenching of Xe_2^* by Xe atoms is small (about 10^{-13} cm^3/s [Ref. 38, 39), and this process shows up at $N_{Xe} > 6 \cdot 10^{20}$ cm^{-3}. At the same time, quenching of AX* by molecules of the halide donor, atoms of A, and even buffer gas atoms[1] cannot be disregarded even for much lower densities of the corresponding components.

Table 4 gives the rate constants of interaction of some exciplexes with various quenching agents (see also Ref. 225, 226). It can be seen that XZ molecules are quite energetic quenching agents. A high rate is also typical of three-particle reactions of RX* with atoms of inert gases, especially in cases where three-atom exciplexes R_2X^* are formed. It must be pointed out that mechanisms of quenching processes have not yet been adequately studied, and the measured values of the constants are not always reliable, since analysis of experimental data usually involves the simplest models of relaxation kinetics in the afterglow without

[1]The reduction of losses of excited particles due to quenching is one of the major reasons for using buffer gases.

TABLE 4

Rate constants of quenching of some exciplexes

(1) Тушитель \ (2) Эксиплекс	XeF	KrF	ArF	HgCl
X_2	$3,5 \cdot 10^{-10}$ [168]; $3,3 \cdot 10^{-10}$ [218]; $3,0 \cdot 10^{-10}$ [219]; $1,2 \cdot 10^{-10}$ [49]	$4,8 \cdot 10^{-10}$ [54]; $7,8 \cdot 10^{-10}$ [220]; $5,7 \cdot 10^{-10}$ [55]	$1,9 \cdot 10^{-10}$ [221, 222]	$1,3 \cdot 10^{-10}$ [223]
NF_3	$1,5 \cdot 10^{-11}$ [218]; $2,8 \cdot 10^{-11}$ [168]; $3,3 \cdot 10^{-12}$ [49]	—	—	—
AX_2	$3,5 \cdot 10^{-10}$ [48]	$1,4 \cdot 10^{-10}$ [54]	—	$9,2 \cdot 10^{-11}$ [65]
He	$4 \cdot 10^{-13}$ [168, 51]; $2 \cdot 10^{-12}$ [49]	—	—	$5 \cdot 10^{-14}$ [223]
Ne	$7,7 \cdot 10^{-13}$ [168]; $3 \cdot 10^{-13}$ [49]	—	—	—
Ne + Ne	$2,5 \cdot 10^{-33}$ [219]	—	—	—
Ar	$1,6 \cdot 10^{-12}$ [218]	$1,8 \cdot 10^{-12}$ [54]	$9 \cdot 10^{-12}$ [221]	$5 \cdot 10^{-14}$ [223]
Ar + Ar	$1,5 \cdot 10^{-32}$ [224]	$1,1 \cdot 10^{-32}$ [54]	$4 \cdot 10^{-31}$ [221] $5,3 \cdot 10^{-31}$ [222]	—
Kr	—	$2 \cdot 10^{-13}$ [220]; $8 \cdot 6 \cdot 10^{-12}$ [54]	$1,6 \cdot 10^{-9}$ [221]	—
Kr + Kr	—	$6,7 \cdot 10^{-31}$ [220]; $2,9 \cdot 10^{-31}$ [55]; $9,7 \cdot 10^{-31}$ [54]	—	—
Xe	$2,9 \cdot 10^{-11}$ [218, 219]; $3,9 \cdot 10^{-11}$ [168]; $6,0 \cdot 10^{-11}$ [49]	—	$4,5 \cdot 10^{-9}$ [221]	$2,4 \cdot 10^{-13}$ [223]
Xe + Xe	$2,4 \cdot 10^{-29}$ [168]	—	—	—
N_2	$4,6 \cdot 10^{-12}$ [218]	—	—	$5 \cdot 10^{-14}$ [223]
CO_2	$1,6 \cdot 10^{-10}$ [218]	—	—	—
HCl	—	—	—	$8,6 \cdot 10^{-11}$ [223]
CCl_4	—	—	—	$1,2 \cdot 10^{-10}$ [223]

Note: Rate constants in cm^3/s for binary reactions, cm^6/s for ternary

KEY: 1--Quenching agent; 2--Exciplex

consideration of the possible influence of intermediate products, transitions to other than the ground state of the exciplex (for example see Ref. 225), self-quenching and so on.

Among the numerous side reactions in exciplex media, mention should be made of the formation of three-atom particles -- ions and molecules [Ref. 199, 227]. Almost nothing is known about how relaxation takes place in a three-atom channel. We also mention parasitic processes of transmission of excitation to oxygen or halide donors, for example:

$$R^* + N_2O \rightarrow N_2^* + R + O \tag{16}$$

or

$$R^* + XZ \rightarrow \begin{cases} XZ^* + R; \\ X^* + R + Z; \\ Z^* + R + X; \\ X + Z + R. \end{cases} \tag{17}$$

When the energy of $R^*(R_2^*)$ is sufficient for excitation of BZ, processes of type (16), (17) effectively compete with (15a)[1]. This explains the increasing difficulty of achieving amplification on exciplexes RX* with a reduction in the ordinal number of R and an increase in the number of X. For instance in a mixture of Ne-F_2, a laser on the NeF* transition could not be triggered [Ref. 228], although it was possible in this case to achieve emission on F_2^*. Media of R'-Xe-XZ lase not only on XeX*, but on atomic and molecular lines of the halide as well (for example F* [Ref. 128], Br_2^* [Ref. 169]).

Side processes can be only partly suppressed by regulating the density and composition of the working mixtures. In addition to quenching reactions they are one of the reasons for low values of η_{cp}. This is due both to losses of excited particles, and to the formation of products capable of absorbing amplified emission (see Section 4). Estimates of the relative output of RX* as calculated per atom of R* give about 0.3 for XeBr* [Ref. 230], and about 0.5 for XeF* [Ref. 190]. The approximate composition of active media R'-R-XZ with regard to the products of side reactions is illustrated by the diagram of population of RX* in Fig. 2.

Among the side processes that are capable of increasing the service life of exciplex lasers are reactions of regeneration of the halide or oxygen donor. The diminution of donor molecules in the process of formation of the active medium leads to a deterioration with time in the emission output parameters that shows up particularly strongly in lasers that operate in the pulse-periodic mode. Spontaneous chemical regeneration of the donor in the working volume, if it is possible, as a rule takes place much more slowly than relaxation of electron excitation. For example let us point out that the rate constant of recombination of

[1]The principle of transmission of excitation from metastable atoms is used in schemes of lasing on X_2^* (see Ref. 13, 228, 229).

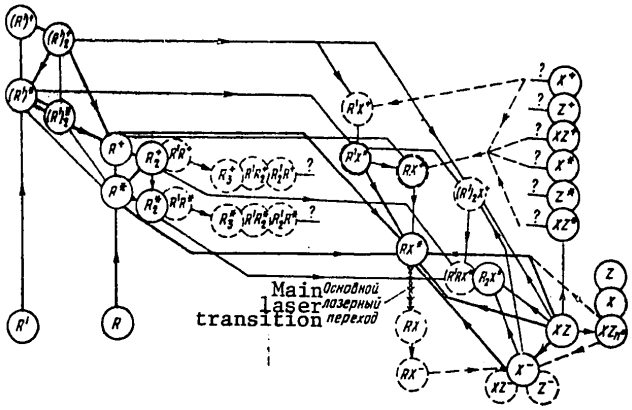

Fig. 2. Fundamental scheme of population of the upper working state of RX* in a plasma of composition R'-R-XZ

fluorine atoms in helium is about $6 \cdot 10^{-34}$ cm^3/s [Ref. 231]. It should be added that X and O atoms may diffuse to the walls of the working chamber, and once there enter into quite active chemical interaction. So far, Hcl has shown the best capacity to regenerate [Ref. 163] (chain reaction of chlorine with hydrogen). After 16,000 lasing pulses on XeCl without a change of gas, there was no loss of lasing energy [Ref. 163].

4. Losses of Working Radiation in the Medium

Photoabsorption of uncontrollable impurities may make an appreciable contribution to $\kappa_{ср}$. This process is most appreciable for excimers and exciplexes with high energy of a quantum of the laser transition: R_2^*, ArCl*, ArF*. In the vacuum ultraviolet, the cross sections of absorption by molecular gases frequently exceed ~10^{-17} cm^3. The influence that the purity of the gas used has on lasing parameters has been shown by experiments with Xe_2^*. For instance, the laser triggering reported in Ref. 84 had been preceded by an unsuccessful attempt by the same authors [Ref. 232] on the same installation with insufficiently pure gas. In Ref. 95, the xenon was purified after each flash, and the lasing energy increased.

Considerable absorption losses may take place directly in the initial components of the working mixture. Usually these can be reduced by adding a buffer gas. These losses may also have an influence on the efficacy of various halide donors. But even choosing initial substances that are practically transparent to the emission being amplified is no guarantee of absence of absorption in the activated medium. Studies of absorption in exciplex laser media have shown that absorption depends in a complicated way on wavelength and mixture composition, and is characterized by different dynamics than amplification (see Ref. 51, 58, 200).

Therefore it is natural to assume that absorption is due to the numerous products of plasma-chemical reactions.

Little is known about absorption by excited particles. According to the calculations of Ref. 233, photoionization cross sections in the 100-300 nm wavelength region for lower metastable levels are less than 10^{-19} cm^2 for Ar, Kr and Xe, less than $2 \cdot 10^{-19}$ cm^2 for Ne, and less than $2 \cdot 10^{-18}$ cm^2 for He. The photoionization cross section for Ar_2^* found in Ref. 74 is much greater: at the maximum on $\lambda \approx 320$ nm it reaches 10^{-16} cm^2. Apparently the dimers of other inert gases must also have photoionization maxima in the near ultraviolet; however, it is not yet clear what role these molecules play in the absorption of working radiation of exciplexes like XeX. The most considerable absorption losses may be associated with the excited particles that are formed in appreciable concentrations. The authors of Ref. 17 suggest that the main contribution to absorption on lasing lines of KrF* is from Kr_2F^* exciplexes, although the estimated cross section of this process given in Ref. 17 is relatively small: of the order of $1.6 \cdot 10^{-18}$ cm^2.

Rather large cross sections are typical of electron photodetachment from a negative ion, especially for halides X^- (of the order of 10^{-17} cm^2 or more [Ref. 234, 235]). Ref. 58 notes that photoabsorption on bound-free transitions of molecular ions (of the R_2^+, $R'R^+$ type) has a considerable effect on lasing on RX*. Subsequent theoretical calculations [Ref. 31, 236-238] and experimental studies [Ref. 236, 200, 239-241] have basically confirmed this conclusion. For example in the case of Ar_2^+ we know the position of the peak is about 292 nm, its half-width is about 90 nm, and the cross section in the maximum is about 10^{-17}-10^{-16} cm^2.

The dynamic behavior of the coefficient of absorption of the active medium is determined by the instantaneous microcomposition and temperature. The reason for the increased intensity of laser emission of KrF* and XeF* with increasing T that was observed in Ref. 131, 199 may be due not only to the temperature dependence of the kinetics of processes that form the population of the upper laser level [Ref. 199], but also to thermal destruction of radiation-absorbing intermediate compounds such as Kr_2F^*, F^-, and possibly Ar_2^+, $ArKr^+$ and ArKrF* as well. Let us note that the temperature also influences the effective (averaged with respect to internal degrees of freedom) absorption cross sections of molecular particles [Ref. 236, 237]. An abrupt fall-off in the intensity of luminescence of exciplexes above 400-500 K may be due in large measure to photoassociation and chemical radiative collisions [Ref. 189].

5. Nature of Nonequilibrium of the Active Medium

The basis of the active medium of exciplex lasers is a nonequilibrium plasma. Depending on the predominance of ionization or recombination electron flux in the plasma, such a medium is called ionization-nonequilibrium or recombination-nonequilibrium (see Ref. 35). Knowledge of the

type of nonequilibrium is important in particular because subsequent improvement of the laser characteristics in these thermodynamically opposite cases is usually realized by opposite means. For example, to intensify the ionization mode we must achieve considerable separation of the electron temperature from the gas temperature, while to intensify the recombination mode we must do the opposite, minimizing the electron temperature (for instance by using a light buffer gas).

In cases where relaxation with respect to electronically excited states is determined by collisions with plasma electrons, the characteristic of the type of nonequilibrium and its measure may be deviation of the electron temperature T_e and concentration N_e from Saha distribution. In the case of appreciable influence of plasma-chemical reactions (dissociative recombination, electron sticking and so on) the degree of ionization (as well as the concentration of heavy charged particles) no longer depends only on the electron temperature, but also on the gas temperature, so that we cannot use a simple nonequilibrium criterion. It is necessary to make a direct comparison of the contributions made by the different fluxes to population of the upper laser level. At present the possibility of such a comparison is quite problematic, and therefore we must judge from indirect data.

The nature of nonequilibrium of the active medium for excimers R_2^* is qualitatively analyzed in Ref. 9, 12, 35; the conclusions drawn have been verified by detailed calculations based on the example of a helium plasma [Ref. 73]. There are grounds for believing that R_2^*-lasers operate in the recombination mode[1]. In the framework of recombination concepts it is easy to explain the reduction in delay time with increasing gas density and pumping intensity, the enhanced laser output with addition of a light buffer gas, and the fact that the delay and lasing times may exceed both the pumping duration and the radiative lifetime of the upper working level. Ionization schemes of amplification on Xe_2^* have been discussed as well [Ref. 244, 245]. However, an experimental verification [Ref. 91] of electron-beam controlled pumping [Ref. 245] in the specific case of Xe_2^* did not yield hopeful results, and a more thorough analysis [Ref. 246] of the ionization model of Ref. 244 has shown that it is difficult to realize. Actually, under conditions where it is still possible to prevent the development of instabilities in the discharge, the excimer concentration M^* is limited from above by the critical value $M^* < M_{cr} \approx 10^{16}$ $[p\ (atm)]^{-1}\ cm^{-3}$, since ionization of Xe_2^* and Xe^* by electron impact becomes appreciable long before M_{cr} is reached [Ref. 246]. In the experiments where lasing has been achieved, the population of Xe_2^* was much greater than M_{cr}.

---

[1]When lasing on excimers was achieved, only a few researchers [Ref. 46, 242] believed that the medium was recombination-equilibrium. The possibility of amplification on photodissociative transitions in a recombining plasma was predicted [Ref. 36, 243] even before triggering of the first Xe_2^* lasers.

We can state with full confidence that amplification of the recombinant type takes place on dimers of helium [Ref. 46] and mercury [Ref. 47]. In fact, since the working states of He_2^* and Hg_2^* are not lower excited states, their population by the scheme $A + e \rightarrow A^{**} + e$, $A^{**} + A + A \rightarrow A_2^* + A$ is unlikely because under the conditions of Ref. 46, 47, the characteristic time of deactivation of A** by electrons must be less than the characteristic time of collisional association. Besides, the cross sections of excitation of A by electron impact usually decrease with an increase in the excitation number. Under discharge conditions [Ref. 247], the threshold of amplification on Hg_2^* ($\lambda = 335$ nm) was not reached.

The complicated plasma chemistry of media that amplify on transitions of monoxides and monohalides so far precludes a detailed investigation of the relation between the various channels of formation and destruction of exciplexes RO* and AX*, as well as intermediate and subsidiary compounds (that influence amplification) as a function of the nature of nonequilibrium. Nevertheless, there is no doubt concerning the important part played by recombination mechanisms in amplification in such media. It was pointed out above that the main channel of population of AX* is apparently recombination of a positive and a negative ion, rather than electronic excitation of A that goes off into the harpoon reaction. There are indications [Ref. 115, 161, 248] that the ionization scheme gives an inadequate description of the kinetics in the case of RX*. The authors of Ref. 248 note in particular the unfavorable role of collisions of the first kind with electrons, and also that the addition of helium suppresses these processes.

In the case of lasing on monohalides, one frequently observes effects typical of amplification in the recombination mode (see Ref. 35, §§21, 23). For example, a fall-off in laser output when a heavy buffer gas is substituted for a light one may be due not only to the increase in absorption (in Ref. 51 it was shown that absorption is appreciable close to a wavelength of 351 nm in mixtures of He-Xe-$F_2(NF_3)$ and even He-$F_2(NF_3)$), but also to deterioration of the conditions of cooling of the electron plasma. In Ref. 178 it is noted that there is an increase in efficiency and power of stimulated emission on HgX* when a molecular gas (nitrogen) is added to the working mixtures that is capable of producing intense cooling of the electrons through vibrational-rotational excitation. Two lasing pulses were observed in the afterglow of a brief (about 10 ns) transverse discharge [Ref. 102]. Finally, it is also typical for the recombination mode that current spikes (with transition to unstable operation) are accompanied by rapid cut-off of amplification (for example see the oscillograms given in Ref. 118, 129; cf. 35, §21).

6. Proposed Laser Media

6.1. Diatomic exciplexes. Continuing research in the field of exciplex lasers is tied up mainly with optimizing pumping conditions and the quantitative and qualitative compositions of media that contain molecules

for which laser activity has already been established. Of interest is the possibility of achieving lasing on other known transitions of these exciplexes, in particular $He_2(A^1\Sigma_u^+) \rightarrow He_2(X^1\Sigma_g^+)$, $RX^*(D^2\Sigma_{1/2}) \rightarrow RX(X^2\Sigma_{1/2})$, and $RO^*(F) \rightarrow RO(X)$.

Among these, the most detailed theoretical study has been done on the case of amplification on a photodissociative decay of He_2^* ($\lambda \approx 80$ nm) [Ref. 173]. Calculations indicate attainability of lasing with pumping by an electron beam ($\kappa \gtrsim 10^{-2}$ cm^{-1}) or in a laser spark ($\kappa \gtrsim 1$ cm^{-1}). In this connection, it is necessary to use rather high gas pressures ($p \geqslant 30$ atm) and input power density ($\dot{Q} \gtrsim 100$ MW/cm^3), which when adjusted to beam parameters correspond to a current density $j \gtrsim 30$ kA/cm^2 at an electron energy of about 1 MeV. It is also necessary to reduce the impurity content in the helium down to a content of the order of 10^{-7} or less. It can be assumed that difficulties of about the same magnitude are typical of amplification on the analogous transition of the dimer Ne_2^*, which was mentioned in Ref. 8 as a possible lasing compound.

Under certain conditions, luminescence intensity on transitions $D \rightarrow X$ of molecules such as XeF* and XeCl* may be considerable [Ref. 249, 250]. However, the states $D^2\Sigma_{1/2}$ have a number of properties [Ref. 25, 27] that prevent lasing. Apparently it would be more realistic to achieve lasing on transitions $F \rightarrow X$ of molecules RO*. Here it would make sense to try oxygen donors for which O^- ions are readily produced by dissociative electron sticking. This would ensure rapid population of the lower ionic state F by ion-ion recombination. Consideration should also be given to higher oxides that ionize with difficulty, for which the electron affinity energy is high, such as CrO_3, ClO_2 and others [Ref. 5]. These compounds should actively participate in harpoon reactions with R*.

We note that for reasons which have not yet been understood, lasing has not been attained on transition $B^2\Sigma_{1/2} \rightarrow X^2\Sigma_{1/2}$ of mercury monofluoride, which is analogous to the other mercury monohalides. It is not even clear whether emission has been observed on this transition (see Ref. 19, p 209), which estimates indicate can be anticipated in the visible or near infrared.

The search for new exciplex compounds of promise for amplification is another important area of work in this field. The lack of detailed information not only on plasma-chemical reaction rates, but also on the structure of electronically excited states is a considerable obstacle to prediction of which transitions of what molecules will certainly be convenient for lasing. More often than not, the required information on the exciplex comes to light after the laser on the given compound has already been triggered. Usually the existence of an exciplex is shown by observation of its emission bands, but of course this is not enough to decide the feasibility of lasing. Some additional considerations may be of use here. Let us list the most general requirements for exciplexes

on which effective lasing can be anticipated, and for the laser media based on such exciplexes:

1. The working transition should correspond to a large cross section of induced radiation (evidently larger than 10^{-19} cm^2).

2. The upper working state should have adequate thermal stability. It is undesirable in the extreme for the term of this state to intersect with the dispersion terms close to the minimum energy.

3. Compounds and media are to be preferred that typically have rapid mechanisms of depopulation of the lower working state.

4. The working mixture should be transparent to the radiation that is being amplified, and should be fairly dense.

The existence of thermally stable electronically excited states of molecules of monohydrides of inert gases has been theoretically predicted [Ref. 251, 252]; so far the existence of such states has been reliably established only for HeH* [Ref. 253] and ArH* [Ref. 254]. Structural parameters of the lower covalent state of RH* (R = He, Ne, Ar, Kr) and the characteristics of its photodissociative decay have been estimated in Ref. 255 (see also Ref. 12, 35]. However, the values used there for the parameters of interaction of unexcited atoms of R and H [Ref. 256] were inexact [Ref. 257]. Results of the most recent estimates with consideration of the corrections of Ref. 257 are given in Table 5. In con-

TABLE 5

Estimates of parameters of photodissociative decay of monohydrides of inert gases

(1) Параметр фотоперехода 2 → 1 / (2) Эксиплекс	HeH	NeH	ArH	KrH
λ_0, нм nm	460	300	340	330
$\Delta\omega_{разл}$, эВ eV	3,9	2,9	2,1	1,9
$A \cdot 10^{-8}$, $с^{-1}$ s^{-1}	1,1	3,0	2,0	2,0
$\bar{\sigma}_+ \cdot 10^{17}$, $см^2$	1,0	1,5	1,8	1,9

KEY: 1--Exciplex; 2--Parameter of phototransition 2→1

trast to Ref. 255, the effective line width here was found by projection of the reversal points of the lower vibrational level of RH*, assuming $\hbar\omega_{КОЛ} \approx 0.2$ eV, and the probability of radiative transition was estimated on the basis of oscillator strengths taken from tables in Ref. 258.

Preliminary experimental studies have been done to detect characteristic radiation of RH* [Ref. 259]. It has been established that in a transverse

breakdown, luminescence of R-H_2 mixtures is much brighter in the spectral region of 200-500 nm than that of the individual components (see also Ref. 12). So far, no more weighty proofs of the presence of RH* in the R-H_2 plasma have been found. In Ref. 260, dense neon doped with $H_2(D_2)$ was excited by a short electron beam pulse. A spectral continuum with maximum close to $\lambda \approx 30$ nm was observed in the afterglow. The author of Ref. 260 attributed this maximum to the known transition $H_2(a\,^3\Sigma_g^+) \rightarrow H_2(b\,^3\Sigma_u^+)$; however, the photodissociative transition of NeH* may have similar characteristics. One of the main difficulties in spectroscopic identification of monohydrides is that different particles (H_2^*, H_3^*, H^-, R_2H^* and others) that are present in a plasma of R-H_2 composition can be emitted and absorbed in a single region of the spectrum. It is possible that predissociation of the upper working state plays an appreciable part [Ref. 254]. A sound theoretical analysis of conditions of amplification on monohydrides is not realistic until additional information has been obtained on the structure of terms of RH* and the kinetics of relaxation of the corresponding active medium.

Let us list some of the diatomic exciplexes that have been discussed in the literature as feasible lasing compounds (in connection with the observation of their luminescence bands). Among the inert gas compounds are RMe* [Ref. 186, 261-265], where R = Ar, Kr, Xe; Me = Li, Na, K, Rb, Cs; HgXe* [Ref. 266, 267] and TlXe [Ref. 268]. In addition, compounds of elements of the second group have been proposed: CdHg* [Ref. 269, 270], ZnHg* [Ref. 271], TlHg* [Ref. 272, 273], Cd_2^* [Ref. 274], KMg* [Ref. 275]. Almost all these complexes are poor in meeting the requirements enumerated above, chiefly because of the inability to ensure high density of the working components, considering that we are dealing with photodissociative transitions, and that the energies of dissociation of the excited states are low.

Sulfur and selenium, like oxygen, are capable of forming exciplexes with heavy inert gases. The structure of the terms of RS, RSe and RO is analogous. With an increase in the atomic number of the chalcogen and a reduction in the atomic number of R, there is a considerable drop in the energy of dissociation of the bound state, as evidenced by the luminescence spectra of these molecules [Ref. 276-278]. Lasing has been attained on mixtures of R with donors of S and Se. However, according to Ref. 276 the observed laser lines are more correctly attributed to atomic transitions $^1S_0 \rightarrow {}^1D_2$ and $^1S_0 \rightarrow {}^3P_1$, the forbiddenness being removed by collisions.

6.2. Polyatomic exciplexes. The spectra of spontaneous emission of media that amplify on RX* show wide bands that are of greater wavelengths than for the working transition. These bands correspond to photodissociation of triatomic exciplexes of the R_2X^* type (for example see Ref. 44, 199, 222). The luminescence intensity of R_2X^* increases with increasing content of R and density in the working gas mixture. This explains the current increased interest in R_2X^* as possible lasing

compounds. Potential surfaces have been calculated for Ne_2F [Ref. 279, 280], Ar_2F [Ref. 280-283], Kr_2F [Ref. 280, 283] and Kr_2Cl [Ref. 280]. The results of these calculations show the existence of stable excited states $^2B_2$ with respect to dissociation on $R(^1S) + RX^*(B^2\Sigma_{1/2})$. The estimated parameters of the transition $^2B_2 \rightarrow {}^2A_1$ agree with the observed spectral characteristics. The experimentally determined values of λ_0, the half-widths of bands $\Delta\lambda$ and radiative lifetimes A^{-1} of exciplexes R_2X^* are shown in Table 6. An estimate of σ_+ based on this table gives $\sim 3 \cdot 10^{-18}$ and 10^{-18} cm^2 for Kr_2F^* and Ar_2X^* respectively.

TABLE 6

Characteristics of luminescence of exciplexes R_2X

(1) Параметр фотоперехода $^2B_2 \rightarrow {}^2A_1$ / (2) Эксиплекс	Xe_2F	Xe_2Cl	Kr_2F	Kr_2Cl	Ar_2F	Ar_2Cl	Ne_2F
λ_0, nm (нм)	460*) [284]	450 [284]	400 [284]; 420 [199]	325 [284]	290 [199, 222, 284]	246 [284]	120 [228]
$\Delta\lambda$, nm (нм)	200—300 [284]	—	60 [284]	—	52,5 [284]	—	—
A^{-1}, ns (нс)	—	—	180 [44]	—	185 [222]	—	—

) In Ref. 49, 285 this band is attributed to the transition $C(3/2) \rightarrow A(3/2)$ of the XeF molecule. Apparently there is considerable overlap of the bands XeF* ($C \rightarrow A$) and Xe_2F^* ($^2B_2 \rightarrow {}^2A_1$).

Exciplexes R_2F (R = Ar, Kr) are formed quite rapidly in ternary collisions [see Section 3.3], and also in ion-ion recombination $R_2^+ + F^- + Y$ [Ref. 211, 286] and in harpoon reactions $R_2^* + F_2$ [Ref. 44]. Molecules of F_2 are not much more effective in quenching three-atom exciplexes than for the corresponding diatomic exciplexes [Ref. 44, 222], and quenching of R_2F^* by atoms of R can be disregarded. To judge from the cited data, amplification on Ar_2F^* and Kr_2F^* is realistic. Possible complications may involve absorption, quenching collisions of excited particles ($R_2F^* + RF^*$ or $R_2F^* + R_2F^*$) and predissociation of the upper working state, since the surfaces of $^2B_2$ and of the repulsion states $^2B_1$ and $^2A_1$ may intersect.

The effect of intersection of the surfaces of the hydrogen trimer $^2B_2$ with $^2B_1$ and $^2A_1$ (nuclei situated at the vertices of an isosceles triangle), and $^2A_2'$ with $^2E'$ (in the configuration of an equilateral triangle) has been found on the basis of numerical calculation of H_3^* ($\lambda_0 \approx 430$ nm) [Ref. 287]. The calculations showed that the intersection takes place in the vicinity of the second vibrational level of H_3^* ($^2B_2$).

Moreover, radiative transition $^2A_2''-^2E'$ is forbidden in the equilibrium configuration D_{3h} of the excited molecule. With displacement of the nuclei in the amplitude range of the principal oscillations, the dipole moment of the electronic transition increases rather insignificantly. All this gives ground for considering photodissociation of H_3^* promising for amplification. Four emission bands in the visible and infrared region corresponding to transitions between excited states of H_3^* were recorded in Ref. 288. An investigation of the possibility of lasing on these transitions is clearly of considerable interest, if only for the simplicity and accessibility of the initial medium.

Analogy of the properties of atoms of alkali metals and R* mentioned in Section 1 is also taken into consideration in the search for polyatomic lasing exciplexes. The existence of lower-lying terms can be assumed in compounds of R with electronegative radicals consisting of two or more atoms. The exciplex XeOH is an example of such a compound. The position of the emission band of XeOH* (224 nm) predicted in Ref. 197 has been confirmed in recent research by experimental observations (234 nm) [Ref. 289]. However, the data of Ref. 289 differ considerably from the results of an earlier report [Ref. 290] in which the spectra of XeOH* were also observed.

In conclusion, let us note that the feasibility in principle of lasing on polyatomic exciplexes was established prior to the production of lasers on diatomic exciplexes. In Ref. 291-293, wide-band lasing was realized in alcohol solutions of coumarin derivatives with pumping by a nitrogen laser. The spectral luminescence range and amplification pulse delay time varied depending on the pH of the medium. Lasing was observed in the visible region with a wavelength tuning range of more than 150 nm; a gain of about 4 cm^{-1} was reached, and energy conversion efficiency of about 15%. The radiating exciplexes have been identified as products of addition of a proton to the electronically excited dye molecules. The corresponding scheme of creation of population inversion based on the difference between the rates of electrolytic dissociation of excited and unexcited molecules had been discussed in 1965 [Ref. 294]. Ir Ref. 295, the second harmonic of a ruby laser was used to achieve lasing on the intramolecular exciplex p-(9-anthryl)-N,N-dimethylaniline dissolved in organic liquids. Ref. 291-293, 295 were devoted mainly to proof of the formation of exciplexes in the investigated systems; the lasing parameters found in this research were on the level of the average indices of dye lasers. Therefore it is possible that this work has not attracted due attention of specialists.

On the whole there is no doubt that new active media based on both diatomic and polyatomic exciplexes will take an important place in the development and creation of lasers of subsequent generations.

REFERENCES

1. J. B. Birks, MOL. PHOTOCHEM., Vol 1, 1969, p 157.

2. J. B. Birks, "The Exciplex," N. Y. - San Francisco - London, Acad. Press, Inc., 1975, p 39.

3. S. K. Searles, APPL. PHYS. LETTS, Vol 28, 1976, p 602.

4. V. N. Lisitsyn, A. M. Razhev, A. A. Chernenko, KVANTOVAYA ELEKTRONIKA, Vol 5, 1978, p 424.

5. L. V. Gurvich et al., "Energiya razryva khimicheskikh svyazey. Potentsialy ionizatsii i srodstvo k elektronu" [Breaking Energy of Chemical Bonds. Ionization Potentials and Electron Affinity], Moscow, Nauka, 1974.

6. J. Tellinghuisen, G. C. Tisone, J. M. Hoffman, A. K. Hays, J. CHEM. PHYS., Vol 64, 1976, p 4796.

7. V. S. Zuyev, A. V. Kanayev, L. D. Mikheyev, D. B. Stavrovskiy, "Second All-Union Seminar on Physical Processes in Gas Lasers," Uzhgorod, 1978, p 107.

8. C. K. Rhodes, IEEE J., QE-10, 1974, p 153.

9. L. I. Gudzenko, L. A. Shelepin, S. I. Yakovlenko, USPEKHI FIZICHESKIKH NAUK, Vol 114, 1974, p 457.

10. S. C. Wallace, G. A. Kenney-Wallace, INT. J. RADIAT. PHYS. & CHEM., Vol 7, 1975, p 345.

11. A. V. Dzhonson, Dzh. B. Zherardo, Ye. L. Patterson, R. A. Gerber, Dzh. K. Rays, F. V. Bingem, KVANTOVAYA ELEKTRONIKA, Vol 3, 1976, p 914.

12. L. I. Gudzenko, I. S. Lakoba, S. I. Yakovlenko, TRUDY FIAN [Proceedings of Lebedev Physics Institute], Vol 90, 1976, p 61.

13. V. A. Danilychev, O. M. Kerimov, I. B. Kovsh, ITOGI NAUKI I TEKHNIKI. SERIYA RADIOTEKHNIKA, Moscow, VINITI, Vol 12, 1977, p 174.

14. R. Veynant, KVANTOVAYA ELEKTRONIKA, Vol 5, 1978, p 1767.

15. Ch. P. Vang, KVANTOVAYA ELEKTRONIKA, Vol 5, 1978, p 1771.

16. A. V. Yeletskiy, USPEKHI FIZICHESKIKH NAUK, Vol 125, 1978, p 279.

17. M. Rokni, J. A. Mangano, J. H. Jacob, J. C. Hsia, IEEE J., QE-14, 1978, p 464.

18. Yu. A. Kudryavtsev, ZARUBEZHNAYA RADIOELEKTRONIKA, No 4, 1978, p 106.

19. B. Rosen, "Tables de constantes et données numériques," N. Y. - London - Toronto, Perg. Press, Vol 17, 1970.

20. W. C. Ermler, Y. S. Lee, K. S. Pitzer, N. W. Winter, J. CHEM. PHYS., Vol 69, 1978, p 976.

21. F. Spiegelman, J.-P. Malrieu, CHEM. PHYS. LETTS, Vol 58, 1978, p 214.

22. T. H. Dunning, P. J. Hay, J. CHEM. PHYS., Vol 66, 1977, p 3767.

23. P. J. Hay, T. H. Dunning, Ibid., Vol 66, 1977, p 1306.

24. P. J. Hay, T. H. Dunning, Ibid., Vol 69, 1978, p 134.

25. P. J. Hay, T. H. Dunning, Ibid., Vol 69, 1978, p 2209.

26. W. R. Wadt, APPL. PHYS. LETTS., Vol 34, 1979, p 658.

27. R. E. Drullinger, M. M. Hessel, E. M. Smith, J. CHEM. PHYS., Vol 66, 1977, p 5656.

28. T. A. Cool, J. A. McGarvey, A. C. Erlandson, CHEM. PHYS. LETTS, Vol 58, 1978, p 108.

29. Y. S. Kim, R. G. Gordon, J. CHEM. PHYS., Vol 61, 1974, p 1.

30. W. J. Stevens, M. Gardner, A. Karo, P. Julienne, Ibid., Vol 67, 1977, p 2860.

31. L. E. Brus, J. MOL. SPECTROSC., Vol 64, 1977, p 376.

32. J. Goodman, J. C. Tully, V. E. Bondibey, L. E. Brus, J. CHEM. PHYS., Vol 66, 1977, p 4802.

33. C. A. Brau, J. J. Ewing, Ibid., Vol 63, 1975, p 4640.

34. M. F. Golde, B. A. Thrush, CHEM. PHYS. LETTS., Vol 29, 1974, p 486.

35. L. I. Gudzenko, S. I. Yakovlenko, "Plazmennyye lazery" [Plasma Lasers], Moscow, Atomizdat, 1978.

36. S. I. Yakovlenko, Preprint IAE-2174, Institute of Atomic Energy, Moscow, 1972.

37. M. F. Golde, J. MOL. SPECTROSC., Vol 58, 1975, p 261.

38. A. W. Johnson, J. B. Gerardo, J. CHEM. PHYS., Vol 59, 1973, p 1738.

39. D. J. Bradley, M. Hutchinson, H. Koetser, OPT. COMMS., Vol 7, 1973, p 187.

40. W. H. Weihoffen, J. CHEM. PHYS., Vol 60, 1974, p 445.

41. A. M. Johnson, J. B. Gerardo, J. APPL. PHYS., Vol 44, 1973, p 4120.

42. F. Mies, MOL. PHYS., Vol 26, 1973, p 1233.

43. F. H. K. Rambow, T. D. Bonifield, G. K. Walters, BULL. AM. PHYS. SOC., Vol 23, 1978, p 148.

44. G. P. Quigley, W. M. Hughes, APPL. PHYS. LETTS., Vol 32, 1978, p 649.

45. M. Diegelmann, W. G. Wrobel, K. Hohla, Ibid., Vol 33, 1978, p 525.

46. C. B. Collins, A. J. Cunningham, S. M. Curry, B. W. Johnson, M. Stockton, Ibid., Vol 24, 1974, p 245.

47. L. A. Schlie, B. D. Guenter, R. D. Rathge, Ibid., Vol 28, 1976, p 393.

48. R. Burnham, N. W. Harris, J. CHEM. PHYS., Vol 66, 1977, p 2742.

49. C. H. Fisher, R. E. Center, Ibid. Vol 69, 1978, p 2011.

50. J. G. Eden, S. K. Searles, APPL. PHYS. LETTS, Vol 30, 1977, p 287.

51. M. C. Gower, R. Exberger, P. D. Rowley, K. W. Billman, Ibid., Vol 33, 1978, p 65.

52. C. A. Brau, J. J. Ewing, Ibid., Vol 27, 1975, p 435.

53. R. Burnham, F. X. Powell, N. Djieu, Ibid., Vol 29, 1976, p 30.

54. J. G. Eden, R. W. Waynant, S. K. Searles, R. Burnham, Ibid., Vol 32, 1978, p 733.

55. G. P. Quigley, W. M. Hughes, Ibid., Vol 32, 1978, p 627.

56. R. Burnham, S. K. Searles, J. CHEM. PHYS., Vol 67, 1977, p 5967.

57. R. S. Bradford, E. R. Ault, M. L. Bhaumik, OPT. COMMS., Vol 18, 1976, p 116.

58. A. M. Hawryluk, J. A. Mangano, J. H. Jacob, APPL. PHYS. LETTS, Vol 31, 1977, p 164.

59. J. A. Mangano, J. H. Jacob, M. Rokni, A. M. Hawryluk, Ibid., Vol 31, 1977, p 26.

60. S. K. Searles, G. A. Hart, Ibid., Vol 27, 1975, p 243.

61. J. Tellinghuisen, A. K. Hays, J. M. Hoffman, G. C. Tisone, J. CHEM. PHYS., Vol 65, 1976, p 4473.

62. I. S. Datskevich, V. S. Zuyev, L. D. Mikheyev, I. V. Pogorel'skiy, KVANTOVAYA ELEKTRONIKA, Vol 5, 1978, p 1456.

63. D. L. Cunningham, K. C. Clark, J. CHEM. PHYS., Vol 61, 1974, p 1118.

64. W. M. Hughes, N. T. Olson, R. Hunter, APPL. PHYS. LETTS., Vol 28, 1976 p 81.

65. J. G. Eden, Ibid., Vol 33, 1978, p 495.

66. R. W. Waynant, J. G. Eden, Ibid., Vol 33, 1978, p 708.

67. J. H. Parks, Ibid., Vol 31, 1977, p 297.

68. M. Ghelfenstein, H. Szwarc, R. Lopéz-Delgado, CHEM. PHYS. LETTS, Vol 49, p 312; Vol 52, 1977, p 236.

69. O. Duduit, R. A. Gutcheck, J. L. Calvé, Ibid., Vol 58, 1978, p 66.

70. P. Millet, A. Birot, H. Brunet, J. Galy, B. Pons-Germain, J. L. Teyssier, J. CHEM. PHYS., Vol 69, 1978, p 92.

71. J. W. Keto, R. E. Gleason, T. D. Bonifield, G. K. Walters, F. K. Soley, CHEM. PHYS. LETTS, Vol 42, 1976, p 152.

72. C. B. Collins, A. J. Cunningham, B. W. Johnson, "11-th Int. Conf. on Phen. in Ionized Gases," Prague, 1973, contr. paper, p 31.

73. L. I. Gudzenko, I. S. Lakoba, Yu. I. Syts'ko, S. I. Yakovlenko, Preprint IAE-2912, Institute of Atomic Energy, Moscow, 1977; KVANTOVAYA ELEKTRONIKA, Vol 6, 1979, p 701; USPEKHI FIZICHESKIKH NAUK, Vol 126, 1978, p 699.

74. T. N. Rescigno, A. U. Hazi, A. E. Orel, J. CHEM. PHYS., Vol 68, 1978, p 5283.

75. M. Shimauchi, S. Karasawa, T. Miura, Ibid., Vol 68, 1978, p 5657.

76. R. M. Hill, D. J. Eckstrom, D. C. Lorents, H. H. Nakano, APPL. PHYS. LETTS, Vol 23, 1973, p 373.

77. H. A. Koehler, L. J. Ferderber, R. L. Redhead, P. J. Ebert, Ibid., Vol 21, 1972, p 198.

78. A. W. Johnson, J. B. Gerardo, "11-th Int. Conf. on Phen. in Ionized Gases," Prague, 1973, contr. papers, p 64.

79. P. W. Hoff, J. C. Swingle, C. K. Rhodes, OPT. COMMS., Vol 8, 1973, p 128.

80. P. W. Hoff, J. C. Swingle, C. K. Rhodes, APPL. PHYS. LETTS, Vol 23, 1973, p 245.

81. W. M. Hughes, J. Shannon, A. Kolb, E. Ault, M. Bhaumik, Ibid., Vol 23, 1973, p 385.

82. E. R. Ault, M. R. Bhaumik, W. M. Hughes, R. L. Jenson, C. P. Robinson, A. C. Kolb, J. Shannon, IEEE J, QE-9, 1973, p 1031.

83. M. Novaro, F. Lagarde, C. R. ACAD. SCI., SÉR. B, Vol 277, 1973, p 671.

84. S. C. Wallace, R. W. Dreyfus, R. T. Hodgson, APPL. PHYS. LETTS, Vol 23, 1973, p 672.

85. P. J. Ebert, L. J. Ferderber, H. A. Koehler, R. W. Kuckuck, R. L. Redhead, IEEE J, QE-10, 1974, p 736.

86. A. W. Johnson, J. B. Gerardo, J. APPL. PHYS., Vol 45, 1974, p 867.

87. D. J. Bradley, D. R. Hull, M. H. R. Hutchinson, M. W. McGeoch, OPT. COMMS, Vol 11, 1974, p 335.

88. W. M. Hughes, J. Shannon, R. Hunter, APPL. PHYS. LETTS., Vol 25, 1974, p 85.

89. S. C. Wallace, R. W. Dreyfus, Ibid., Vol 25, 1974, p 498.

90. D. J. Bradley, D. R. Hull, M. H. R. Hutchinson, M. W. McGeoch, OPT. COMMS, Vol 14, 1975, p 1.

91. N. G. Basov, V. A. Danilychev, V. A. Dolgikh, O. M. Kerimov, A. N. Lobanov, A. S. Podsosonnyy, A. F. Suchkov, KVANTOVAYA ELEKTRONIKA, Vol 2, 1975, p 28.

92. G. L. Oomen, M. J. Witteman, "Proc. 4 Colloq. on Electronic Transition Lasers," Munich, 1977, p 49.

93. C. E. Turner, APPL. PHYS. LETTS, Vol 31, 1977, p 659.

94. F. Collier, P. Cottin, OPT. COMMS, Vol 25, 1978, p 89.

95. P. D. Slade, IEEE J., QE-14, 1978, p 637.

96. W. M. Hughes, J. Shannon, R. Hunter, APPL. PHYS. LETTS, Vol 25, 1974, p 488.

97. E. R. Ault, R. S. Bradford, M. L. Bhaumik, Ibid., Vol 27, 1975, p 413.

98. R. Burnham, N. W. Harris, N. Djieu, Ibid., Vol 28, 1976, p 86.

99. C. P. Wang, H. Mirels, D. C. Sutton, S. N. Suchard, Ibid., Vol 28, 1976, p 326.

100. B. Goddard, M. Vannier, OPT. COMMS., Vol 18, 1976, p 206.

101. V. N. Ishchenko, V. N. Lisitsyn, A. M. Razhev, PIS'MA V ZHURNAL TEKHNICHESKOY FIZIKI, Vol 2, 1976, p 839.

102. C. P. Wang, APPL. PHYS. LETTS, Vol 29, 1976, p 103.

103. C. P. Christensen, L. W. Brawerman, W. H. Steier, C. Wittig, Ibid., Vol 29, 1976, p 424.

104. J. A. Mangano, J. H. Jacob, J. B. Dodge, Ibid. Vol 29, 1976, p 426.

105. N. G. Basov, A. N. Brunin, V. A. Danilychev, V. A. Dolgikh, A. G. Degtyarev, O. M. Kerimov, PIS'MA V ZHURNAL TEKHNICHESKOY FIZIKI, Vol 2, 1976, p 1057.

106. R. Burnham, N. Djieu, APPL. PHYS. LETTS, Vol 29, 1976, p 707.

107. Yu. A. Kudryavtsev, N. P. Kuz'mina, KVANTOVAYA ELEKTRONIKA, Vol 4, 1977, p 220.

108. I. V. Tomov, R. Fedosejevs, N. C. Richardson, W. J. Sarjeant, A. J. Alcock, APPL. PHYS. LETTS, Vol 30, 1977, p 146.

109. L. F. Champagne, J. G. Eden, N. W. Harris, N. Djieu, S. K. Searles, Ibid., Vol 30, 1977, p 160.

110. P. G. McKee, B. P. Stoicheff, S. C. Wallace, Ibid., Vol 30, 1977, p 278.

111. C. P. Christensen, Ibid., Vol 30, 1977, p 483.

112. W. J. Sarjeant, A. J. Alcock, K. E. Leopold, Ibid. Vol 30, 1977, p 635.

113. C. H. Fisher, R. E. Center, Ibid., Vol 31, 1977, p 106.

114. S. Watanabe, T. Sato, H. Kashiwagi, OPT. COMMS, Vol 22, 1977, p 143.

115. D. E. Rothe, R. A. Gibson, Ibid. Vol 22, 1977, p 265.

116. V. Hasson, C. M. Lee, R. Exberger, K. W. Billman, P. D. Rowley, APPL. PHYS. LETTS, Vol 31, 1977, p 167.

117. L. F. Champagne, N. W. Harris, Ibid., Vol 31, 1977, p 513.

118. Yu. I. Bychkov, N. V. Karlov, I. N. Konovalov, G. A. Mesyats, A. M. Prokhorov, V. F. Tarasenko, PIS'MA V ZHURNAL TEKHNICHESKOY FIZIKI, Vol 3, 1977, p 1041.

119. I. M. Isakov, A. G. Leonov, V. Ye. Ogluzdin, PIS'MA V ZHURNAL TEKHNICHESKOY FIZIKI, Vol 3, 1977, p 1066.

120. J. Goldhar, J. Dickie, L. P. Bradley, L. D. Pleasanse, APPL. PHYS. LETTS, Vol 31, 1977, p 677.

121. N. G. Basov, V. S. Zuyev, L. D. Mikheyev, D. B. Stavrovskiy, V. I. Yalovoy, KVANTOVAYA ELEKTRONIKA, Vol 4, 1977, p 2453.

122. B. Fontaine, B. Forestier, OPT. COMMS, Vol 25, 1978, p 97.

123. V. Yu. Baranov, V. M. Borisov, F. N. Vysikaylo, S. G. Mamonov, B. B. Kiryukhin, Yu. Yu. Stepanov, "Abstracts of Papers of the Second All-Union Seminar on Physical Processes in Gas Lasers," Uzhgorod, 1978, p 102.

124. C. P. Wang, APPL. PHYS. LETTS, Vol 32, 1978, p 360.

125. L. F. Champagne, N. W. Harris, Ibid., Vol 33, 1978, p 248.

126. L. A. Newman, Ibid., Vol 33, 1978, p 501.

127. M. Mareta, R. Salimbeni, OPT. COMMS, Vol 25, 1978, p 251.

128. I. M. Isakov, A. G. Leonov, V. Ye. Ogluzdin, PIS'MA V ZHURNAL TEKHNICHESKOY FIZIKI, Vol 4, 1978, p 1228.

129. Yu. I. Bychkov, I. N. Konovalov, G. A. Mesyats, V. F. Tarasenko, ZHURNAL TEKHNICHESKOY FIZIKI, Vol 48, 1978, p 1908.

130. V. Yu. Baranov, V. M. Borisov, Yu. B. Kiryukhin, Yu. Yu. Stepanov, KVANTOVAYA ELEKTRONIKA, Vol 5, 1978, p 2285.

131. J. C. Hsia, J. A. Mangano, J. H. Jacob, M. Rokni, APPL. PHYS. LETTS, Vol 34, 1979, p 208.

132. R. M. Hill, P. L. Trevor, D. L. Huestis, D. C. Lorents, Ibid., Vol 34, 1979, p 137.

133. N. G. Vlasov, V. S. Zuyev, A. V. Kanayev, L. D. Mikheyev, D. B. Stavrovskiy, KVANTOVAYA ELEKTRONIKA, Vol 6, 1979, p 1074.

134. W. K. Bishel, H. H. Nakano, D. J. Eckström, R. M. Hill, D. H. Huestis, D. C. Lorents, APPL. PHYS. LETTS, Vol 34, 1979, p 565.

135. J. J. Ewing, C. A. Brau, APPL. PHYS. LETTS, Vol 27, 1975, p 350.

136. G. C. Tisone, A. K. Hays, J. M. Hoffman, OPT. COMMS, Vol 15, 1975, p 188.

137. J. A. Mangano, J. H. Jacob, APPL. PHYS. LETTS, Vol 27, 1975, p 495.

138. M. L. Bhaumik, R. S. Bradford, E. R. Ault, Ibid., Vol 28, 1976, p 23.

139. D. G. Sutton, N. S. Suchard, D. L. Gibb, C. P. Wang, Ibid., Vol 28, 1976, p 522.

140. J. M. Hoffman, A. K. Hays, G. C. Tisone, Ibid., Vol 28, 1976, p 538.

141. J. Goldhar, J. R. Murray, OPT. LETTS, Vol 1, 1977, p 199.

142. N. G. Basov, A. N. Brunin, V. A. Danilychev, O. M. Kerimov, A. I. Milanich, D. D. Khodkevich, PIS'MA V ZHURNAL TEKHNICHESKOY FIZIKI, Vol 3, 1977, p 1297.

143. A. A. Andrews, A. J. Kearsley, C. E. Webb, S. C. Haydon, OPT. COMMS, Vol 20, 1977, p 265.

144. W. J. Sarjeant, A. J. Alcock, K. E. Leopold, IEEE J, QE-14, 1978, p 177.

145. T. R. Loree, K. D. Butterfield, D. L. Barker, APPL. PHYS. LETTS, Vol 32, 1978, p 171.

146. S. Watanabe, S. Shiratori, T. Sato, H. Kashiwagi, Ibid., Vol 33, 1978, p 141.

147. R. W. Waynant, Ibid., Vol 30, 1977, p 234.

148. J. A. Mangano, J. Hisa, J. H. Jacob, B. N. Srivastava, Ibid. Vol 33, 1978, p 487.

149. R. S. Taylor, W. J. Sarjeant, A. J. Alcock, K. E. Leopold, OPT. COMMS, Vol 25, 1978, p 231.

150. J. I. Levatter, R. S. Bradford, APPL. PHYS. LETTS, Vol 33, 1978, p 742.

151. S. Sumida, M. Obara, T. Fujioka, Ibid., Vol 33, 1978, p 913.

152. T. S. Fahlen, J. APPL. PHYS. Vol 49, 1978, p 455.

153. G. L. Oomen, W. J. Witteman, APPL. PHYS. LETTS, Vol 33, 1978, p 878.

154. Yu. A. Kudryavtsev, N. P. Kuz'mina, APPL. PHYS., Vol 13, 1977, p 107.

155. J. Tellinghuisen, J. M. Hoffman, G. C. Tisone, A. K. Hays, J. CHEM. PHYS., Vol 64, 1976, p 2484.

156. V. N. Ischenko, V. N. Lisitsyn, A. M. Razhev, OPT. COMMS, Vol 21, 1977, p 30.

157. Yu. I. Bychkov, V. F. Losev, G. A. Mesyats, V. F. Tarasenko, PIS'MA V ZHURNAL TEKHNICHESKOY FIZIKI, Vol 3, 1977, p 1233.

158. R. Burnham, OPT. COMMS, Vol 24, 1978, p 161.

159. Yu. I. Bychkov, N. V. Karlov, V. F. Losev, G. A. Mesyats, A. M. Prokhorov, V. F. Tarasenko, PIS'MA V ZHURNAL TEKHNICHESKOY FIZIKI, Vol 4, 1978, p 83.

160. M. Maeda, T. Yamashita, Y. Miyazoe, JAP. J. APPL. PHYS., Vol 17, 1978, p 969.

161. J. I. Levatter, J. H. Morris, Shao-Chi Lin, APPL. PHYS. LETTS, Vol 32, 1978, p 630.

162. P. Burlamacchi, R. Salimbeni, OPT. COMMS, Vol 26, 1978, p 233.

163. R. S. Sze, P. B. Scott, APPL. PHYS. LETTS, Vol 33, 1978, p 419.

164. L. F. Champagne, Ibid., Vol 33, 1978, p 523.

165. L. Burlamacchi, P. Burlamacchi, R. Salimbeni, APPL. PHYS. LETTS, Vol 34, 1979, p 33.

166. J. R. Murray, H. T. Powell, Ibid., Vol 29, 1976, p 252.

167. J. G. Eden, S. K. Searles, Ibid., Vol 29, 1976, p 350.

168. J. G. Eden, R. Waynant, J. CHEM. PHYS., Vol 68, 1978, p 2850.

169. R. S. Sze, P. B. Scott, APPL. PHYS. LETTS, Vol 32, 1978, p 479.

170. I. N. Konovalov, V. F. Tarasenko, KVANTOVAYA ELEKTRONIKA, Vol 6, 1979, p 400.

171. H. T. Powell, J. R. Murray, C. K. Rhodes, APPL. PHYS. LETTS, Vol 25, 1974, p 730.

172. N. G. Basov, Yu. A. Babeyko, V. S. Zuyev, L. D. Mikheyev, V. K. Orlov, I. V. Pogorel'skiy, D. B. Stavrovskiy, A. V. Startsev, V. I. Yalovoy, KVANTOVAYA ELEKTRONIKA, Vol 3, 1976, p 930.

173. V. S. Zuyev, L. D. Mikheyev, I. V. Pogorel'skiy, Preprint FIAN, No 279, Lebedev Physics Institute, Moscow, 1978.

174. J. H. Parks, APPL. PHYS. LETTS, Vol 31, 1977, p 192.

175. J. G. Eden, Ibid., Vol 31, 1977, p 448.

176. K. Y. Tang, R. O. Hunter, J. Oldenettel, G. Howton, D. Huestis, D. Ecstrom, D. Perry, M. McCusker, Ibid., Vol 32, 1978, p 239.

177. W. T. Whitney, Ibid., Vol 32, 1978, p 239.

178. R. Burnham, Ibid., Vol 33, 1978, p 156.

179. E. J. Schimitschek, J. E. Celto, J. A. Trias, Ibid., Vol 31, 1977, p 608.

180. E. J. Schimitschek, J. E. Celto, OPT. LETTS, Vol 2, 1978, p 64.

181. S. P. Bazhulin, N. G. Basov, V. S. Zuyev, Yu. S. Leonov, Yu. Yu. Stoylov, KVANTOVAYA ELEKTRONIKA, Vol 5, 1978, p 684.

182. A. N. Didenko, V. P. Grigor'yev, Yu. P. Usov, "Moshchnyye elektronnyye puchki i ikh primeneniye" [Powerful Electron Beams and Their Applications], Moscow, Atomizdat, 1977.

183. I. J. Bigio, IEEE J, QE-14, 1978, p 75.

184. Mod. TAC-11 150 XR, Tachisto, Inc. USA; Mod. EMG-500, Lambda Physik, BRD.

185. D. L. Borovich, V. S. Zuyev, ZHURNAL EKSPERIMENTAL'NOY I TEORETICHESKOY FIZIKI, Vol 58, 1970, p 1794.

186. A. A. Belyayeva, R. B. Dushin, Ye. V. Nikiforov, Yu. B. Predtechenskiy, L. D. Shcherba, DOKLADY AKADEMII NAUK SSSR, Vol 198, 1971, p 1117.

187. S. E. Harris, A. H. Kung, E. A. Stappaerts, J. F. Young, APPL. PHYS. LETTS, Vol 23, 1973, p 232.

188. A. M. Bonch-Bruyevich, S. N. Busov, G. A. Skorobogatov, KVANTOVAYA ELEKTRONIKA, Vol 1, 1974, p 1994.

189. L. I. Gudzenko, L. V. Gurvich, V. S. Dubov, S. I. Yakovlenko, ZHURNAL EKSPERIMENTAL'NOY I TEORETICHESKOY FIZIKI, Vol 73, 1977, p 2067.

190. G. H. Miley, S. J. S. Nagalingam, F. P. Boody, M. A. Prelas, TRANS. AM. NUCL. SOC., Vol 30, 1978, p 26.

191. J. Eden, J. Golden, R. A. Mahaffey, J. A. Pasour, R. W. Waynant, APPL. PHYS. LETTS, Vol 35, 1979, p 133.

192. N. G. Basov, O. V. Bogdankevich, V. A. Danilychev, G. N. Kashnikov, O. M. Kerimov, N. P. Lantsov, KRATKIYE SOOBSHCHENIYA PO FIZIKE, Lebedev Physics Institute, No 7, 1970, p 68.

193. N. G. Basov, V. A. Danilychev, Yu. M. Popov, D. D. Khodkevich, PIS'MA V ZHURNAL EKSPERIMENTAL'NOY I TEORETICHESKOY FIZIKI, Vol 12, 1970, p 473.

194. R. W. Dreyfus, S. C. Wallace, OPT. COMMS, Vol 13, 1975, p 218.

195. G. C. Tisone, E. L. Patterson, J. K. Rice, APPL. PHYS. LETTS, Vol 35, 1979, p 437.

196. R. Hunter, "7-th Winter Colloq. on High Power Visible Lasers," Park City, Utah, Feb 1977.

197. D. J. Bradley, "Proc. 4-th Colloq. on Electronic Transition Lasers," 1977, p 19.

198. O. Cheshnovsky, B. Raz, J. Jortner, CHEM. PHYS. LETTS, Vol 15, 1972, p 475.

199. N. G. Basov, V. A. Danilychev, V. A. Dolgikh, O. M. Kerimov, V. S. Lebedev, A. G. Molchanov, PIS'MA V ZHURNAL EKSPERIMENTAL'NOY I TEORETICHESKOY FIZIKI, Vol 26, 1977, p 20; KVANTOVAYA ELEKTRONIKA, Vol 6, 1979, p 1010.

200. T. G. Finn, L. J. Palumbo, L. F. Champagne, APPL. PHYS. LETTS, Vol 33, 1978, p 148.

201. S. F. Fulgham, I. P. Herman, M. S. Field, A. Javan, Ibid., Vol 33, 1978, p 926.

202. V. Yu. Baranov et al., Preprint IAE, Institute of Atomic Energy, No 3080, Moscow, 1978.

203. G. D. Sides, T. O. Tiernan, J. CHEM. PHYS. Vol 65, 1976, p 3392.

204. Hao-Lin Chen, R. E. Center, D. W. Trainor, W. I. Fyfe, APPL. PHYS. LETTS, Vol 30, 1977, p 99.

205. K. J. Nygaard, S. R. Hunter, J. Fletcher, S. R. Fottyn, Ibid., Vol 32, 1978, p 351.

206. D. W. Trainor, M. J. W. Boness, Ibid., Vol 32, 1978, p 604.

207. B. I. Schneider, C. A. Brau, Ibid. Vol 33, 1978, p 569.

208. L. I. Gudzenko, V. I. Derzhiyev, S. I. Yakovlenko, TRUDY FIAN [Proceedings of Lebedev Physics Institute], Vol 120, 1979.

209. M. R. Flannery, T. P. Yang, APPL. PHYS. LETTS, Vol 32, 1978, p 327.

210. M. R. Flannery, CHEM. PHYS. LETTS, Vol 56, 1978, p 43.

211. M. R. Flannery, T. P. Yang, APPL. PHYS. LETTS, Vol 33, 1978, p 574.

212. G.-H. Chen, M. G. Payne, IEEE J, QE-15, 1979, p 149.

213. V. A. Aleksandrov, V. Yu. Vinogradov, V. V. Lugovskiy, I. V. Podmoshenskiy, OPTIKA I SPEKTROSKOPIYA, Vol 41, 1976, p 390.

214. D. R. Herschbach, ADV. CHEM. PHYS., Vol 10, 1966, p 319.

215. Ye. Ye. Nikitin, "Teoriya elementarnykh atomno-molekulyarnykh protsessov v gazakh" [Theory of Elementary Atomic-Molecular Processes in Gases], Moscow, Khimiya, 1970.

216. J. E. Velazco, J. H. Kolts, B. W. Setser, J. CHEM. PHYS., Vol 65, 1976, p 3468.

217. W. B. Lacina, D. B. Cohn, APPL. PHYS. LETTS, Vol 32, 1978, p 106.

218. H. C. Brashears, D. W. Setser, D. Desmarteau, CHEM. PHYS. LETTS, Vol 48, 1977, p 84.

219. M. Rokni, J. H. Jacob, J. A. Mangano, R. Brochu, APPL. PHYS. LETTS, Vol 32, 1978, p 223.

220. J. H. Jacob, M. Rokni, J. A. Mangano, R. Brochu, Ibid., Vol 32, 1978, p 109.

221. M. Rokni, J. H. Jacob, J. A. Mangano, R. Brochu, Ibid., Vol 31, 1977, p 79.

222. C. H. Chen, M. G. Payne, J. P. Judish, J. CHEM. PHYS., Vol 69, 1978, p 1626.

223. A. Mandl, J. H. Parks, APPL. PHYS. LETTS, Vol 33, 1978, p 498.

224. M. Rokni, J. H. Jacob, J. A. Mangano, R. Brochu, Ibid., Vol 30, 1977, p 458.

225. H. C. Brashears, D. W. Setser, APPL. PHYS. LETTS, Vol 33, 1978, p 821.

226. J. G. Eden, R. W. Waynant, Ibid., Vol 34, 1979, p 324.

227. B. L. Borovich, V. S. Zuev, D. B. Stavrovsky, J. QUANT. SPECTRY RAD. TRANSFER, Vol 13, 1973, p 1241.

228. J. K. Rice, A. K. Hays, J. R. Woodworth, Ibid., Vol 32, 1977, p 31.

229. J. A. Mangano, J. H. Jacob, J. J. Ewing, OPT. COMMS, Vol 18, 1976, p 205.

230. S. K. Searles, G. A. Hart, APPL. PHYS. LETTS, Vol 28, 1976, p 384.

231. C. J. Ultee, CHEM. PHYS. LETTS, Vol 46, 1977, p 366.

232. S. C. Wallace, R. T. Hodgson, R. W. Dreyfus, APPL. PHYS. LETTS, Vol 23, 1973, p 22.

233. K. J. McCann, M. R. Flannery, Ibid., Vol 31, 1977, p 599.

234. D. E. Rothe, PHYS. REV., Vol 177, 1969, p 93.

235. A. Mandl, Ibid., Vol A3, 1971, p 251.

236. J. T. Moseley, R. P. Saxon, B. A. Huber, P. C. Cosby, R. Abouaf, M. Tradjeddine, J. CHEM. PHYS., Vol 67, 1977, p 1659.

237. W. R. Wadt, D. C. Cartwright, J. C. Cohen, APPL. PHYS. LETTS, Vol 31, 1977, p 672.

238. C. F. Bender, N. W. Winter, Ibid., Vol 33, 1978, p 29.

239. J. A. Vanderhoff, J. CHEM. PHYS., Vol 68, 1978, p 3311.

240. M. Rokni, J. H. Jacob, J. A. Mangano, APPL. PHYS. LETTS, Vol 32, 1978, p 622.

241. R. O. Hunter, J. Oldenettel, C. Howton, BULL. AM. PHYS. SOC., Vol 23, 1978, p 135.

242. E. V. George, C. K. Rhodes, APPL. PHYS. LETTS, Vol 23, 1973, p 139.

243. L. G. Gudzenko, S. I. Yakovlenko, DOKLADY AKADEMII NAUK SSSR, Vol 207, 1972, p 1085.

244. M. M. Mkrtchyan, V. T. Platonenko, PIS'MA V ZHURNAL EKSPERIMENTAL'-NOY I TEORETICHESKOY FIZIKI, Vol 17, 1973, p 28.

245. A. G. Molchanov, Yu. M. Popov, KVANTOVAYA ELEKTRONIKA, Vol 1, 1974, p 1122.

246. M. M. Mkrtchyan, V. T. Platonenko, KVANTOVAYA ELEKTRONIKA, Vol 3, 1976, p 2562.

247. E. R. Mosburg, M. Wilke, J. CHEM. PHYS., Vol 66, 1976, p 5682.

248. J. G. Eden, S. K. Searles, APPL. PHYS. LETTS, Vol 29, 1976, p 356.

249. J. E. Velazco, J. H. Kolts, D. W. Setser, J. A. Coxon, CHEM. PHYS. LETTS, Vol 46, 1977, p 99.

250. R. Shuker, APPL. PHYS. LETTS, Vol 29, 1976, p 785.

251. H. H. Michels, F. E. Harris, J. CHEM. PHYS., Vol 39, 1963, p 1464.

252. V. Bondybey, P. K. Pearson, H. F. Schaefer, J. CHEM. PHYS., Vol 57, 1972, p 1123.

253. J. Gray, R. H. Tomlinson, CHEM. PHYS. LETTS, Vol 4, 1969, p 251.

254. J. W. C. Johns, J. MOL. SPECTROSC., Vol 36, 1970, p 448.

255. L. I. Gudzenko, I. S. Lakoba, KRATKIYE SOOBSHCHENIYA PO FIZIKE, No 6, 1975, p 3.

256. Yu. N. Belyayev, N. V. Kamyshov, V. B. Leonas, KHIMIYA VYSOKIKH ENERGIY, Vol 4, 1970, p 260.

257. V. B. Leonas, USPEKHI FIZICHESKIKH NAUK, Vol 107, 1972, p 29.

258. L. A. Vanshteyn, I. I. Sobel'man, Ye. A. Yukov, "Secheniya vozbuzhdeniya atomov i ionov elektronami" [Electronic Excitation Cross Sections of Atoms and Ions], Moscow, Nauka, 1973.

259. L. I. Gudzenko, L. A. Kulevskiy, I. S. Lakoba, A. A. Medvedev, KRATKIYE SOOBSHCHENIYA PO FIZIKE, No 1, 1976, p 21.

260. J. K. Rice, BULL. AM. PHYS. SOC., Vol 21, 1976, p 155.

261. A. A. Belyayeva, R. B. Dushin, Yu. B. Predtechenskiy, L. D. Shcherba, DOKLADY AKADEMII NAUK SSSR, Vol 199, 1971, p 628.

262. A. C. Tam, G. Moe, R. B. Bulos, W. Hopper, OPT. COMMS, Vol 16, 1976, p 376.

263. J. G. Eden, B. E. Cherrington, J. T. Ferdeyen, IEEE J, QE-12, 1976, p 698.

264. J. Marek, J. PHYS., B10, 1977, p L325.

265. K. Tachibana, M. Ohara, Y. Urano, JAP. J. APPL. PHYS., Vol 16, 1977, p 1859.

266. J. R. Woodworth, BULL. AM. PHYS. SOC., Vol 21, 1976, p 155.

267. L. K. Lam, A. Gallagher, R. Drullinger, J. CHEM. PHYS., Vol 68, 1978, p 4411.

268. L. A. Schlie, D. A. Drummond, BULL. AM. PHYS. SOC., Vol 23, 1978, p 155.

269. G. R. Fournier, M. W. McGeoch, OPT. COMMS, Vol 18, 1976, p 121.

270. M. W. McGeoch, G. R. Fournier, P. Ewart, J. PHYS. B9, 1976, p L121.

271. J. G. Eden, OPT. COMMS, Vol 25, 1978, p 201.

272. D. L. Drummond, L. A. Schlie, J. CHEM. PHYS., Vol 65, 1976, p 3554.

273. R. B. Benedict, L. A. Schlie, D. L. Drummond, BULL. AM. PHYS. SOC., Vol 23, 1978, p 142.

274. R. E. Drullinger, M. Stock, J. CHEM. PHYS., Vol 68, 1978, p 5299.

275. D. J. Benard, P. J. Love, W. D. Slafer, CHEM. PHYS. LETTS, Vol 48, 1977, p 321.

276. J. R. Murray, C. K. Rhodes, J. APPL. PHYS., Vol 47, 1976, p 5041.

277. G. Black, R. J. Sharpless, T. G. Slanger, J. CHEM. PHYS., Vol 69, 1978, p 794.

278. R. V. Taylor, W. C. Walker, APPL. PHYS. LETTS, Vol 35, 1979, p 359.

279. C. F. Bender, H. F. Schaefer, CHEM. PHYS. LETTS, Vol 53, 1978, p 27.

280. N. E. Schlotter, D. L. Huestis, BULL. AM. PHYS. SOC., Vol 23, 1978, p 132.

281. H. H. Michels, R. H. Hobbs, L. A. Wright, CHEM. PHYS. LETTS, Vol 48, 1977, p 158.

282. W. R. Wadt, P. J. Hay, APPL. PHYS. LETTS, Vol 30, 1977, p 573.

283. W. R. Wadt, P. J. Hay, J. CHEM. PHYS. Vol 68 1978, p 3850.

284. D. C. Lorents, D. L. Huestis, M. W. McCusker, H. H. Nakano, R. M. Hill, Ibid., Vol 68, 1978, p 4657.

285. D. Kliegler et al., APPL. PHYS. LETTS, Vol 33, 1978, p 39.

286. M. R. Flannery, T. P. Yang, Ibid., Vol 32, 1978, p 357.

287. L. I. Gudzenko, A. I. Dement'yev, I. S. Lakoba, V. Ya. Simkin, TRUDY FIAN [Proceedings of Lebedev Physics Institute], Vol 120, 1979.

288. G. Herzberg, J. CHEM. PHYS., Vol 70, 1979, p 4806.

289. M. H. R. Hutchinson, CHEM. PHYS. LETTS, Vol 54, 1978, p 359.

290. J. Goodman, L. E. Brus, J. CHEM. PHYS., Vol 67, 1977, p 4858.

291. C. V. Shank et al., APPL. PHYS. LETTS, Vol 16, 1970, p 405.

292. A. Diens, C. V. Shank, A. M. Trozzolo, Ibid., 1970, p 189.

293. C. V. Shank, A. Diens, W. T. Silfvast, Ibid., Vol 17, 1970, p 307.

294. M. G. Kuz'min, in: "Elementarnyye protsessy khimii vysokikh energiy" [Elementary Processes in High-Energy Chemistry], Moscow, Nauka, 196, p 304.

295. N. Nakashima, N. Mataga, C. Yamanaka, R. Ide, S. Misumi, CHEM. PHYS. LETTS, Vol 18, 1973, p 386.

[155-6610]

6610
CSO: 1862

UDC 533.9.011+621.378.53

A CLOSED-CYCLE GASDYNAMIC CO_2 LASER WITH GAS SEPARATOR

Moscow KVANTOVAYA ELEKTRONIKA in Russian Vol 7, No 4(94), Apr 80
pp 764-769

[Article by A. G. Velikanov, N. M. Gorshunov, I. S. Knyazev, N. I. Lagunov, Yu. P. Neshchimenko and G. A. Sulaberidze, Moscow Engineering Physics Institute]

[Text] At the present time among CO_2 gasdynamic lasers the greatest specific powers and efficiencies are realized on devices with selective heating of nitrogen, and admixture of CO_2-He in the supersonic nozzle. Calculations have shown the feasibility of further raising specific energy of emission to 200 J/cm^3 [Ref. 1] and efficiency to 2-3% in lasers with an open gasdynamic cycle.

Closed-cycle gasdynamic lasers provide the opportunity for using the thermal energy that remains in the working gas after passage through the resonator, which should additionally increase efficiency to 5-10% [Ref. 2]. Thus the efficiency of a closed-cycle gasdynamic laser with selective heating may approach that of electric-discharge lasers with pumping of the gas. Besides, when selective heating is used the molecules do not enter the heater, and consequently the working mixture remains usable much longer than in electric-discharge lasers. Despite these advantages, according to Ref. 1 the closed-cycle gasdynamic laser has not yet been realized, although it is in the developmental phase.

Development of a closed-cycle gasdynamic laser with heating of the entire working mixture is scarcely feasible since the CO_2 molecules would be dissociated in the heater, and the mixture would soon be unusable. The main difficulty in creating a closed-cycle gasdynamic laser with selective heating of nitrogen is separation of the stream of working fluid into nitrogen and CO_2-He after passage through the cavity.

We propose that a cascade consisting of membrane type separating stages be used as the gas separator in the gasdynamic laser. This enables separation of the nitrogen from the radiating CO_2 gas and the relaxant gases. A gasdynamic laser design is being considered with selective heating of nitrogen and a gas separator, as shown in Fig. 1.

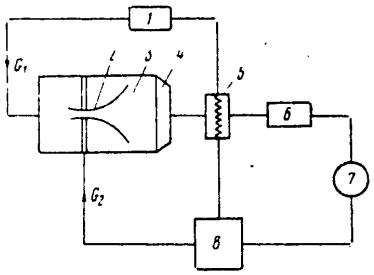

Fig. 1. Diagram of gasdynamic laser with selective heating of nitrogen and a gas separator

A stream of nitrogen G_1 with stagnation pressure p_{01} and stagnation temperature T_{01} comes from heater 1 into the supersonic nozzle system 2. In the supersonic part of the nozzles, stream G_2 (CO_2-He) is mixed with the flow. This stream has stagnation pressure p_{02} and stagnation temperature of 300 K. After mixing and cooling in the supersonic nozzle, the working mixture $G = G_1 + G_2$ with stagnation parameters p_0, T_0 goes to the region of resonator 3, and then to diffuser 4. It is assumed that the coefficient of losses of dynamic pressure is σ_N in the nozzle and σ_D in the diffuser, and that the compressor raises the the pressure of the working mixture from $\sigma_N\sigma_D p_0$ to p_{01}. It was assumed that heat exchanger 5 equalizes the temperatures of the streams of nitrogen coming from gas separator 8, and the temperature of the working mixture coming from the diffuser, resulting in a temperature

$$T_5 = (c_{pN_2} G_1 \cdot 300\ \text{K} + \Sigma c_{pi} T_0 G_i)/(G_1 c_{pN_2} + \Sigma c_{pi} G_i).$$

In cooler 6, the temperature of the mixture is reduced from T_5 to 300 K, and in heater 1 the temperature of the nitrogen is raised from T_5 to T_{01}. The powers taken by the compressors were calculated for isothermal gas compression.

The gas mixture is separated on polymer membranes as a result of the different rates of diffusion of the mixture components through the membrane [Ref. 3]. The equipment used is simple in design and comparatively inexpensive. The packing density in the elements of the film membranes is 800-1000 m^2/m^3, and in the elements of membranes in the form of hollow fibers -- up to 5000 m^2/m^3 [Ref. 3]. The process can take place at ambient temperature, and is not accompanied by phase transformations. The flow of separated mixture is readily changed by appropriately changing the area of the membranes in the elements.

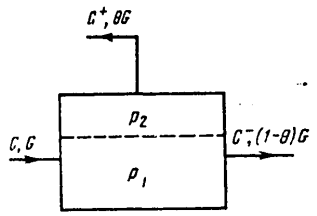

Fig. 2. Diagram of a membrane separating element

Fig. 2 shows a diagram of a membrane separating element. The stream of gas mixture G with concentration C of the more penetrating component enters the element. After passage over the membrane, the concentration of this component falls to C^-. Part of the flow θG passes through the membrane, and in doing so becomes enriched with the more penetrating component to concentration C^+. The process of separation depends on the

value of the coefficient of flow division θ, dynamic gas pressures p_1 and p_2 in the cavities preceding and following the membrane, the penetration factors of the components of the mixture for the given material of the membrane, and the gasdynamic currents in the element.

The membrane material should be chosen so that the penetration factor of nitrogen differs appreciably from that of the other components of the mixture. This requirement is met by a membrane of polyvinyltrimethylsilane polymer (PVTMS). The penetration factors of components used in working mixtures are summarized in Table 1 for this membrane [Ref. 4].

TABLE 1

Gas	CO_2	He	H_2	N_2
Q, $\frac{nm^3 \cdot m}{m^2 \cdot s \cdot N/m^2}$	$1.67 \cdot 10^{-15}$	$1.38 \cdot 10^{-15}$	$1.8 \cdot 10^{-15}$	$8.1 \cdot 10^{-17}$

This table shows that the penetration factors for nitrogen are much lower than those of carbon dioxide, helium and hydrogen. This means that nitrogen can be effectively separated from the mixture since it will penetrate the membrane much more poorly than the other components. Also note that the penetration factors of CO_2, He and H_2 are similar in magnitude, so that the mixture to be separated can be treated as a two-component mixture.

Since it is impossible to attain the required degree of separation on a single element, a cascade must be used that consists of several elements connected in series. The arrangement for connecting the elements can be the simplest symmetric arrangement of a counterflow cascade in which the streams enriched with the more penetrating component on each stage are fed to the inputs of the next stages, and those with lower concentration of the more penetrating component are fed to the inputs of the preceding stages. A diagram of a symmetric cascade is shown in Fig. 3.

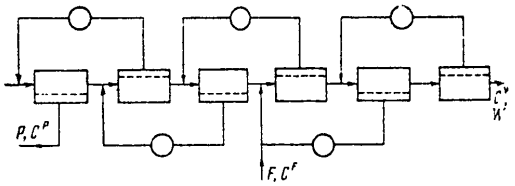

Fig. 3. Diagram of a symmetric separating cascade

As the mixture to be separated circulates in the cascade, the concentration of nitrogen as the less penetrating component will increase toward the last stage, from which a sample is taken with nitrogen

concentration C^W. Contrariwise, the concentration of nitrogen will decrease toward the first stage, and as a result a mixture will be obtained in flow P that is nitrogen-depleted to concentration C^P. Supply F with nitrogen concentration C^F is fed to some intermediate stage in the cascade.

Since the overall area of the membranes in the cascade and inputs of electric energy must be minimized, it is advisable to use a cascade in which there is no mixing of flows with different concentrations at the inlets to the elements, and as a result there are no thermodynamic losses of work on separation of the mixture due to mixing.

In calculation it was assumed that the pressure of the mixture at the inlets to the elements was constant along the entire cascade, and the compressors that raise gas pressure from p_2 to p_1 are situated on lines of the fractions that penetrate through the membranes [Fig. 3].

For the sake of definiteness it was also assumed that the cascade consists of elements in which no longitudinal intermixing takes place in the high-pressure cavity, while the gas flow in the low-pressure cavity is directed perpendicular to the surface of the membrane. The method of calculating these elements is given in Ref. 5.

The cascade was designed by a technique developed on the basis of the general theory of designing cascades with arbitrary enrichment on an element [Ref. 6, 7]. This technique enables calculation of all possible modifications of cascades for given values of the concentrations in the supply and at the output.

An estimate of the efficiency of a laser configured as shown in Fig. 1 was done for three modes of laser operation. The parameters of these working conditions are summarized in Table 2, where w_L is specific lasing power corresponding to a working gas flowrate G = 1 g/s.

TABLE 2

Mode Режим	Mixture Состав смеси	T_{01}, K	p_{01}, атм	p_{02}, атм	J/g w_L, Дж/г
1	CO_2:N_2:He = 14,2:28,8:57	1900	8,0	4,0	17,5
2	CO_2:N_2:He = 45,4:44,6:10	2780	14,0	2,7	54,0
3	CO_2:N_2:H_2:He = 32:45,5:6,5:16	2000	48,8	25,8	6,5

Mode 1 was experimentally realized on a laser facility with quasi-cw operation [Ref. 8]. This paper does not give the stagnation pressure of the ejected gas p_{02}, but only the pressure in the valve before it opens. By numerical calculation of the gain for mode 1 on a computer at different values of p_{02}, we found that when p_{02} = 1 atm, the calculated

gain coincides with that measured in Ref. 8. The specific lasing output power of 25 J/g given in Ref. 8 was calculated without consideration of the flowrate of the ejected gas. In calculating the overall flowrate for mode 1 we get $w_L = 17.5$ J/g.

Mode 2 is obtained as a result of analytical multiparameter optimization of the parameters of a gasdynamic laser with selective heating of nitrogen with respect to weak-signal gain on line P (20) in the 10.6 μm band [Ref. 9]. The quantity w_L was calculated from an approximate formula for the power of the gasdynamic laser with a cavity having a flow length that gives maximum energy extraction, while the reflectivities of the mirrors are the optimum with consideration of gain saturation. According to our calculations, mode 3 is close to optimum for maximum gain in the 16 μm band in the case of cascade lasing of a gasdynamic laser with pulsed Q-switching first triggered in Ref. 10. For pulsed lasing, w_L is calculated as the average lasing power $w = Ev/XG$, where E is the energy of a lasing pulse in the 16 μm band, v is the flowrate of the working gas in the resonator, X is the length of the resonator mirrors along the flow. It is implied that the Q-switching frequency of the cavity corresponds to the time of flight of the gas through the cavity.

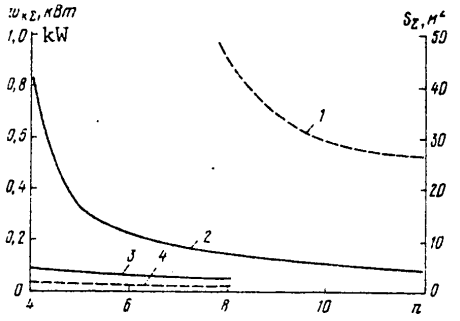

Fig. 4. Total area of membranes S_Σ (1, 2) and total power $w_{k\Sigma}$ (3, 4) consumed by the compressors of the separator in modes 1 (1, 3) and 3 (2. 4) as a function of the number of stages n in the cascade

The parameters of the gas separator (Fig. 4) were taken so as to ensure cv operation of the laser facility with the parameters shown in Table 2. the nitrogen concentration at the takeoff was $C^W = 0.99$. To extend the life of the working mixture and increase the laser efficiency it is desirable to take $C^W = 1$; however, as C^W approaches unity there is a considerable increase in the required membrane area and in the energy consumed by the compressors. The necessary parameters of the separated flows can be obtained in several versions that differ in the number of stages.

Fig. 4 shows the way that the number of stages in the cascade depends on the overall area of the membranes S_Σ and the overall power $w_{k\Sigma}$ consumed by the compressors of the separator in modes 1 and 3. The given values of S_Σ and $w_{k\Sigma}$ ensure separation of a unit flow ($G = 1$ g/s) of the given working mixtures.

The figure shows that the area of the membranes and the consumption of electric energy decrease with an increase in the number of stages right

up to the maximum number possible for the given scheme of stage connection and the given values of concentrations in the external flows of the cascade. The efficiency of these lasers is defined as

$$\eta = w_L/(w_{heat} + w_{k\Sigma} + w_{comp}),$$

where w_{heat}, $w_{k\Sigma}$, w_{comp} are the specific expenditures on heating, compression in the compressors of the separator, and in compressor 7 (see Fig. 1) respectively.

The values of w_L were taken from Table 2, and the corresponding specific expenditures of energy were calculated as $w_{heat} = c_{pN_2}(T_{01} - T_5)[N_2]\mu$, where c_{pN_2} is molecular heat; $[N_2]$ is the mole fraction of nitrogen in the mixture, μ is the molecular weight of the mixture; $w_{comp} = 10.4T \times \ln(p_{01}/\sigma_N\sigma_D p_0)/\mu$. Since the Mach number in the resonator is close to 5 for the three given modes, it was assumed that $\sigma_N = 0.3$ and $\sigma_D = 0.15$ (see Ref. 11); $w_{k\Sigma}$ was taken as equal to the minimum value of the corresponding quantity on the curve of Fig. 4. The results of calculations of specific losses and efficiencies are summarized in Table 3.

TABLE 3

Mode	w_{heat}, J/g	$w_{k\Sigma}$, J/g	w_{comp}, J/g	η, %
1	157	802	715	1.1
2	109	503	397	5.4
3	156	431	560	0.6

This table shows that a considerable part of the energy input in the given laser is used on the compressors in the gas separator. The efficiency of the laser facility should increase when η is optimized with consideration of w_{heat}, $w_{k\Sigma}$ and w_{comp}. Such optimization was not done in our research. Despite this, the overall efficiency of the laser in mode 2 is comparable to that of open-cycle electric discharge lasers that emit in the 10.6 μm band. The advantage of the proposed laser over conventional designs is the much greater service life of the working mixture, which is important when developing cw lasers for technological operations.

REFERENCES

1. A. Gertsberg, RAKETNAYA TEKHNIKA I KOSMONAVTIKA, Vol 16, No 2, 1978.

2. S. A. Losev, "Gazodinamicheskiye lazery" [Gasdynamic Lasers], Moscow, Nauka, 1977.

3. "Tekhnologicheskiye protsessy s primeneniyem membran" [Technological Processes Using Membranes], Moscow, Mir, 1976, chapter 13.

4. "Vsespyuznaya konferentsiya po membrannym metodam razdeleniya smesey. Tezisy dokladov" [All-Union Conference on Membrane Methods of Separating Mixtures. Abstracts of the Papers], Moscow, 1973.

5. N. I. Nikolayev et al., TEORETICHESKIYE OSNOVY KHIMICHESKOY TEKHNOLOGII, Vol 13, No 10, 1979.

6. N. A. Kolokol'tsov, N. I. Laguntsov, ATOMNAYA ENERGIYA, Vol 27, 1969, p 560.

7. N. I. Laguntsov, ATOMNAYA ENERGIYA, Vol 35, 1973, p 205.

8. A. V. Krauklis, V. M. Kroshko, R. I. Soloukhin, N. A. Fomin, FIZIKA GORENIYA I VZRYVA, Vol 12, 1976, p 792.

9. A. G. Velikanov, N. M. Gorshunov, Yu. A. Kunin, Yu. P. Neshchimenko, "Report of Moscow Engineering Physics Institute," reg. No 78039336, 1977.

10. T. J. Manuccia, J. A. Stregack, N. W. Harris, B. L. Wexler, APPL. PHYS. LETTS, Vol 29, 1976, p 360.

11. G. N. Abramovich, "Prikladnaya gazovaya dinamika" [Applied Gas Dynamics], Moscow, Nauka, 1969.

[155-6610]

6610
CSO: 1862

UDC 621.378.324

PROSPECTS FOR USING AN AC DISCHARGE TO PUMP FAST-FLOW CLOSED-CYCLE CARBON DIOXIDE TECHNOLOGICAL LASERS

Moscow KVANTOVAYA ELEKTRONIKA in Russian Vol 7, No 4(94), Apr 80
pp 775-780

[Article by A. V. Kondarenko, V. D. Gavrilyuk, V. S. Golubev, F. V. Lebedev and M. M. Smakotin]

[Text] 1. The extensive prospects that have been noted in recent years on the introduction of laser technology for cutting, welding, heat treatment and doping metals and alloys call for the development of powerful CO_2 lasers, which are characterized by high economy, simplicity, reliability and compactness. Among the numerous pumping methods that have been proposed for pumping in such systems, the AC discharge technique deserves particular attention [Ref. 1, 2]. The use of this method eliminates the need for ballast resistors, and the associated losses of energy, which in the case of a transverse DC discharge may reach 30-50% [Ref. 3] of the total energy taken from the power supply, and also simplifies the design of the gas discharge chamber in the case where a capacitive discharge is used [Ref. 1, 2]. Another reason for interest in use of an AC discharge is the availability of Soviet-made compact stationary power supplies with frequency of 10 kHz or less that have a specific power output of 50-100 kW from one cu. m of structure, with output power of up to 250 kW. The very earliest research on the characteristics of a transverse AC discharge with frequency of 10 kHz showed that its total oscillatory efficiency η_{osc} in a nitrogen stream exceeds 60% [Ref. 2], and the total efficiency η of a CO_2 laser using an AC discharge for pumping may reach 13-15% [Ref. 4].

In this paper we investigate the outlook for using such a discharge to pump fast-flow technological CO_2 lasers. We give data on the specific characteristics of an AC discharge with frequency of 10 kHz for different working mixtures under conditions of an increased interelectrode gap, on limiting energy inputs and amplification factors of the medium under closed-cycle conditions, and also discuss the feasibility of producing a technological laser with power of 25-50 kW based on the investigated type of discharge.

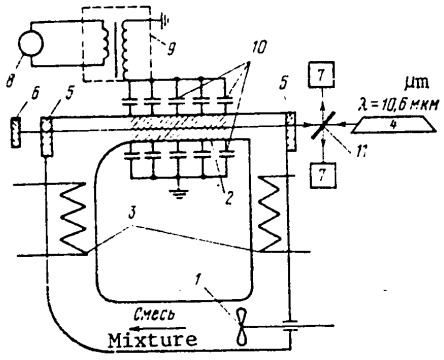

Fig. 1. Diagram of the experimental facility: 1--circulating unit; 2--gas-discharge chamber; 3--heat exchangers; 4--diagnostic laser; 5--KCl windows; 6--metal mirror; 7--power meter; 8--motor-generator set; 9--step-up transformer; 10--ballast capacitors; 11--beam splitter

2. Most of the experimental results were obtained on a closed-cycle facility (Fig. 1) comprising a gasdynamic channel that consists of circulating unit 1, gas-discharge chamber 2, two heat exchangers 3 and gas lines. The volumetric flowrate of the gas mixture circulating through the loop was about 400 liters per second. The dielectric discharge chamber had the form of a rectangular channel with cross section of 60 x 80 mm. The flow length of the discharge zone was 600 mm. The electrode plates were the upper and lower walls of the discharge chamber containing an array of copper rods about 2-4 mm in diameter separated by a space of 12 mm. Capacitor 10 of 47-100 pF was connected in the circuit of each electrode. The discharge power supply was electric generator 8 with frequency of 10 kHz, and step-up transformer 9. The working mixture (N_2--50%, He--40-48.5%, CO_2--1.5-10% by volume) was pumped through the discharge chamber at a rate of 80 m/s with static pressure from 30 to 80 mm Hg. The mixture was not replenished during the experiment. Leakage of atmospheric air into the loop did not exceed 0.3 mg/s.

The gain of the medium was determined by diagnostic CO_2 laser 4 stabilized on vibrational-rotational transition P(18). The integral amplification of weak-intensity radiation with double pass of a beam along the gas flow was measured in the experiment.

3. The electrode plate design that was used enabled us to raise the parameters jE (j is the density of the discharge current, E is the electric field) and W_g corresponding to the specific volumetric and mass energy inputs to the AC discharge as compared with the results of our earlier research [Ref. 2, 4]. Under closed-cycle conditions for the given mixture at pressures of 30-50 mm Hg and an interelectrode gap of 60 mm, the values of W_g for diffuse discharge combustion reached 500-700 J/g, and the value of jE was about 4.5-5 W/cm^3 when the discharge length along the flow was $l = 600$ mm, and about 7-8 W/cm^3 at $l = 300$ mm.

Data on the limiting energy inputs to various lasing mixtures that can be achieved under open-cycle conditions with an interelectrode gap of about 10 cm and $l = 20$ cm are summarized in the table. The limiting values of jE increased with increasing flow velocity v and fell with increasing length l of the discharge zone $\sim 1/\sqrt{l}$.

TABLE

Working Mixture	p, mm Hg	v, m/s	jE, W/cm^3	W_g, J/g
50% He + 45% N_2 + 5% CO_2	50	100	6-7	250-300
50% He + 45% N_2 + 5% CO_2	50	50	4.5-5	350-400
20% air + 75% N_2 + 5% CO_2 + 0.2% H_2O	30	100	5-5.5	200-220
95% air + 5% CO_2	25	100	4.5-5	210-240

According to the results of the experiments, the integral gain of the diagnostic laser J/J_0 depends on the CO_2 content X_{CO_2} in the mixture, the pressure p of the mixture, the power input to the discharge, and also the duration of continuous operation of the facility.

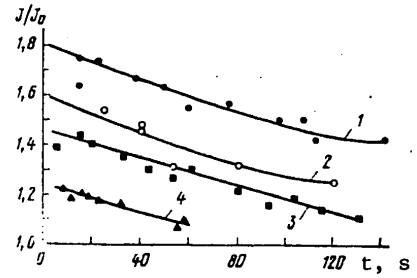

Fig. 2. Integral gain of diagnostic laser signal as a function of the operating time of the unit: l = 60 cm, p = 30 (1, 2) and 50 mm Hg (3, 4); X_{CO_2} = 2, 5 (1), 5 (2, 3) and 7.5% (4); X_{N_2} = 50%; X_{He} = 47.5 (1), 45 (2, 3) and 42.5% (4); W_g = 390 (1, 2) and 340 J/g (3, 4)

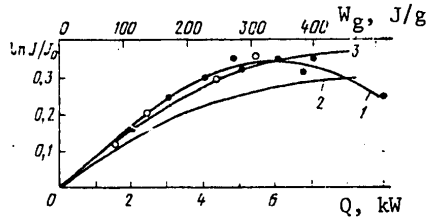

Fig. 3. $\ln J/J_0$ as a function of the mass energy input: mixture 50% N_2 + 47.5% He + 2.5% CO_2; p = 50 mm Hg; 1--experiment at l = 30 (○) and 60 (●) cm; 2--calculation at l = 60 cm, η_{osc} = 0.6, η_T = 0.25; 3--calculation for l = 60 cm, η_{osc} = 0.75, η_T = 0.15

Typical behavior of time dependences of J/J_0 for different values of X_{CO_2} and p at optimum values of W_g is shown in Fig. 2. Fig. 3 shows the experimental curves for $\ln (J/J_0) = 2\int k_0\, dx$ (k_0 is the gain of the medium) as a function of the electric power input to the discharge Q and W_g for different flow lengths of the discharge l. This figure also shows the calculated curves for $\ln J/J_0$ (W_g) for two versions of energy balance in the discharge that differ with respect to the oscillatory efficiency η_{osc} and the fraction of energy expended on direct heating of the gas η_T.

The integral values of $\ln (J/J_0)$ were calculated on a computer by the method used in Ref. 5.

4. The resultant experimental data enable us to analyze the outlook for using this kind of discharge for pumping fast-flow closed-cycle technological lasers and to predict the major characteristics of such systems.

To maintain time stability of the properties of the active medium of the laser, the mixture circulating through the loop must be partially replenished [Ref. 3,

6, 8]. In our work we did not look into the causes of deterioration of the amplifying properties of the medium with time. This effect may be associated with dissociation of CO_2 [Ref. 6-8], formation of substances in the discharge that lead to rapid collisional relaxation of N_2 and CO_2 molecules, and also with entry of these substances from the heated structural elements of the gas discharge chamber. Since an analytical relation cannot be established between the reduction in J/J_0 and the required replenishment of the mixture q under such conditions, we were restricted to an upper estimate of q from the experimentally established slope of the curve for J/J_0 as a function of time.

Let us take a value of about 10% of the J/J_0 under open-cycle conditions (i. e. at $t = 0$) as the admissible reduction in gain of the diagnostic laser signal. Then we can see from Fig. 2 that the time required for such a reduction is about 50 s for typical laser operating conditions (curve 3). Since the time of passage of the mixture through the channel of the facility is about 0.5 s under our experimental conditions, the gas passes through the discharge channel about 100 times during the time of the given reduction in J/J_0. Thus replenishment of the working mixture in an amount of $q \approx 1\%$ of the flowrate of the gas in the loop will maintain J/J_0 on the level we have chosen.

Considering that the reduction in J/J_0 is proportional to the reciprocal of q, and using the relations for $J/J_0(t)$ in Fig. 2, we can determine the necessary values of q for different conditions of laser operation. The results show that replenishment of the mixture on a level of 0.5-1% gives a value of J/J_0 under closed-cycle conditions that differs by no more than 5-10% from the open-cycle values. Such a degree of replenishment of the medium is typical for stationary closed-cycle lasers [Ref. 3, 6, 8] without regeneration systems.

The nonmonotonic behavior of the curves for $\ln(J/J_0) = f(W_g)$ that are shown in Fig. 3 evidences the intense relaxation of vibrationally excited molecules during passage along the optical axis of the system, and the inadvisability of using a cavity with an axis that coincides with the direction of gas flow. Fast-flow lasers ordinarily use transverse placement of the resonator with respect to the gas flow [Ref. 1, 6]. To optimize the working conditions of such a laser it is necessary to know the distribution of gain of the medium k_0 along the flow.

The lack of accurate data on the energy balance in the discharge that we used precludes reliable computer calculation of the distribution $k_0(x)$. However, the accuracy of such calculations can be considerably improved by normalizing $2\int k_0(x)\,dx$ to the experimentally measured integral values of J/J_0. The distribution of gain with respect to the flow can be represented as

$$k_0(x) \sim (jE\eta_{osc}X_{CO_2}/\Delta\nu)F(jE,\ X_{CO_2},\ \eta_{osc},\ \eta_T,\ x,\ \tau_r(T),\ldots),$$

where η_T is the percentage of energy expended by the source on direct heating of the gas, $\Delta\nu$ is the width of the amplification line, $\tau_r(T)$ is the time of relaxation of the vibrational energy. Calculations and estimates showed that the main error in determining k_0 is from the imprecise value of η_{osc}. For example, the difference in values of the function F in calculation of $k_0(x)$ for the case $\eta_{osc} = 0.6$, $\eta_T = 0.25$ and $\eta_{osc} = 0.75$, $\eta_T = 0.15$ did not exceed 5%, whereas the calculated values of k_0 in accordance with the curves in Fig. 3 differed by 20-25%. Therefore normalization of $2\int k_0(x)\,dx$ by using the experimental values of J/J_0 eliminates the main error in determination of the values of k_0, and gives more exact values of the oscillatory efficiency of an AC discharge. As implied by Fig. 3, the value of η_{osc} at $p = 50$ mm Hg, $X_{CO_2} = 2.5\%$ and $W_g \lesssim 350$ J/g is about 0.7-0.75.

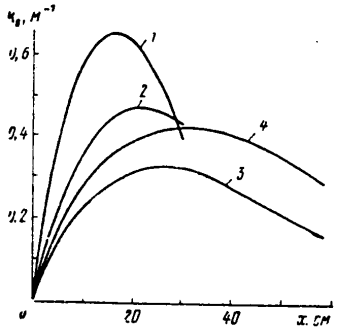

Fig. 4. Distribution of weak-signal gain with respect to the flow; x is reckoned from the beginning of the discharge zone: $p = 50$ (1-3) and 30 mm Hg (4); $X_{CO_2} = 5$ (1, 3, 4) and 2.5% (2); $X_{N_2} = 50\%$; $X_{He} = 45$ (1, 3, 4) and 47.5% (2); $W_g = 340$ (1-3) and 370 J/g (4); $l = 30$ (1, 2) and 60 cm (3, 4)

Typical distributions of k(x) for different values of X_{CO_2} and lengths of the discharge zone are shown in Fig. 4. These data evidence the high efficiency of AC discharge pumping. For comparison we can point out that in lasers with DC discharge pumping the maximum value of k_0 under closed-cycle conditions at pressure $p \approx 30$-50 mm Hg, $X_{CO_2} \sim 5\%$ and mixture replenishment of ~0.5% did not exceed 0.4 m^{-1} [Ref. 6, 9].

5. The realized values of $k_0 \approx 0.65$ m^{-1} on a length of $l \approx 20$ cm suggest a rather simple and effective electro-optical design for a powerful technological laser with AC discharge pumping. Let the height of the interelectrode gap be $H = 10$ cm, and let the flow length of the discharge chamber be $l = 30$ cm. The dimension of the chamber along the optical axis transverse to the flow is taken as 200 cm. Let the working mixture (50% N_2 + 45% He + 5% CO_2) be fed to the inlet of the discharge chamber at a velocity of 80 m/s with static pressure of 50 mm Hg. Let the volumetric energy input be $jE = 5$ W/cm^3. As can be seen from the data given above, such values of jE can be reached under closed-cycle conditions at $H = 10$ cm, and degree of mixture replenishment of about 1%. The calculations that we did for two versions of the optical arrangement (a single-pass unstable confocal resonator completely coinciding with the discharge zone with a rectangular output mirror, and a three-pass unstable confocal resonator with circular output mirror) showed that the output power of such a laser with optimum transparency of the optical cavity will be about 40 kW when the total

efficiency of the system is 13-15%, and the specific power output is about 50 J/g. An increase in flow velocity to 100-120 m/s should further increase the output power and efficiency of the device.

The mentioned values of total efficiency and specific emission output are much greater than the characteristics attained up to now on existing closed-cycle lasers with DC discharge pumping [Ref. 6, 9], where they come to $\lesssim$5-8% and $\lesssim$30-35 J/g respectively.

6. The cited experimental and theoretical data show the promise of using an AC discharge with frequency of about 10 kHz for exciting powerful lasers. The given type of discharge does not lead to anomalously rapid poisoning of the working mixture under closed-cycle conditions. It does away with ballast resistors, produces a fairly simple design of the gas-discharge chamber with interelectrode gap increased to about 10 cm in which a uniform discharge is maintained by the simplest power supply mentioned in the literature: a motor-generator set and a transformer.

High volumetric energy inputs give the necessary values of W_g with short lengths of the discharge along the flow, which under conditions of an increased interelectrode gap enables the use of simple electro-optical systems with a small number of passes. Coefficients of amplification of the medium can be reached that are higher than with pumping by a DC discharge, shortening the optical length of the laser and thus improving the configuration of the technological laser as a whole. All this recommends the 10 kHz AC discharge for pumping the active medium in technological lasers with a closed cycle.

In conclusion the authors thank N. I. Katsuro and G. G. Selivanov for designing and making the closed-cycle facility, and also A. B. Kuznetsov for doing the computer calculations.

REFERENCES

1. V. Kh. Goykhman, V. M. Gol'dfarb, ZHURNAL PRIKLADNOY SPEKTROSKOPII, Vol 21, 1974, p 456.

2. V. D. Gavrilyuk, A. F. Glova, V. S. Golubev and F. V. Lebedev, KVANTOVAYA ELEKTRONIKA, Vol 4, 1977, p 2034.

3. F. K. Kosyrev, N. P. Kosyreva, Ye. I. Lunev, AVTOMATICHESKAYA SVARKA, No 9, 1976, p 174.

4. V. D. Gavrilyuk, A. F. Glova, V. S. Golubev, A. B. Kuznetsov, F. V. Lebedev, V. A. Feofilaktov, KVANTOVAYA ELEKTRONIKA, Vol 6, 1979, p 548.

5. B. F. Gordiyets, A. I. Osipov, Ye. V. Stupenchenko, L. A. Shelepin, USPEKHI FIZICHESKIKH NAUK, Vol 108, 1972, p 655.

6. G. A. Abil'siitov, L. I. Antonova, A. V. Artamonov, V. S. Golubev, S. V. Drobyazko, Yu. A. Yegorov, N. I. Katsuro, A. V. Kazhiuub, F. V. Lebedev, Yu. M. Senatorov, Ye. M. Sidorenko, V. V. Sumerin, V. B. Turundayevskiy, V. M. Frolov, KVANTOVAYA ELEKTRONIKA, Vol 6, 1979, p 204.

7. V. N. Ochkin, TRUDY FIAN [Proceedings of Lebedev Physics Institute], Vol 78, 1974.

8. S. S. Vorontsov, A. I. Ivanchenko, R. I. Soloukhin, A. A. Shelepenko, ZHURNAL PRIKLADNOY MEKHANIKI I TEKHNICHESKOY FIZIKI No 3, 1977, p 6

9. A. V. Artamonov, Yu. A. Yegorov, A. V. Kazhidub, N. I. Katsuro, F. V. Lebedev, Y. M. Sidorenko, V. V. Sumerin, V. N. Frolov, KVANTOVAYA ELEKTRONIKA, Vol 5, 1978, p 920.

[155-6610]

6610
CSO: 1862

UDC 621.375

SPATIAL COHERENCE OF EMISSION OF A LASER WITH A RESONATOR THAT IS FILLED WITH A RANDOMLY INHOMOGENEOUS MEDIUM

Moscow KVANTOVAYA ELEKTRONIKA in Russian Vol 7, No 4(94), Apr 80
pp 764-769

[Article by I. A. Deryugin, A. P. Pogibel'skiy, N. D. Ustinov and I. A. Fedulov]

[Text] Random spatial inhomogeneities of the index of refraction of the active medium have a considerable effect on angular divergence of laser emission. Scattering of light by these inhomogeneities increases both the number of excited modes of waveforms and the divergence of individual modes. In this paper we will examine the influence that inhomogeneities of the medium have on the angular divergence of the fundamental mode of oscillations of an optical cavity that consists of two identical flat mirrors with reflectivity decreasing toward the edges in accordance with gaussian law. It is assumed that fluctuations of the index of refraction of the medium filling the cavity are uniform and isotropic.

To find field parameters like spatial and angular intensity distribution of emission, it is sufficient to know the mutual coherence function (MCF) of the field, which is defined as follows:

$$\Gamma(z, \mathbf{r}_1, \mathbf{r}_2) = \langle U(z, \mathbf{r}_1) U^*(z, \mathbf{r}_2) \rangle,$$

where $\mathbf{r} = \{x, y\}$ is a two-dimensional vector in the plane perpendicular to the direction of beam propagation. The angle brackets denote that averaging has been done with respect to spatial fluctuations of the index of refraction.

The MCF in a randomly inhomogeneous medium satisfies the equation of propagation [Ref. 1-3]:

$$\Gamma(z, \mathbf{R}, \mathbf{p}) = \left(\frac{k}{2\pi z}\right)^2 \int d^2\mathbf{R}' \int d^2\mathbf{p}' \Gamma(0, \mathbf{R}', \mathbf{p}') \exp\left[\frac{ik}{z}(\mathbf{R} - \mathbf{R}')(\mathbf{p} - \mathbf{p}')\right] \times$$
$$\times \exp\left\{-4\pi^2 k^2 z \int_0^1 dt \int dK K \Phi(K) [1 + J_0(|\mathbf{p}' + (\mathbf{p} - \mathbf{p}') \cdot t| K)]\right\}, \qquad (1)$$

where $\Phi(K)$ is the three-dimensional Fourier transform of the correlation function of fluctuations of the index of refraction of the medium; $J_0(x)$ is a zero-order Bessel function of the first kind; $\Gamma(0,R,p)$ is the MCF in the plane $z = 0$; $p = r_1 - r_2$, $R = \frac{1}{2}(r_1 - r_2)$ are new variables. The region of applicability of equation (1) is

$$ka \gg 1; \quad \langle \mu^2 \rangle k^2 a^3 \ll 1,$$

where $\langle \mu^2 \rangle$ is the mean square of fluctuations of the index of refraction of the medium, a is the size of the inhomogeneities, $\langle \mu^2 \rangle k^2 a$ is the coefficient of attenuation of the wave due to scattering in the Born approximation. Thus the size of the inhomogeneities must be much smaller than a wavelength, and the attenuation of the wave due to scattering at the distance equal to the size of the inhomogeneities must be small.

Let us write the integral equation for the MCF of the emission as

$$\Gamma(\mathbf{R}, \mathbf{p}) = A \int d^2\mathbf{R}' \int d^2\mathbf{p}' \Gamma(\mathbf{R}', \mathbf{p}') \rho\left(\mathbf{R}' + \frac{1}{2}\mathbf{p}'\right) \rho\left(\mathbf{R}' - \frac{1}{2}\mathbf{p}'\right) \times$$
$$\times \exp\left(-i\frac{2k}{F}\mathbf{R}'\mathbf{p}'\right) \exp\left[\frac{ik}{z}(\mathbf{R} - \mathbf{R}')(\mathbf{p} - \mathbf{p}')\right] \times$$
$$\times \exp\left\{-4\pi^2 k^2 L \int_0^1 dt \int dK K \Phi(K) [1 + J_0(|\mathbf{p}' + (\mathbf{p} - \mathbf{p}')t| K)]\right\}, \qquad (2)$$

where ρ is the reflectivity of the mirrors over the field, F is the radius of curvature of the mirrors, and L is the distance between them. We disregard effects associated with the fact that the radiation after reflection from the mirror passes through the same inhomogeneities, which is permissible when $L/k \gg a^2$. The index of the next to last exponential function of the kernel of integral equation (2) can be represented as $(p^2 + pp' + p'^2)$, where $q = \langle \mu^2 \rangle k^2 L \sqrt{\pi}/3a$ in the case of spatial fluctuations of the index of refraction described by the correlation function $B(z_1 - z_2, \rho) = \langle \mu^2 \rangle \exp\{-[(z_1 - z_2)^2/a^2] - \rho^2/a^2\}$. As we see, the inhomogeneous medium will now be characterized by a single parameter q, which in the Born approximation is directly proportional to the attenuation of radiation due to scattering on length L, and inversely proportional to the square of the size of inhomogeneities, i. e. the coefficient increases with the scattering capacity of the medium and the angle of scattering of emission.

Let the reflectivity of the mirrors be

$$\rho(r) = \exp(-r^2/2r_0^2). \qquad (3)$$

Then equation (2) takes the form

$$\Gamma(\mathbf{R}, \mathbf{p}) = A \int d^2\mathbf{R}' \int d^2\mathbf{p}' \Gamma(\mathbf{R}', \mathbf{p}') \exp\left[-(\mathbf{R}'^2/r_0^2) - (\mathbf{p}'^2/4r_0^2) + i\beta\mathbf{R}'\mathbf{p}'\right] \times$$
$$\times \exp[i\alpha(\mathbf{R} - \mathbf{R}')(\mathbf{p} - \mathbf{p}')] \exp[-q(\mathbf{p}^2 + \mathbf{p}\mathbf{p}' + \mathbf{p}'^2)], \qquad (4)$$

where $\alpha = k/L$, $\beta = -2k/F$. Mirrors with gaussian distribution of reflectivity have an ideally flat polar pattern; reflection from such mirrors does not produce additional diffraction maxima in the angular distribution of radiation. This should considerably simplify solution of the equation.

The simplest solution of equation (4) that corresponds to the MCF of the lower mode of resonator oscillations can be written as

$$\Gamma(\mathbf{R}, \mathbf{p}) = B \exp\left[-(M-1/r_0^2)R^2-(N-1/4r_0^2)p^2-S\,\mathbf{Rp}\right]. \quad (5)$$

The lower mode of our resonator is the lower mode of a cavity with a randomly inhomogeneous medium that is averaged with respect to all realizations of this medium. Let us note that the correlation function of the lower mode of our resonator may have a correlation radius much shorter than the beam radius.

Substitution of (5) in equation (4) leads to a system of three equations; the solution of this system for the case of weak inhomogeneities ($q<<1/r_0^2$) with large Fresnel numbers ($\alpha r_0^2>>1$) and $\beta = 0$ gives

$$\Gamma(\mathbf{R}, \mathbf{p}) = B \exp\left[-\frac{\sqrt{\alpha}}{r_0\sqrt{2}}\left(1-3r_0^2q\right)R^2-\frac{\sqrt{\alpha}}{4r_0\sqrt{2}}\left(1+9r_0^2q\right)p^2+\frac{i\sqrt{\alpha}}{r_0\sqrt{2}}\left(1+3r_0^2q\right)\mathbf{Rp}\right]. \quad (6)$$

The modulus of the complex degree of coherence takes the form

$$|\gamma| = \frac{|\Gamma(\mathbf{R}, \mathbf{p})|}{[\Gamma(\mathbf{R}+\mathbf{p}/2,0)\,\Gamma(\mathbf{R}-\mathbf{p}/2,0)]^{1/2}} = \exp\left(-\frac{\sqrt{\alpha}}{r_0\sqrt{2}}3r_0^2qp^2\right).$$

For a homogeneous medium, $q = 0$; then

$$\Gamma(\mathbf{R}, \mathbf{p}) = U(\mathbf{R}+\mathbf{p}/2)\,U^*(\mathbf{R}-\mathbf{p}/2),$$

where U(r) is the distribution over the mirror for the fundamental mode of a plane resonator with mirrors having reflectivity decreasing toward the edges in accordance with gaussian law [Ref. 4]. In the given case, $|\gamma| = 1$, which should have been anticipated since we are not considering spontaneous emission of the active medium.

In the case of strong inhomogeneities, where $qr_0^2>>1$, $q<<\alpha^2r_0^2$, we get

$$\Gamma(\mathbf{R}, \mathbf{p}) = B \exp\left(-\sqrt[4]{\frac{\alpha^2}{48r_0^6q}}R^2-\sqrt[4]{\frac{27}{16}\alpha^2r_0^2q^3}\,p^2+i\sqrt[4]{\frac{3\alpha^2q}{r_0^2}}\mathbf{Rp}\right), \quad (7)$$

$$|\gamma| = \exp\left(-\sqrt[4]{\frac{27}{16}\alpha^2r_0^2q^3}\,p^2\right).$$

The intensity distribution of the field over the mirror takes the form $I(R) = \Gamma(R,0)$. It is clear from expression (6) that in the case of weak inhomogeneities, the characteristic dimension of the region occupied by the lower mode of the resonator with inhomogeneous medium is equal to $(M - 1/r_0^2)^{1/2}$, increasing by a small amount over the dimension of the region occupied by the lower mode of an empty resonator.

The angular distribution of intensity of the light beam is determined by the MCF averaged over the beam [Ref. 5]:

$$\gamma(\mathbf{p}) = \int d^2R\,\Gamma(\mathbf{R}, \mathbf{p}).$$

The angular width of the beam is determined by the characteristic scale of the function $\gamma(p)$, which is called the effective radius of coherence, and does not coincide with the radius of coherence defined as the characteristic scale of the modulus of the complex degree of coherence $|\gamma|$. In our case the effective radius of coherence is

$$\rho_{эф}=\left[\frac{\left(M-1/r_0^2\right)\left[N-1/\left(4r_0^2\right)\right]+{}^1/_4S^2}{M-1/r_0^2}\right]^{1/2}.$$

For small q, the angle of divergence of the radiation is

$$\varphi=\sqrt[4]{2\alpha/r_0^2}\left(1+9r_0^2q/2\right)/k, \qquad (8)$$

for large q

$$\varphi=\sqrt[4]{(27/16)\,\alpha^2r_0^2q^3}/k. \qquad (9)$$

It is clear that for small q, i. e. in the case of weak inhomogeneities, the divergence is determined chiefly by the parameters of the mirrors, and it is only slightly worsened by the inhomogeneities of the active medium. In the case of large q, the random inhomogeneities of the medium have the major effect on divergence.

Formulas (8) and (9) give the divergence of the lower averaged mode of oscillations, i. e. the lower limit of divergence of the radiation that is reached in the case of single-mode lasing; but even this limiting divergence of laser emission may be considerably greater than the diffraction divergence.

REFERENCES

1. L. M. Dolin, IZVESTIYA VUZOV: SERIYA RADIOFIZIKA, Vol 11, 1968, p 840.

2. V. I. Tatarskiy, ZHURNAL EKSPERIMENTAL'NOY I TEORETICHESKOY FIZIKI, Vol 56, 1969, p 2106.

3. H. T. Yura, APPL. OPTICS, Vol 11, 1972, p 1399.

4. N. G. Vakhitov, RADIOTEKHNIKA I ELEKTRONIKA, Vol 10, 1965, p 1676.

5. A. I. Kon, V. I. Tatarskiy, IZVESTIYA VUZOV: SERIYA RADIOFIZIKA, Vol 15, 1972, p 1547.

[155-6610]

6610
CSO: 1862

UDC 621.373.826.038.823

A PULSE-PERIODIC EXCIMER LASER

Moscow KVANTOVAYA ELEKTRONIKA in Russian Vol 7, No 4(94), Apr 80
pp 896-898

[Article by V. Yu. Baranov, G. S. Baronov, V. M. Borisov, Yu. B. Kiryukhin and S. G. Mamonov, Institute of Atomic Energy imeni I. V. Kurchatov, Moscow]

[Text] In recent years, considerable interest has developed in excimer lasers with emission in the ultraviolet region of the spectrum. The comparatively high efficiency of this class of lasers and their high peak power make them of interest from the standpoint of use in various kinds of research, for example in separation of isotopes and ultrapurification of materials [Ref. 1]. A pulse-periodic laser with high pulse repetition frequency is convenient for applications of this kind. Such a mode of operation is most simply realized on electric discharge versions of the excimer laser. Electric discharge excimer lasers are not as efficient as electron-beam-controlled lasers, but the simplicity of design, the absence of foils and the possibility of using thyratron commutators in the circuit makes them preferable.

At the present time, one work is known [Ref. 2] that gives the experimental results on development of a pulse-periodic electric discharge KrF excimer laser with pulse repetition frequency of 1 kHz and average power of 10 kW. The rate of circulation of the gas mixture in the discharge zone is 70 m/s. The electric circuit is based on sections of coaxial lines and a thyratron commutator. The efficiency of the laser facility in the pulse-periodic mode is 0.15%, and the energy in an individual pulse did not exceed 10 mJ. In Ref. 3 a report is given on attainment of an average power of 40 W at a pulse repetition frequency of about 1 kHz in a KrF laser, i. e. energy in the isolated pulse is 40 mJ.

The purpose of our research was to develop a pulse-periodic laser with elevated lasing pulse energy, which is necessary for a number of applications of excimer lasers of this type. Luminous energy of 0.2 J in a pulse is attained at a pulse repetation rate of 100 Hz and efficiency of about 0.5%.

A closed cycle of circulation of the gas mixture is realized in a loop that includes a compressor with capacity of 200 l/s, a cooler, a gas line and a laser chamber. The rate of circulation of the mixture in the discharge zone is 6 m/s. The electric power supply system consists of a low-inductance KMVD-50-0.5 storage capacitor with capacitance of 0.05 mF and a TGI-2500/50 thyratron commutator. Resonant-diode charging of the storage capacitor was used in the work. The design of the laser chamber, the method of UV preionization and the configuration of the electrodes are analogous to Ref. 4. The active volume is about 200 cc (0.7 x 4 x 70 cm). The laser cavity is formed by an opaque aluminum mirror and a plane-parallel CaF plate separated by a distance of 1 m. With an arc gap as commutator, the lasing energy on KrF was 1 J in this electric discharge arrangement at a discharge voltage of 70 kV. The use of a thyratron as a commutator reduces the lasing characteristics of the system somewhat, although they remain fairly high. The growth of specific lasing and average power of the facility when the charging voltage is increased is limited by the maximum voltage that can be applied to the thyratron. A discharge voltage just above 40 kV led to unstable operation of the thyratron commutator in the pulse repetition mode and accordingly to a reduction in lasing power.

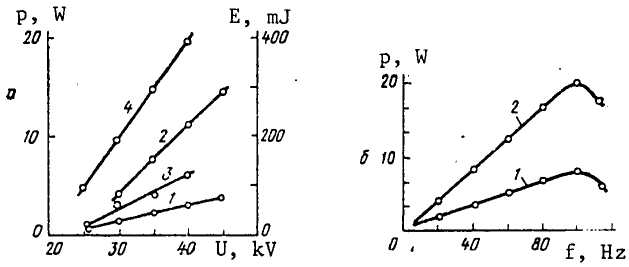

Fig. 1. Specific lasing and average emission power for KrF and XeCl lasers as functions of the voltage across the storage capacitor (a), and average power as a function of pulse repetition frequency (b): 1--mixture HCl:Xe:He = 1:20:1000, p = 1.5 atm; 2--mixture F_2:Kr:He = 1:25:500, p = 1.75 atm; 3--mixture HCl:Xe:He = 1:20:1000, p = 1.5 atm, f = 100 Hz; 4--mixture F_2:Kr:He = 1:25:500, p = 1.75 atm, f = 100 Hz

Specific lasing and average emission power are shown as functions of the charging voltage across the storage capacitor for KrF and XeCl in Fig. 1a. The pressures and the mixture composition were optimized for the given electric discharge system. It should be noted that theoretical and experimental research [Ref. 5] has shown that an increase in charging voltage U_{ch} produces little change in the parameter $E/p = U_m/dp$ (U_m is the voltage across the discharge plasma, d is interelectrode spacing and p is gas pressure), which is 5 kV/cm·atm for typical laser mixtures. The energy input to the discharge as U_{ch} rises, increases chiefly due to

the growth in discharge current. At $U_{ch} = 40$ kV, the amplitude of the current through the discharge at a duration of about 80 ns reaches 20 kA and is provided by the discharge of a peaking capacitor connected to a small inductance in parallel with the electrodes and pulse-charged from the main capacitor. Fig. 1b shows the average power as a function of the pulse repetition frequency. This figure implies that the reduction in average power with increasing frequency occurs when the repetition frequency exceeds 100 Hz, which is less than the limiting prf $f_0 = v/b$, where v is flowrate and b is the width of the discharge along the flow.

Apparently pulse-periodic excimer lasers are subject to the same mechanisms that limit the pulse repetition frequency in CO_2 lasers [Ref. 6]. Nevertheless, the presence of strongly electronegative gases such as F_2, HCl and NF_3 in the gas mixtures of excimer lasers, and also noble gases like Xe, Ar and Kr is responsible for both the specifics of the discharge and the level of limitation of repetition frequency.

Observed discharge peculiarities in gas mixtures that are typical of excimer lasers are shown in Fig. 2 in photographs of the integral discharge luminescence. This figure shows a photograph of the discharge in a mixture of HCl:Xe:He = 1:20:1000 at a low level of specific energy input of about 50 J/l, corresponding to $U_{ch} = 20$ kV. Lasing was not observed. An increase in the energy stored in the capacitor to the level of the energy input to the discharge of about 150 J/l ($U_{ch} = 35$ kV) leads to brighter channels in the discharge along with diffuse uniform luminescence, and lasing appears. The emission intensity increases with an increase in the voltage across the storage capacitor (Fig. 1), and more channels appear (see Fig. 2b). At higher halide concentrations (HCl:Xe:He = 1:20:500), p = 1.5 atm, and specific energy inputs to the discharge of about 150 J/l, there is a reduction in brightness of the diffuse part of the discharge, and one or two regions appear with strong luminescence (see Fig. 2c); lasing was not observed. Similar patterns show up in operation of a laser facility with pulse repetition frequency of 1-100 Hz.

a b c

Fig. 2. Photographs of integral discharge luminescence in an excimer mixture for different charging voltages and halide concentrations: a--$U_{ch} = 20$ kV, mixture of HCl:Xe:He = 1:20:1000, p = 1.5 atm; b--$U_{ch} = 35$ kV, mixture of HCl:Xe:He = 1:20:1000, p = 1.5 atm; c--$U_{ch} = 35$ kV, mixture of HCl:Xe:He = 1:20:500, p = 1.5 atm.

The laser loop contains about 200 liters of gas mixture, enabling the facility to operate for some time without replacing the gas. For a KrF mixture the duration of operation was limited to 10^4 light flashes with a fall-off in lasing power to half. Such a rapid reduction in lasing may be due to the generation of F_2 in the discharge, drift of atomic fluorine to the walls of the chamber and the loop, and also the formation of products that absorb strongly in the 250 nm region in the discharge. This question requires further research. The lasing power for XeCl falls to half after $2.2 \cdot 10^5$ light flashes.

Thus a pulse-periodic electric-discharge excimer laser has been made with lasing energy of 0.2 J in an isolated pulse and closed cycle of circulation of the working gas at average power of 20W on KrF and 7 W on XeCl with pulse repetition frequency of 100 Hz. An increase in the rate of circulation of the gas mixture could considerably increase the pulse repetition frequency, and hence the average power.

REFERENCES

1. J. H. Clark, APPL. PHYS. LETTS, Vol 32, 1978, p 46.

2. T. S. Fahlen, J. APPL. PHYS., Vol 49, 1978, p 455.

3. LASER FOCUS, Vol 14, No 1, 1978, p 28.

4. V. Yu. Baranov, V. M. Borisov, F. I. Vysikaylo, S. G. Mamonov, Yu. Yu. Stepanov, KVANTOVAYA ELEKTRONIKA, Vol 7, No 5, 1980.

5. V. Yu. Baranov, V. M. Borisov, F. I. Vysikaylo, Yu. B. Kiryukhin, I. V. Kochetov, S. G. Mamonov, V. G. Pevgov, V. D. Pis'mennyy, Yu. Yu. Stepanov, O. B. Khristoforov, "Issledovaniye kharakteristik razryada i generatsii eksimernykh lazerov" [Investigation of the Characteristics of Discharge and Stimulated Emission of Excimer Lasers], Preprint, Institute of Atomic Energy, Moscow, 1979, p 12.

6. V. Yu. Baranov, V. V. Breyev, D. D. Malyuta, V. G. Niz'yev, KVANTOVAYA ELEKTRONIKA, Vol 4, 1977, p 1861.

[155-6610]

6610
CSO: 1862

NUCLEAR PHYSICS

UDC 621.384.6

LIU-10 HIGH-POWER ELECTRON ACCELERATOR

Moscow DOKLADY AKADEMII NAUK SSSR in Russian Vol 250, No 3, 1980 pp 1118-1122

[Article by A. I. Pavlovskiy, V. S. Bosamykin, V. A. Savchenko, A. P. Klement'yev, K. A. Morunov, V. S. Nikol'skiy, A. I. Gerasimov, V. A. Tananakin, V. F. Basmanov, D. I. Zenkov, V. D. Selemir, and A. S. Fedotkin; presented by Academician Yu. B. Khariton 27 September 1979]

[Text] A new direction in accelerator technology for the construction of high-power generators of beams of charged particles with acceleration energies of tens of megaelectron volts has developed over the last few years - linear induction accelerators (LIA) with inductors on the radial lines [1-3], which combine the possibility of changing the acceleration energy by varying the scales of the accelerating system with the high-current feature characteristic of low-impedance lines having distributed parameters. The construction of such accelerators is of great interest from the standpoint of the development of technology for accelerating high-power beams of charged particles (electrons and ions) up to high energies and obtaining solutions of wide range of physical problems, such as collective acceleration methods, the interaction between radiation fluxes and a material, the interaction between ultrarelativistic beams and plasmas, process for generating electromagnetic waves, etc.

The development of this new trend requires a wide range of research into and the solution of several theoretical electrophysical problems, among the most important of which are: the construction of high-power multi-component accelerating systems with hundreds (∿400 in the LIU-10) of spark gaps, which are switched on with subnanosecond accuracy according to a specified program and which are commutated by low-impedance (∿1 Ohm)

radial lines; the development of methods for generating high-current (tens of kiloamperes) electron beams and transmitting them considerable distances; the development of reliable interrelationships between the units and components operating under the complicated conditions for electric fields close to the limit and for static and shock loads, and the accumulation of irreversible changes. One of the most important advantages of the LIA is the sequential modular structure of the accelerating system. The uniformity and replaceability of the modules significantly reduces the working area and simplifies the manufacture and operation of the accelerators.

The first model of such accelerators - the LIU-10 high-power electron accelerator - was put into operation in 1977. The accelerating system of the LIU-10 consists of 14 series-connected modules, with each contributing ~1 MeV to the acceleration energy. The dimensions of the device are: a length of 7 m, a width of 4 m, and a height of 2.2 m (Fig. 1). Individual accelerator modules consist of three functionally connected units - the inductor unit (of the acceleration sections), the pulse voltage generator (PVG) providing a pulsed capacitance charge to the inductors, and the generator shaping the starting pulses of the switches of the accelerator sections (GES). The modules are automatic both in construction and in the electrical circuit. They can be used to construct devices of various sizes with an accelerating energy range from unity to tens of megaelectron volts. In designing the LIU-10 units in which liquid (water, glycerin, transformer oil) and gaseous (SF_6 and nitrogen mixture) insulators were used, special attention was given to the polarity distribution of the electric potentials. In the pulse-charged capacitance storage rings the high-voltage electrodes have negative-charge potential; the control units of the gas-filled trigatron spark gaps were placed in the positive electrodes. Some results on the development of the commutators are given in [4, 5]. Individual components, units, and accelerator modules were subjected during operation to multiple lifetime tests in series with $(5\text{-}10)\cdot 10^3$ switch-ons.

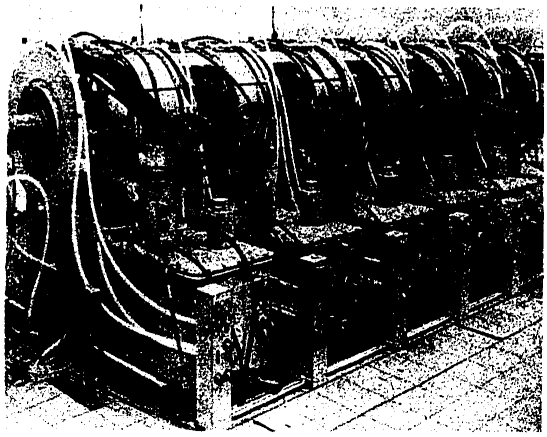

Fig. 1. Overall view of the LIU-10 accelerator

The most important unit in an LIA in the block of inductors. It consists of three series-connected inductors on the radial lines, which are connected in parallel through the triggering circuit with one PVG. An individual inductor is formed by a torus-shaped retarding electrode, open along the internal radius, with an internal cavity containing a high-voltage disk electrode [3]. The inductor line is closed over the perimeter of one of the output gaps with the aid of a multi-channel ring commutator; another output gap is connected to the load through the same commutator. The no-load inductor generates rectangular pulses of accelerating voltage with an amplitude close to the charging voltage. The duration of the first pulse along the base is equal to an electric line length of 20 nsec, while the second and succeeding pulses of alternating polarity are 40 nsec long. The accelerating voltage of the three inductors is additive under series connection. Deionized water is used as the insulation for the radial lines. The ring commutator is formed by eight separate gas-filled trigatron spark gaps operating at 500 kV. The spread in the gap switch-on time is ±1 nsec with a reserve of electrical resistance in the gas gap of 1.7. A polyethelene accelerator tube was placed along the axis of the inductor block. A solenoid was placed on the inner surface of the tube to generate the magnetic field when the external capacitor bank discharged and to remove the electrons scattered from the accelerated beam. With a series connection of the units a single vacuum accelerator channel was formed

with a longitudinal homogeneous magnetic field of ~5 kOe. The parameters of the unit with the accelerator sections are: a charging voltage -500 kV; duration of the charging pulse along the base of 0.8 μsec; maximum amplitude of the accelerating voltage of 1.2 MV; short-circuit current of 180 kA; number of spark gaps is 24; dimensions of the units are an outer diameter of 1 m, a longitudinal dimension of 0.45 m, and a high-voltage gap in the lines of ~5 cm.

The capacitance of the inductor unit was charged from a generator constructed according to a modified Arkad'yev-Marx circuit. The five PVG stages were formed by IK 100-0.25U4 capacitors, gas-filled trigatron commutators operating at 100 kV, liquid resistors, and current-carrying buses. Transformer oil was the insulator. All the spark gaps were controlled and, with the exception of the gap of the first stage, were started by pulses shaped by the operation of the gap of the previous stage with the aid of resistor circuits. The spread in the switch-on time of the PVG gap with a dc voltage of 100 kV was ±3 nsec with an electrical resistance reserve in the gas gap of 2. The 14 generators were synchronized to within ±10 nsec. The electrical system of the PVG was screened by a retarding metal frame which was connected to the inductor unit by a 500 kV coaxial high-voltage output lead, which contains a filter for suppressing "reverse" high-voltage pulses propagating along the lead-in when the inductor lines are switched. The PVG is triggered by a 50 kV pulse with a duration of $\geqslant$30 nsec and a rise time of $\leqslant$10 nsec. The energy reserve of one generator was 6.25 kJ, the pulsed current was 50 kA, and the charge voltage was +100 kV. The dimensions of the PVG were a length of 1.3 m and a width and height of 0.75 m.

The multichannel commutators of the block were triggered by 24 simultaneous pulses of positive polarity with a rise time of $\leqslant$5 nsec, a duration of $\geqslant$15 nsec, an amplitude of +60 kV, and transmission over a cable line. The GES producing them consists of a double shaping line (DSL) with glycerin insulation, which is switched on by the operation of a one-channel trigatron spark gap. To sharpen the leading edge up to 2 nsec, a hydrostatic gas-filled peaking spark gap was used with ring electrodes, and it operated as a multispark gas gap with a pressure of the gas mixture of 6 tech. atmosphere. The DSL impedance is 3.3 Ohm, the pulsed charge voltage is -100 kV, and the charge duration is 0.8 μsec. The GES is started by one pulse with the same parameters that obtain at its output. The spread in the operation of each GES is not poorer than ±0.7 nsec, which allows the starting time of the accelerator blocks to be regulated by changing the time the starting pulse arrives

at the single-channel DSL spark gap. The GES capacitance is charged from the second PVG stage though the high-voltage charging circuit mounted inside the PVG housing.

Thus, the function of a module involves a dc charging pulse for the PVG, two starting pulses for the PVG and the GES, and a pulsed current to excite an axial magnetic field. The modules are placed in pairs on mobile mounts.

The high-voltage synchronizing system contains two generators similar in design to the GES; one of them simultaneously triggers all 14 PVG's, while the other triggers through delay cable lines of variable length the set of 14 PVG's controlling the connection of the inductor blocks. The generators are charged from a pulsed device which also generates a high-voltage pulse; a time shift of 0.8 μsec suffices for the starting generator for the PVG, one of whose pulses in turn connects the starting generator of all the GES's with a delay of 0.8 μsec. The accelerator is started by pulses with an amplitude of 10 kV, which are controlled by the spark gaps of the capacitor bank in order to excite the magnetic field and by the commutator of the pulsed charging device in the synchronizing system. Monitoring of the initial parameters, the starting of the device, and automatic protection measures during emergencies are carried out from the control panel. Resistor, capacitance, and induction transducers monitor the accuracy of the synchronization of the units and the charging voltages.

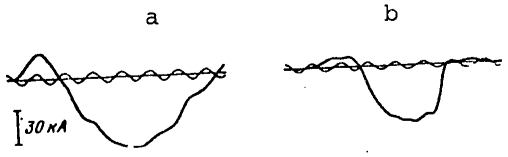

Fig. 2. Current pulses in the injector diode (a) and electron beam current behind the fourth inductor block (b) with acceleration during the second voltage pulse of the inductors; the marks are 100 MHz.

The total accelerating voltage of all three blocks is supplied to a field-emission foil-less diode with magnetic insulation by a logitudinal field; the diode shapes a tubular electron beam with an energy of ∿2.5 MeV and injects it into the accelerating channel. With a beam propagating along the vacuum (10^{-5} Torr) accelerating channel, the transit time of the relativistic electrons ∿20 nsec is comparable to the duration

of the accelerating pulses, the blocks were switched on according to a selected time program with a shift in operation every 3 - 1.5 nsec. The beam diameter was varied by changing the diameter of the ring emitter up to 180 mm, and the thickness of the electron layer increased during acceleration from 5 to 20 mm. Experiments in which the injection current was recorded by a Rogowski loop, as well as the beam current as it propagates along the acceleration channel (Fig. 2), indicate that the transmission efficiency is 0.75 with respect to the diode current. An increasing magnetic field at the accelerator output changes the transverse beam dimensions by a factor of ~2. The results of measurements of the electron limiting energy and the spectrum of the hard γ radiation over the nuclear threshold reactions by a set of activation detectors shows a good agreement with the acceleration energy calculated according to the current-voltage characteristics of the inductor block.

The charged particles can be accelerated either during the first pulse or only during the second pulse of the inductor accelerating voltage of different duration, depending on the directions of the electric field and the electron motion. The output parameters of the device are: electron limiting energy of 13.5 MeV; amplitude of the current pulse of the electron beam of 50 kA; maximum duration of the current pulses is 20 or 40 nsec, respectively. A two-fold increase in the accelerator power is possible due to an increase in the inductor diameter up to ~1.5 m and in the PVG capacitance.

At the present time, the following basic factors affecting the formation, transmission efficiency, and acceleration of electron beams are being investigated: injection efficiency of turbular beams from diodes with magnetic insulation; limiting beam currents in the presence of accelerating and magnetic fields; the interaction between a high-current relativistic electron beam and an accelerating system; the degree of homogeneity in fields in the accelerator channel and also scattered fields. In a series of experiments a beam was injected into the atmosphere with stable transmission within a diameter of 10 cm in the azimuthal magnetic field of linear current flowing along the beam axis, with injection from the region of a homogeneous axial field. The electron beam was also focused with a diameter of ~2 cm in an increasing azimuthal magnetic field. The development and successful operation of the first model of this new device allowed us to obtain data necessary to design more powerful accelerators and accelerators with higher energies and longer pulses.

REFERENCES

1. V. S. Bosamykin and A. I. Pavlovskiy, Author's Certificate No. 270913; BYULL. IZOBRET., No. 34, p. 223, 1971.

2. A. I. Pavlovskiy and V. S. Bosamykin, AT. ENERG., Vol. 37, No. 3, p. 228, 1974.

3. A. I. Pavlovskiy, V. S. Bosamykin, et al., DOKL. AKAD. NAUK SSSR, Vol. 222, No. 4, p. 817, 1975.

4. B. A. Afanas'yev, A. I. Gerasimov, et al., PRIB. TEKH. EKSP., No. 3, p. 136, 1976.

5. A. I. Gerasimov, G. D. Kuleshov, et al., PRIB. TEKH. EKSP., No. 5, p. 111, 1975.

[8144/1301-9307]

9370
CSO: 8144/1301

-END-